



U.S. DEPARTMENT OF COMMERCE

Frederick B. Dent, Secretary

NATIONAL OCEANIC AND ATMOSPHERIC ADMINISTRATION

Robert M. White, Administrator

ENVIRONMENTAL DATA SERVICE

Thomas S. Austin, Director

Solar-Geophysical Data

DESCRIPTIVE TEXT

**NATIONAL GEOPHYSICAL AND SOLAR - TERRESTRIAL DATA CENTER
BOULDER, COLORADO**

FEBRUARY 1974

SOLAR-GEOPHYSICAL DATA

I N T R O D U C T I O N

This pamphlet contains the description and explanation of the data contained in the monthly publication *Solar-Geophysical Data*, issued by the Environmental Data Service of the National Oceanic and Atmospheric Administration. The monthly bulletins are available on a data exchange basis through the World Data Center A for Solar-Terrestrial Physics, NOAA, Boulder, Colorado 80302, or at a nominal cost through the National Climatic Center.* These data reports continue the series which were issued by the Central Radio Propagation Laboratory of the National Bureau of Standards, known since 1956 as the CRPL-F series Part B. The CRPL became the Institutes of Environmental Research in October 1965. The latter were reorganized as the ESSA Research Laboratories in November 1967. In October 1970 in a governmental reorganization ESSA was absorbed as part of the National Oceanic and Atmospheric Administration (NOAA). Since June 1965, the compilations and editing have been done by Miss Hope I. Leighton under the supervision of Mr. Dale B. Bucknam and Miss J. Virginia Lincoln.

The reports are intended to keep research workers abreast of the major particulars of solar activity and the associated ionospheric, radio propagation and other geophysical effects. This report series is made possible through the cooperation of many observatories, laboratories and agencies as recorded in the detailed descriptions which follow.

Beginning with the July 1969 issue the publication was divided into two Parts (I and II). Part I contains data for the month one month before the month of publication and for the second month before. Part II contains data for the sixth month before the month of publication and the seventh month before. Special data for miscellaneous times are given from time to time in Part II. These reports should not be considered as definitive publications because of the rapid publication schedule involved for the data from months one and two before that of publication. Errata or revisions are included from time to time. Additions to the descriptive text will appear with the data when new material is added, or revision is made.

The first page of each issue gives the general contents and is backed by a running index to locate data for a specific month for the past year. A complete index for data since July 1957 is given in the blue section of this text.

A useful reference containing descriptions of many solar and geophysical phenomena as well as directing the reader to more detailed discussions is the *Handbook of Correlative Data*, issued February 1971 by the National Space Science Data Center, NASA, Goddard Space Flight Center, Greenbelt, Md. (The Handbook is also available through World Data Center A for Solar-Terrestrial Physics.)

*For sale through the National Climatic Center, Federal Building, Asheville, NC 28801, Attn: Publications. Subscription Price: \$30.50 annually for both Part I (Prompt Reports) and Part II (Comprehensive Reports) or \$15.50 annually for either part. Extra issue included. For foreign mailing add \$8.00 for both parts or \$4.00 for either part. Single issue price \$1.25 for either part and 75¢ for the extra issue. Make checks and money orders payable to: Department of Commerce, NOAA.

To standardize referencing these reports in the open literature, the following format is recommended:

Solar-Geophysical Data, CRPL-FB 135⁺, pages, issue date, U.S. Department of Commerce, (Boulder Colorado, U.S.A. 80302).

⁺CRPL-FB 135 through 269
IER-FB 270 through 298
299 Part I or 299 Part II to number of current issue.

TABLE OF CONTENTS

Page

Data for One Month Before Month of Publication

Alerts	4
Daily Solar Indices	6
Solar Flares	8
Solar Radio Waves	10
Solar Wind Measurements	12
Solar Proton Monitoring	14
Interplanetary Magnetic and Electric Fields	15
Solar Proton Events (Provisional)	17

Data for Two Months Before Month of Publication

Daily Solar Activity Centers	20
Solar X-Ray Radiation	28
Sudden Ionospheric Disturbances	28
Solar Radio Waves	32
Cosmic Rays	35
Geomagnetic Activity	37
Radio Propagation Indices	39

Data for Six Months Before Month of Publication

Solar Flares	44
Solar Radio Waves	45
Solar X-Ray Radiation	53
Solar Proton Monitoring	53
Reduced Magnetograms	57

Data for Seven Months Before Month of Publication

Abbreviated Calendar Record	60
Flare Index by Region	61

Data for Miscellaneous Time Periods

Retrospective World Intervals	61
-------------------------------	----

Acknowledgements

Index to Volumes for 1957-1973

Key to Index for <i>Solar-Geophysical Data</i>	67
Index Tables	71

Stonyhurst Disks

DATA FOR ONE MONTH BEFORE MONTH OF PUBLICATION

TABLE OF CONTENTS

	<u>Page</u>
<u>Alert Periods</u>	
H.60 IUWDS Alert Periods (Advance and Worldwide)	4
<u>Daily Solar Indices</u>	
A.2,A.8 Relative Sunspot Numbers and Adjusted 2800 MHz Solar Flux	6
A.2,A.8 Combined Sunspot Numbers and Solar Flux Values	6
A.2 Graph of Sunspot Cycle	6
A.2 Predicted and Observed Relative Sunspot Numbers	6
<u>Solar Flares</u>	
C.1 Flares of Numerical Importance 1 or Greater	8
C.1 Subflares	8
C.1d No-Flare-Patrol Chart	9
<u>Solar Radio Waves</u>	
A.10 Solar Interferometric Charts	10
A.10 East-West Solar Scans	10
C.3 Outstanding Occurrences at Fixed Frequencies (SELECTED)	11
<u>Solar Wind Measurements</u>	
A.13a Measurements of Pioneers 6, 7, 8 and 9	12
<u>Solar Proton Monitoring</u>	
A.12ba Pioneer 6	13
A.12bb Pioneers 8 and 9	15
<u>Interplanetary Magnetic and Electric Fields</u>	
A.17 Interplanetary Magnetic Field - Pioneers 8 and 9	15
A.18 Interplanetary Electric Field - Pioneers 8 and 9	16
A.17c Inferred Interplanetary Magnetic Field	16
<u>Solar Proton Events</u>	
Provisional Data	17

A L E R T P E R I O D S (H.60)

The table gives the Advance Geophysical Alerts (PRESTO) as initiated by (or received by) the Western Hemisphere Regional Warning Center of the International Ursigram and World Days Service (IUWDS) at Boulder, Colorado, and also the Worldwide Geophysical Alerts (GEOALERTS) as designated by the IUWDS World Warning Agency, Boulder, Colorado.

These alerts are of the types recommended by the International Ursigram and World Days Service. A description of the IUWDS program can be found in *Synoptic Codes for Solar and Geophysical Data*, Third Revised Edition 1973, revised by RWC Circular Letters. This code book and its revisions are available from the IUWDS Secretary for Ursigrams, Mr. R. B. Doeker, NOAA, Boulder, Colorado, U.S.A., 80302.

The PRESTO messages are originated by the reporting observatory or at the Regional Warning Centers. They are for advance reporting of major events. The format of these messages follows (extracted from *Synoptic Codes for Solar and Geophysical Data*):

PRESTO

1. Content.

- Report of major events to the other RWC and to the local or regional customers.

2. General form.

PRESTO observatory JJHHmm report

3. Definition of symbols.

PRESTO = key word for RAPID reporting of major events

observatory = name of reporting observatory in clear text

JJHHmm = Greenwich date and time of issue of message in hours and minutes UT

report = one or more of statements as below

For GEOMAGNETIC ACTIVITY

MAGSTORM BEGINS JJHHmm

STRONG MAGSTORM IN PROGRESS JJHHmm (A≥50)

WEAK MAGSTORM IN PROGRESS JJHHmm (30≤A<50)

Note: One may add plain language comments related to auroral reports or Forbush effect expected

For MAJOR FLARES

SOFLARE - importance class - coordinates (i.e. N20 E78)
- JJHHmm

(date and time) - "duration in minutes given" or statement "in progress"

Note: One may add plain language comments like "X-shaped" or "covering spots" or "suspected proton flare"

For TENFLARE (solar radio emission outburst at 10 cm>100% over background)

TENFLARE - XX units - JJHHmm for onset - duration in minutes, or statement "in progress" at the time of PRESTO, or statement "observed until hours and minutes UT"

Note: Units give the increase of the flux density over the pre-burst level in conventional units ($10^{-22} \text{ Wm}^{-2} \text{ Hz}^{-1}$) by significant digits and words such as "1700 units over background"

For PROTON EVENT

COSMIC RAY INCREASE - JJHHmm - percent increase above normal based on neutron monitor

POLCAP ABSORPTION - JJHHmm - dB of absorption by riometer or ionospheric forward scatter technique

PROTON EVENT - JJHHmm - specify energy range from a spacecraft report

Notes: 1. PRESTO should be circulated as soon as the event has been recognized.

2. The PRESTO will only report events and no forecasts. Any change of a forecast would be sent to the interested customers as a GEOSOL, GEOALERT or in plain language.

3. If the observatories follow this scheme, it is not necessary to report the kind of experiment

SOFLARE signifies a chromospheric report
TENFLARE signifies a centimetric outburst
COSMIC RAY INCREASE signifies a neutron monitor count increase
POLCAP ABSORPTION signifies a ground based polar cap report
PROTON EVENT signifies spacecraft reports only

The GEOSOL or GEOALERT messages are originated by the Regional Warning Center or by the World Warning Agency in Boulder, Colorado, U.S.A. They are for the purposes of reporting the current level of solar activity and for forecasting solar-geophysical events. The format of these messages follows:

GEOSOL
or
GEOALERT

1. Content.

- For sending combined data and forecasts to other RWCs and for general data users
- For sending ADVICE information to other RWCs

2. General form.

GEOALERT IIINN DDHHmm
or
GEOSOL date time group of message in UT
warning center of origin, serial number of message

key word - [use GEOALERT when ADVICE included in message]

9HHJJ	laaab	2cccd	3eeef	4gggh
				cosmic ray intensity and events
				geomagnetic A index and events
				10 cm flux and number of bursts
				relative sunspot number, and number of new spot groups
signifies indices for preceding 24 hours follow				

Notes: 1. Events are classified as below:

- a) Chromospheric Events: some flares are just Chromospheric Events without Centimetric Bursts or Ionospheric Effects. (SID). (Class C flare)
 - b) Radio Event: flares with Centimetric Bursts and/or definite Ionospheric Event. (SID).
 - c) Geophysical Event: flare (Importance two or larger) with Centimetric Outbursts (maximum of the flux higher than the Quiet Sun flux, duration longer than 10 minutes) and/or strong SID. Sometimes these flares are followed by Geomagnetic Storms or small PCA. (Class M flare)
 - d) High Energy Event: flare (class two or more) with outstanding Centimetric Bursts and SID. High Energy Protons are reported at the Earth in case of most of these events occurring on the western part of the solar disk. (Class X flare)
2. Some quiet groups being of very little importance, these can be reported only by their number.
 3. If the word CAUTION is inserted between QXXYY group and the description word, it signifies one cannot forecast real evolution of the group at time of the message.
 4. If the word DOUBTFUL is inserted between QXXYY group and description word, it signifies it is impossible to determine definitely the true class of activity expected.

ADVICES AND ALERTS

---ALERT--- key word(s) to describe one or more of the following situations during the next 24 hours or longer:

SOLNIL } End of active period
MAGNIL } or
PROTONNIL } Beginning of period of very low activity

SOLQUIET - No active regions on the solar disk
MAGQUIET - Only sporadic weak geomagnetic activity

SOLALERT JJ/KK - increased solar activity expected between days JJ and KK
MAGALERT JJ/KK - increased geomagnetic activity expected between days JJ and KK

MAJOR FLARE ALERT JJ/KK QXXYY - large bright flare (Class X) expected between days JJ and KK in region QXXYY

PROTON FLARE ALERT JJ/KK QXXYY - protons expected in earth's vicinity as a result of proton flare predicted to occur between days JJ and KK in region QXXYY

PRESTO PROTON ARRIVAL ALERT KK/JJHHmm - forecast of arrival of protons in earth's vicinity on day KK from flare which occurred on day JJ at HHmm (UT)

STRATWARM STARTS ---- } includes day of week and
STRATWARM EXISTS ---- } geographical area
STRATWARM ENDS

- Notes:
- 1) The Alert section is always included in the GEO-ALERT code format as it is used as ADVICE by RWCs & WWA.
 - 2) More than one type of Alert may be included in a message
 - 3) Previous transmission of ALERT (SOL, MAG, MAJOR FLARE, PROTON FLARE, PRESTO PROTON ARRIVAL) requires the eventual transmission of appropriate NIL (SOL, MAG, PROTON)
 - 4) Transmission of STRATWARM STARTS or EXISTS requires the eventual transmission of STRATWARM ENDS
 - 5) GEOALERTS are converted by WWA to plain language and broadcast on WWV and WWVH as described in Circular letter RWC-123.

DAILY SOLAR INDICES (A.2, A.8)

Relative Sunspot Numbers and Adjusted 2800 MHz Solar Flux -- The first table presents Zürich relative sunspot numbers, R_z , for the month. The corresponding data for eleven earlier months are reprinted to permit the trend of solar activity to be followed. On the same page is presented a similar table of twelve months of daily solar flux values at 2800 MHz adjusted to one Astronomical Unit, S_a , as reported by the Algonquin Radio Observatory (ARO) of the National Research Council near Ottawa.

Combined Sunspot Numbers and Solar Flux Values -- The next table gives several available daily indices for the month preceding that of publication. In addition to the calendar date, the table gives the day-number of the year and the day-number of the standard 27-day (solar rotation) cycle. The data presented are Zürich relative sunspot numbers, (R_z), American relative sunspot numbers, (R_A), daily solar flux values at 2800 MHz, (S), and daily solar flux values, (S_a), adjusted to 1 A.U. for 15400, 8800, 4995, 2800, 2695, 1415, 606, 410 and 245 MHz.

Graph of Sunspot Cycle and Table of Predicted and Observed Relative Sunspot Numbers -- A graph illustrates the recent trend of Cycle 20 of the 11-year sunspot cycle with predictions of the future level of activity. The customary "12-month" smoothed index, R_{12} , is used throughout, the data being final R_z numbers except for the current year.

$$R_{12} = 1/12 \left\{ \sum_{k=n-5}^{n+5} (R_k) + 1/2 (R_{n+6} + R_{n-6}) \right\} \quad \text{in which } R_k \text{ is the mean value of } R \text{ for a single}$$

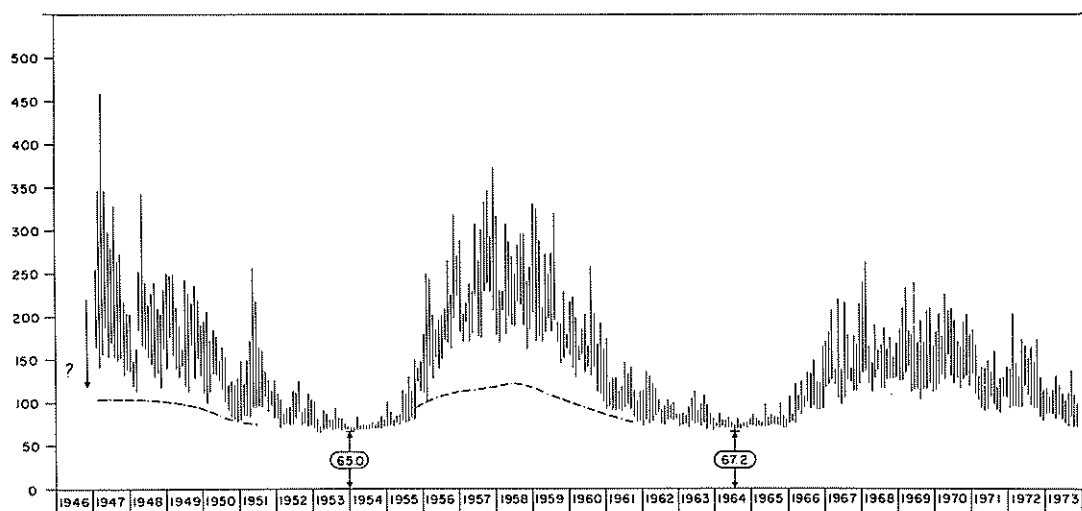
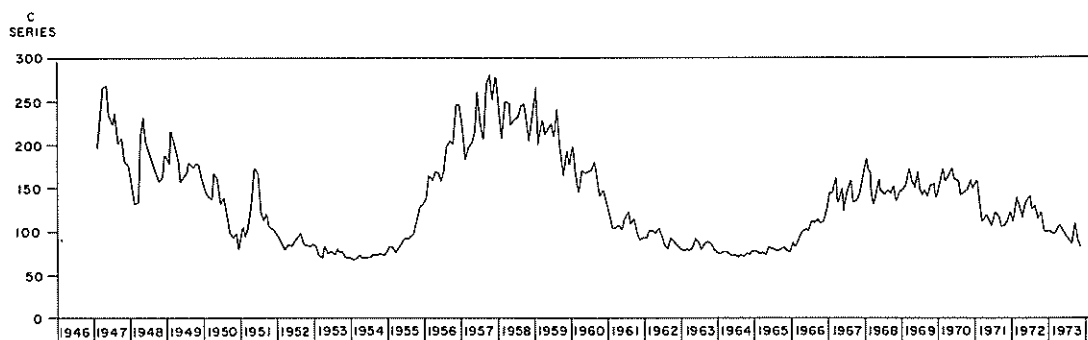
month k and R_{12} is the smoothed index for the month represented by $k = n$. Predictions shown are those made for one year after the latest available datum by the method of A. G. McNish and J. V. Lincoln [Trans. Am. Geophys. Union, 30, 673-685, 1949] modified by the use of regression coefficients and mean cycle values recomputed for Cycles 8 through 19. The last prediction made also shows the 90% prediction interval, an indication of the uncertainty above and below the predicted number. Cycle 20 began October 1964, when the minimum R of 9.6 was reached. The values of observed and predicted Zürich smoothed relative sunspot numbers are given for cycle 20 in the table. The predicted values again are based on observed data available and will change as calculated each month and new observations are included. The 90% prediction interval is shown in parentheses for each month. The observed values also appear regularly in *Ionospheric Data*, issued by the Environmental Data Service, NOAA, Boulder, Colorado 80302.

Relative Sunspot Numbers -- The relative sunspot number is an index of the activity of the entire visible disk of the sun. It is determined each day without reference to preceding days. Each isolated cluster of sunspots is termed a sunspot group and it may consist of one or a large number of distinct spots whose size can range from 10 or more square degrees of the solar surface down to the limit of resolution (e.g. 1/25 square degree). The relative sunspot number is defined as $R = K(10g + s)$, where g is the number of sunspot groups and s is the total number of distinct spots. The scale factor K (usually less than unity) depends on the observer and is intended to effect the conversion to the scale originated by Wolf. The provisional daily Zürich relative sunspot numbers, R_z , based upon observations made at Zürich and its two branch stations in Arosa and Locarno are communicated by M. Waldmeier of the Swiss Federal Observatory. The daily American relative sunspot numbers, R_A , are compiled by Casper Hossfield, for the Solar Division of the American Association of Variable Star Observers. The R_A observations for sunspot numbers are made by a rather small group of extraordinarily faithful observers, many of them amateurs, each with many years of experience. The counts are made visually with small, suitably protected telescopes.

Final values of R_z appear in the *IAU Quarterly Bulletin on Solar Activity*, these reports, and elsewhere. They usually differ slightly from the provisional values. The American numbers, R_A , being computed solely from observations made under favorable conditions selected from the reports of numerous observers, are final numbers and do not require revision.

Daily Solar Flux Values - Ottawa-ARO -- Daily observations of the 2800 MHz radio emissions which originate from the solar disk and from any active regions are made at the Algonquin Radio Observatory (ARO) of the National Research Council of Canada with a reflector 1.8 meters diameter. These are a continuation of observations which commenced in Ottawa in 1947. Numerical values of flux in the tables refer to a single calibration made near local noon at 1700 UT. When the flux changes rapidly, or there is a burst in progress at that time, the reported value is the best estimate of the undisturbed level

SOLAR RADIO FLUX, 10.7 CM
ADJUSTED TO I.A.U.



UPPER CURVE - MONTHLY MEANS OF RADIO FLUX
LOWER CURVE - MONTHLY HIGH & LOW VALUE OF SLOWLY VARYING COMPONENTS
CURVE (---) APPROXIMATELY SEPARATES SUNSPOT COMPONENT FROM BASIC COMPONENT
⊕ MAGNITUDE OF THE RADIO QUIET SUN AT SUNSPOT MINIMUM SHOWN

and provides the reference level for measuring the burst intensity. The various types of outstanding events are listed separately in another table. The observed flux values have variations resulting from the eccentric orbit of the earth in its annual path around the sun. Although these radio values are suitable to use with observed ionospheric and other data, an adjustment must be introduced when the observations are used in studies of the absolute or intrinsic variation of the solar radio flux. Thus the tables show both the observed flux, S , and the flux adjusted to 1 A.U., S_a . The observations are made for a single North-South polarization but reduced for the assumption of two equal orthogonal polarizations. Graphs showing the monthly mean adjusted flux and the monthly high and low values since 1947 are shown in this text. Relative errors over long periods of time are believed to be $\pm 2\%$, over a few days may be $\pm 0.5\%$. The characteristics of the observations are surveyed in "Solar Radio Emission at 10.7 cm" by A. E. Covington [*J. Royal Astron. Soc., Canada*, 63, 125, 1969]. Experiments conducted during the past few years indicate that a multiplying factor of 0.90 should be applied to the reported flux values in order to derive the absolute flux value. A review of the history of the absolute calibration of the Ottawa series as well as a number of other series of observations made within the microwave region has been prepared by H. Tanaka of the Research Institute of Atmospheric Physics, Nagoya University, as convener of a Working Group of Commission 5 of URSI, [H. Tanaka et al., "Absolute calibration of solar radio flux density in the microwave region," *Solar Physics*, 29, 243, 1973].

The reported correction factor includes a correction of 0.01 for the atmospheric attenuation referred to the zenith as well as the appropriate modification for the zenith angle of the sun at the times of calibrations. In data taken previously to 1966, this correction was neglected. A provisional summary of corrected daily flux values prior to 1966 has been made so that the early values may be compared on the same basis as later values. It has also been found necessary to incorporate a correction of -4% for the period July 1967 to May 1968. [ERB 790 Radio and Electrical Engineering Division, NRC.]

These solar radio noise indices are being published in accordance with a CCIR Recommendation originally from the Xth Plenary Assembly, Geneva, 1963 (maintained at Oslo, 1966 and New Delhi, 1970), which states "that the monthly-mean value of solar radio-noise flux at wavelengths near 10 cm should be adopted as the index to be used for predicting monthly median values of foE and foF1, for dates certainly up to 6, and perhaps up to 12 months ahead of the date of the last observed value of solar radio-noise flux".

Daily Solar Flux Values - AFCRL Sagamore Hill -- The Sagamore Hill Solar Radio Observatory of the Air Force Cambridge Research Laboratories (located at 42°37' 54.36"N, 70°49' 15.15"W) in 1966 began operating solar patrols at 8800, 4995, 2695, 1415, and 606 MHz. The patrol was extended to 15400 MHz in 1967, to 245 MHz in early 1969 and 410 MHz was added in early 1971. Flux calibrations are made at about meridian transit each day. All flux data are corrected to sun-earth distance of 1 A.U. Corrections are also made for atmospheric attenuation based on the following average vertical attenuations:

15400 MHz	0.085 dB	4995 MHz	0.055 dB	1415 MHz	0.05 dB
8800	0.070	2695	0.051	606	0.045

S O L A R F L A R E S (C.1)

The solar flare data from the month before that of publication are divided into two tables. The first table is restricted to the record of solar flares for which one or more observatories assigned a numerical importance of "1" or greater.* The heading is marked PARTIAL LISTING to emphasize these reports are those received at NOAA on a rapid schedule. To make the report of occurrence of flares more comprehensive, the flares reported only as subflares are listed in the second table by time of beginning in UT and coordinates only. In the section of these bulletins presenting data for the sixth month before that of publication, verification of questionable values has been attempted and in addition a separation is made between Confirmed and Unconfirmed flares.

The solar flare reports are received from throughout the world at World Data Center A for Solar-Terrestrial Physics, NOAA, Boulder, Colorado, 80302. Observations are made in the light of the center of H α line unless noted otherwise. NOAA operates the flare patrol at Boulder, and NOAA contracts support and operates the flare patrol at Culgoora. Tehran and Palehua are operated by the USAF using NOAA equipment. The USAF operates Ramey and Athens. Manila receives support from the USAF.

The columns in the table are as follows:

- reporting observatory using *IAU Quarterly Bulletin on Solar Activity* designations;
- the Universal date;
- beginning and ending times in UT;
- time of maximum phase in UT;
- the heliographic coordinates in degrees for the "center of gravity" of the emission region, corresponding to the time of maximum intensity;

* The complete provisional listings can be made available at cost through the World Data Center A for Solar-Terrestrial Physics, NOAA, Boulder, Colorado U.S.A. 80302.

- the distance from center of disk in units of the disk radius;
- McMath serial number of the associated plage region;
- the time of central meridian passage of the position of the flare in tenths of the Universal date;
- duration in minutes;
- the flare importance on the IAU scale of Sf* to 4b (see below);
- observing conditions where 1 means poor, 2 fair and 3 good;
- nature and completeness of available observations where

C^{\dagger} = a complete, or quasi complete sequence of photographs was obtained,
 P^{\dagger} = one or a few photographs of the event were obtained resulting in incomplete time coverage,
 V = all (or most of) the development of the flare was visually observed, or
 S = flare was seen visually for a small part of its probable duration;

- time of measurement for either tabulated width of $H\alpha$ to nearest $1/10\text{\AA}$ or for tabulated area;
- measured (i.e. projected) area at maximum intensity in heliographic square degrees (reported originally in millionths of disk by observatory) -- this is not necessarily the maximum area;
- corrected area in square degrees (see below);
- maximum effective line-width in $H\alpha$ to nearest $1/10\text{\AA}$;
- maximum intensity expressed in percent of the local continuum; ††
- and remarks in the IAU system of notes where

A = Eruptive prominence, base at $>90^\circ$.
 B = Probably the end of a more important flare.
 C = Invisible 10 minutes before.
 D = Brilliant point.
 E = Two or more brilliant points.
 F = Several eruptive centers.
 G = No spots visible in the neighborhood.
 H = Flare with high velocity dark surge.
 I = Very extensive active region.
 J = Plage with flare shows marked intensity variations.
 K = Several intensity maxima.
 L = Filaments show effects of sudden activation.
 M = White-light flare.

N = Continuous spectrum shows effects of polarization.
 O = Observations have been made in the calcium II lines H or K.
 P = Flare shows helium D₃ in emission.
 Q = Flare shows the Balmer continuum in emission.
 R = Marked asymmetry in $H\alpha$ line.
 S = Brightening follows disappearance of filament (same position).
 T = Region active all day.
 U = Close and somewhat parallel bright filaments (|| or Y shape).
 V = Occurrence of an explosive phase.
 W = Great increase in area after time of maximum intensity.
 X = Unusually wide $H\alpha$ emission.
 Y = Onset of a system of loop-type prominences.
 Z = Major sunspot umbra covered by flare.

The following symbols are used in the table to explain accuracy of the times reported:

D = greater than
 E = less than
 U = approximate

All times are Universal Time (UT or GCT).

The no-flare patrol observations matching the solar flare table are given in graphical form. The observatories reporting the patrols are indicated. The dark areas at the bottom half of each day are times of no cinematographic patrol. The dark areas at the top half of the day are times of neither visual nor cinematographic patrol.

The dual importance scheme used which was adopted January 1, 1966 at IAU Commission 10, is summarized in the following table:

"Corrected" area in square degrees	Relative Intensity Evaluation		
	Faint (f)	Normal (n)	Brilliant (b)
≤ 2.0	Sf	Sn	Sb
2.1 - 5.1	1f	1n	1b
5.2 - 12.4	2f	2n	2b
12.5 - 24.7	3f	3n	3b
>24.7	4f	4n	4b

* For easier visual selection of the more important flares a minus sign, "-", is used to indicate subflares instead of "S". "--" signifies the subflare has been confirmed by the NOAA grouping program but is not included in the IAU Quarterly Bulletin on Solar Activity, nor is it used in deriving the Flare Index for the day.

† Circumstances C and P can occur with any type of photographic patrol, whether automatic or not. Combinations of two symbols can be used for intermediate circumstances, example: VP = continuous visual watch plus a few photographs.

†† Catania and Anacapri-S report their intensity as referred to the local undisturbed chromosphere.

The area to be used in assigning the first figure of the dual importance, is the area of the flaring region at the time of maximum brightness. The observatory measures apparent area in millionths of the solar disk. For flares less than 65° from the center of the solar disk, the formula relating apparent and corrected area is:

$$\text{"corrected" area} = \frac{\text{apparent area}}{97} \times \sec \theta$$

where apparent area is in millionths of the disk and corrected area is in heliographic square degrees.

For flares more than 65° from the center, the "sec θ law" becomes unsatisfactory. The first importance figure can be estimated from the table below where areas are given in millionths of the disk.

Angle	0°	----	65°	70°	80°	90°
Limit S-1	200	sec θ law	90	75	50	45
Limit 1-2	500	sec θ law	280	240	180	170
Limit 2-3	1200	sec θ law	600	500	350	300

The intensity scale shown as the second importance figure is only a qualitative one where each observatory uses its experience to decide if a flare is rather faint (f), normal (n), or rather bright (b).

The table on page 11 gives the solar flare observatories presently cooperating in international data interchange through the World Data Centers originally established during the International Geophysical Year. For each observatory are given the code numbers used on the punched cards at NOAA; the four letter IAU abbreviations; name, place and country; and type of patrol where C, V and P have the meanings explained above.

Note: All the flare data are recorded on punched cards. As errata are received the punched cards are corrected. These errata are not always published in these reports. Copies of the cards, tabulations from them or magnetic tapes of the data are available at cost through the World Data Center A for Solar-Terrestrial Physics, NOAA, Boulder, Colorado U.S.A. 80302.

S O L A R R A D I O W A V E S (A.10, C.3)

Interferometric Observations -- The chart presents solar interferometric observations at 169 MHz as recorded around local noon at Nancay, France (47°23'N, 8°47'E) the field station of the Meudon Observatory.

The main lobes are parallel to the meridian plane: the half-power width is 3.8 minutes of arc in the East-West direction. The main lobes are about 1° apart [*Ann. Astroph.*, 20, 155, 1957]. The records give the strip intensity distribution from the center of the disk to 30' to the West and East.

These daily distributions are plotted on the same chart giving diagrams of evolution. Points of equal intensity given in relative units are joined day after day in the form of isophotes. Four equal intensity levels have been chosen to draw the isophotes. These intensities are proportional to 0.6, 1, 1.5 and 2. The first level corresponds to the sun without any radio storm center.

In each noisy radio region the smoothed intensity around noon is given in $10^{-22} \text{ W m}^{-2} \text{ Hz}^{-1}$.

East-West Solar Scans -- Algonquin 10.7 cm -- East-West solar scans at 10.7 cm are taken daily at the Algonquin Radio Observatory of the National Research Council of Canada (N 45°56'43", W 78°3'33").

The antenna consists of an array of 32 3-meter paraboloids having interference fringes separated by approximately 1°. The zero order fringe on the meridian (where most of the published curves are taken) has an east-west width of 1.5', but the width increases to 1.7' for fringes 30° from the meridian. The antennas are kept fixed during each drift curve to avoid changes in sensitivity due to scanning and an effort is made to maintain a constant sensitivity from one day to another. When necessary, however, the receiver gain is adjusted to accommodate large fluxes. (Antenna specification can be found in *Solar Phys.*, 1, 465-473, 1967 and details of the antenna performance appear in *Astron. J.*, 73, 749-755, 1968.)

The position of the limbs of the photosphere are indicated on each curve by the vertical bars at the ends of the horizontal line, which itself represents the cold sky level. The estimated level of the quiet sun, shown at the center of the photosphere, is based on an assumed quiet sun of 60 solar flux units (one solar flux unit = $10^{-22} \text{ W m}^{-2} \text{ Hz}^{-1}$). This level is determined for each curve by comparing the area under the curve with the total solar flux at 10.7 cm. (Prior to December 1968 the quiet sun level

SOLAR FLARE OBSERVATORIES

COMPUTER CODE NO.	OBS. TYPE	I.A.U. ABBREV.	NAME, PLACE AND COUNTRY
824	C	ABST	ABASTUMANI, GEORGIAN SSR
512	VP	ARCE	ARCETRI, FLORENCE, ITALY
521	VP	AROS	AROSA, SWITZERLAND
508	VC	ATHN	NATL OBS., ATHENS, GREECE
647	VC	BOUL	BOULDER, COLORADO, USA
560	VC	BUCA	NATL OBS., BUCHAREST, ROMANIA
557	VC	CANR	GRAN CANARIA, CANARY ISLANDS
506	VP	CAPF	ANACAPRI, ITALY (GERMAN)
519	VP	CAPS	ANACAPRI, ITALY (SWEDISH)
570	VC	CATA	CATANIA, ITALY
826	C	CRIM	SIMFIS, CRIMEA, USSR
403	VC	CRON	CARNARVON, AUSTRALIA
402	C	CULG	CULGOORA, AUSTRALIA
478	C	HALE	HALEAKALA, MAUI, HAWAII, USA
537	VP	HERS	R. GREENWICH OBS., HERSTMONCEUX, ENGLAND
563	C	HTPR	HAUTE-PROVENCE, FRANCE
718	C	HUAN	GEOPHYSICAL INST., HUANCAYO, PERU
358	V	ISTA	UNIV. OBS., ISTANBOUL, TURKEY
827	VP	KHAR	KHARKOV, UKRAINIAN SSR
828	C	KIEV	KIEV, GAO, UKRAINIAN SSR
309	V	KODA	KODAIKANAL, INDIA
522	VP	LOCA	LOCARNO, SWITZERLAND
876	C	LVOV	LVOV, UKRAINIAN SSR
468	VC	MANI	MANILA, PHILIPPINES
642	C	MCMA	MCMATH-HULBERT, PONTIAC, MICHIGAN, USA
505	C	MEUD	MEUDON, FRANCE
314	C	MITK	MITAKA, TOKYO, JAPAN
555	C	MONT	MONT MARIO OBS., ROME, ITALY
504	V	ONDR	ONDREJOV, PRAGUE, CZECHOSLOVAKIA
476	VC	PALE	PALEHUA, HAWAII, USA
648	VC	RAMY	RAMEY SOLAR OBSERVATORY, RAMEY AFB, PUERTO RICO
862	VP	SIBE	SIBERIE (SIBERIAN IZMIR), IRKUTSK, USSR
823	VC	TACH	TACHKENT, UZBECK SSR
341	VP	TFHR	TEHRAN, IRAN
514	C	UPIC	UPICE, CZECHOSLOVAKIA
834	VC	VORO	VOROSHILOV, USSR
546	VP	WEND	WENDELSTEIN, GFR
523	PC	ZURI	EIDGENOSSISCHE STERNWART, ZURICH, SWITZERLAND

was estimated each day from a calibrating noise signal inserted between the antenna and receiver. The present method was begun in December 1968 when it was discovered that the quiet sun levels shown for September and October 1968 were approximately 8% too low.)

East-west scans with 30 seconds of arc resolution (recorded simultaneously with the 1.5 minute scans) have been taken at selected intervals between 1969 and November 1971. Commencing November 1, 1971 they have been obtained on a routine basis along with circular polarization data. These data have not been included in the monthly summaries but can be made available on request.

East-West Solar Scans -- Fleurs 21 cm and 43 cm -- East-West strip scans of the sun at 21 cm and 43 cm are made possible by the "Fleurs" Radio Astronomy Station of the University of Sydney, Sydney, Australia.

For the East-West solar scans from the 21 cm solar radio array the fan-beam has 2' of arc resolution. The two short horizontal lines drawn crossing the center line indicate the cold-sky level and the estimated quiet-sun level. The gain may differ from day to day. The curves have not been normalized to account for these gain variations otherwise than by the indication of the estimated quiet-sun level.

For the East-West solar scans from the 43 cm solar radio array the fan beam has a resolution of 4' of arc. The estimated quiet sun is indicated on the published profiles in the same manner as for the 21 cm scans. The curves have not been normalized for variations in gain.

Outstanding Occurrences (SELECTED) -- A list of SELECTED centimeter and millimeter wavelength events at fixed frequencies is published one month following observation. Selections are made to provide 24-hour coverage as nearly as possible. See page 45, Outstanding Occurrences, for descriptions of the types of events and observatory characteristics.

S O L A R W I N D M E A S U R E M E N T S (A.13)

Pioneers 6,7,8 and 9 -- The NASA Ames Research Center plasma probe solar wind velocity data from Pioneers 6 through 9 are supplied by John H. Wolfe. These data include the date, the Deep Space Network (DSN) coverage period, the observation time in UT, the solar wind bulk velocity, U_{H+} , in kilometers/second, the density, N_{H+} , in particles/cubic centimeter, the temperature, T_{H+} , in millions of degrees Kelvin, the Earth-Sun-Probe (ESP) angle in degrees and the co-rotation delay time in days.

The U_{H+} , the N_{H+} and the T_{H+} are derived by a least squares computer fit of the solar wind energy distribution to a Maxwell-Boltzmann distribution in a moving frame of reference. The velocity represents the bulk or convective velocity of the solar wind.

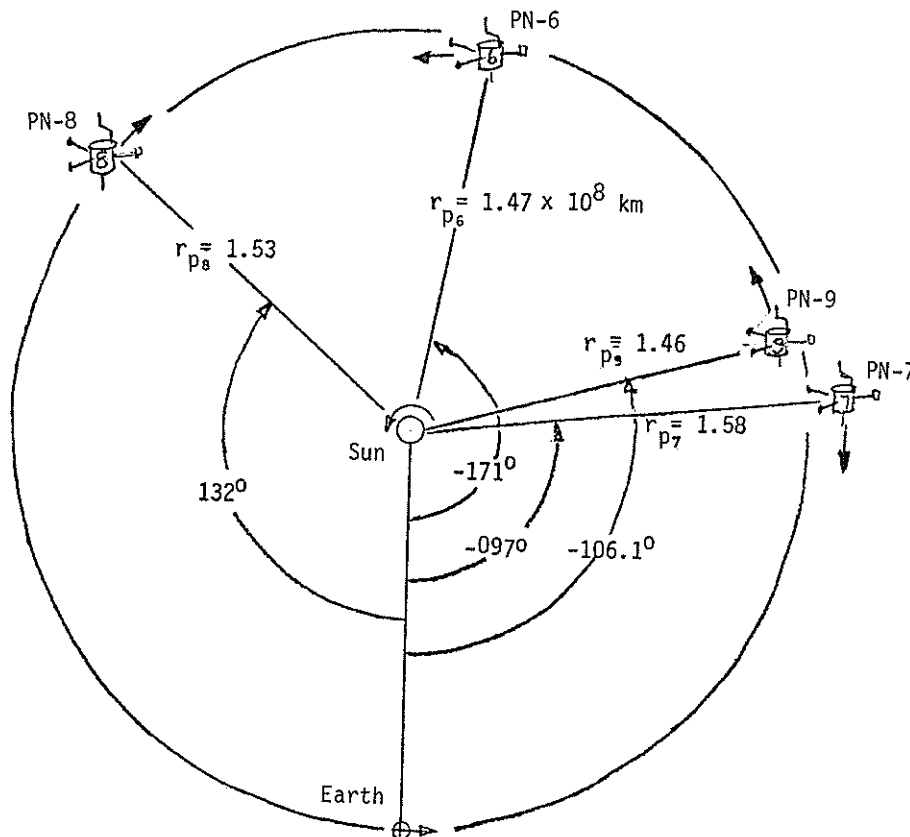
The co-rotation delay, τ , is defined as the time in days required for a steady state solar co-rotating plasma beam to rotate from the spacecraft to earth. A diagram showing the angular positions of Pioneers 6 through 9 with respect to the earth is on page 12. Viewing from the North Ecliptic Pole onto the Ecliptic plane, note that Pioneer 8 is lagging the earth and therefore the τ is positive. Pioneers 6, 7 and 9 are leading the earth and therefore their τ is negative. The co-rotation delay depends on the heliocentric radial distance of the earth and the spacecraft, the angular separation between the earth and the spacecraft, the solar angular velocity and the solar wind bulk velocity which defines the degree of the hose angle of the co-rotating Interplanetary Magnetic Field.

The equation used to compute the co-rotation delay, τ , follows:

$$\tau(\text{in seconds}) = \phi/\omega - (r_p - r_e)/U_{H+}$$

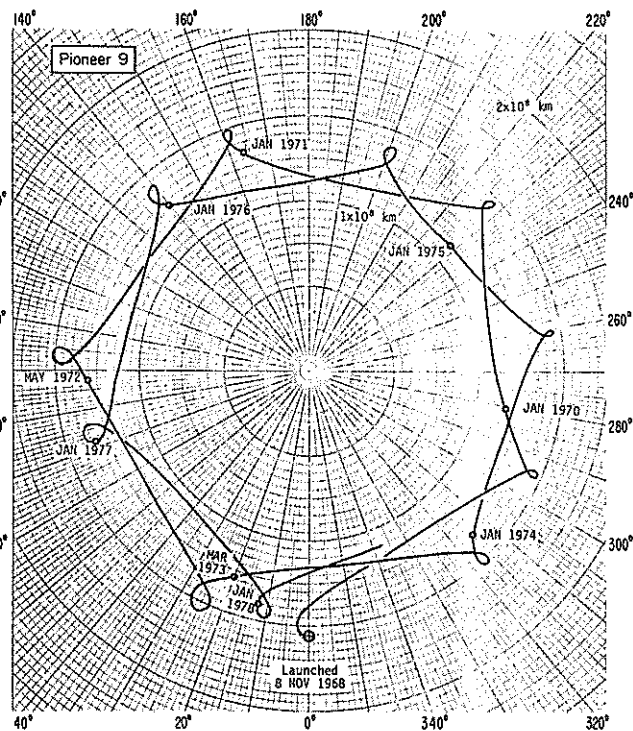
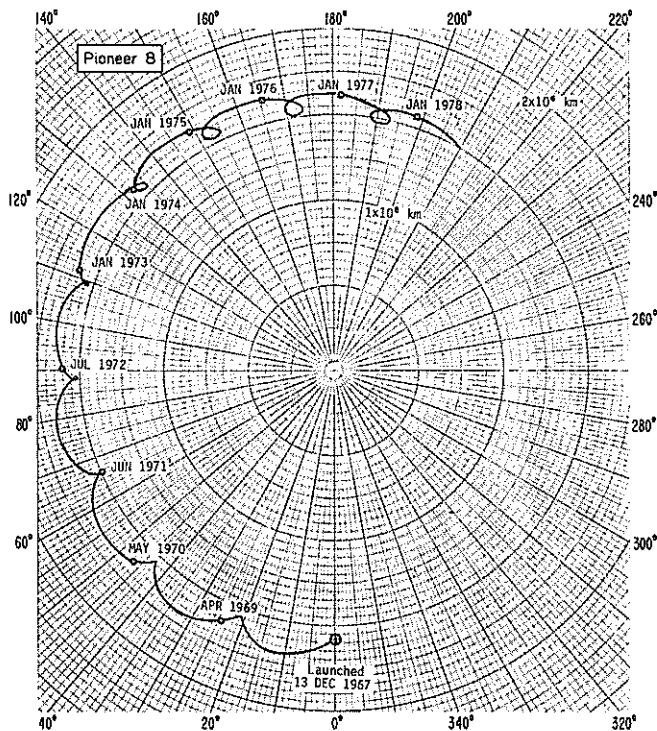
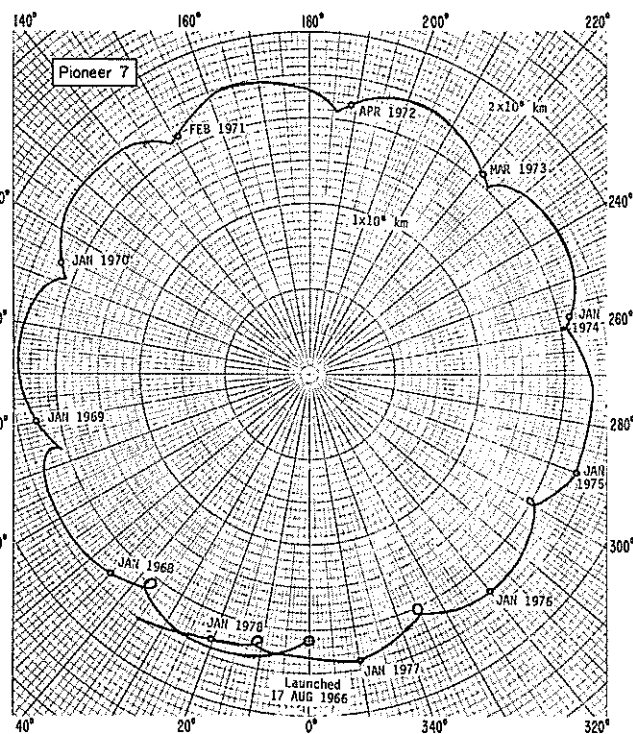
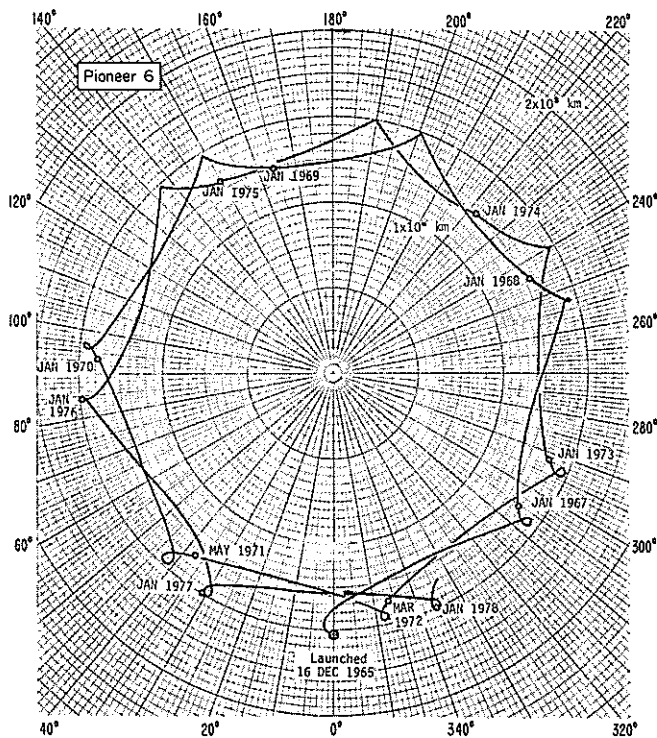
where ω is the angular velocity of the sun (in radians/second) corresponding to a 27 day solar synodical rotation period, and ϕ is the Earth-Sun-Probe angle (in radians).

Instead of using the solar equatorial projection of the Earth-Sun-Probe (ESP) angle ϕ' , the ESP angle itself, ϕ , is used. The error caused by this substitution can be no more than approximately 0.008 radians (0.5°), as explained in the following paragraphs.



Locations of Pioneers 6 through 9 on 1 Jul 74 in the Ecliptic Plane relative to the Earth (in a fixed Sun-Earth line plot) as viewed from the North Ecliptic Pole.

4



The above diagrams illustrate the position of Pioneers 6, 7, 8 and 9. Several types of observations are reported from these spacecraft as discussed in the accompanying descriptions.

Because the solar equatorial plane is inclined approximately 7.25° to the ecliptic plane, and also the ESP angles for the Pioneers are all very nearly in the ecliptic plane, the projection of the ESP angle in the solar equatorial plane, ϕ' , can be related to the ESP angle, ϕ , as follows: Define ϕ as $\alpha_2 - \alpha_1$. α_2 is the angle in the ecliptic plane of the Earth from the "northern crossing" side of the line defined by the intersection of the ecliptic plane and the solar equatorial plane. The "northern crossing" side of this line is the side where the Earth crosses into the space to the north of the equatorial plane from the space to the south as it circles the Sun. α_1 is similarly defined for the Pioneer spacecraft. Then ϕ' (the projection of the ESP angle, ϕ , in the solar equatorial plane) can be expressed:

$$\phi' = \tan^{-1}(\cos 7.25^\circ \tan \alpha_2) - \tan^{-1}(\cos 7.25^\circ \tan \alpha_1)$$

$$\text{or } \phi' = \tan^{-1}(0.9925 \tan \alpha_2) - \tan^{-1}(0.9925 \tan \alpha_1)$$

A difference of approximately 0.008 radians (0.5°) between ϕ' and ϕ occurs when $\alpha_2 = 45^\circ$ and $\alpha_1 = 135^\circ$ (or vice versa). The difference is less than 0.50 for other combinations of α_2 and α_1 . Hence using ϕ rather than ϕ' is sufficiently accurate for the purposes of these calculations.

Pioneers 6 and 7 -- The MIT plasma experiment on the Pioneer 6 and 7 spacecraft analyses the positive ion components of the solar wind by measuring particle fluxes in 14 contiguous energy/charge channels extending from 75 to 9500 ev. These data are supplied by A. J. Lazarus.

Wind Speed, U_p -- The preliminary estimate of the convected speed of the proton component of the solar wind is an average speed obtained by using the mean speed of each energy channel to determine the number density of protons contributing flux to that channel. The average speed is then determined by weighting the mean speed of each channel by the fraction of the total number density contributing to the flux in that channel. The averaging is carried out up to an energy/charge at which alpha particle fluxes begin to become important.

Number Density, N_p -- The observed total proton flux is compared to the flux expected from an isotropic Maxwellian distribution with a most probable thermal speed of 40 km/sec, a number density of 1 proton/cc, and convected with the observed speed. The number density at the point of observation is the ratio of the observed to the calculated total proton flux. The tabular value of the number density has been extrapolated to 1 A.U. by assuming an inverse square dependence on radial distance from the sun.

Detailed analysis of the data indicates that these early values of wind speed and number density have approximate precisions of ± 10 km/sec for U_p and $\pm 10\%$ for N_p . The tabular values are averages starting at the indicated times, of the few samples available on a quick-look basis. The standard deviation, σ , is given for speed and number density unless only one observation is available for that time period.

Predicted Earth Arrival Time -- We calculate the time at which the solar wind would be expected to arrive at the vicinity of the earth by assuming that the plasma was emitted radially from a point on the sun, that the sun rotates with a synodic period of 27 days, and that the plasma moves radially with a constant convective speed U_p .

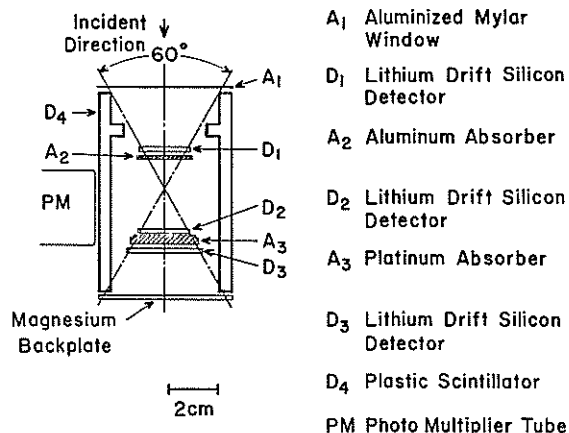
SOLAR PROTON MONITORING (A.12)

Pioneer 6 -- These data are provided by Professor J. A. Simpson and his coworkers at the University of Chicago. Cosmic-ray particle counting rates are provided for three ascending energy ranges, from 0.6 to >175 Mev/nucleon. Counting rate measurements are made by the University of Chicago cosmic ray telescopes aboard Pioneer 6. These are supplied, when possible, both at the beginning and at the end of each tracking pass.

Both instruments consist of a stack of three solid-state detectors separated by absorbers, surrounded by an anti-coincidence cylinder. The Figure shows a cross-section view of the particle telescope.

Counting rates are provided for the coincidence modes $D_1 \bar{D}_2 \bar{D}_4$ (protons and helium nuclei 0.6-13 Mev/nucleon, electrons 400-700 kev), $D_1 D_2 \bar{D}_4$ (protons 13-175 Mev, helium nuclei >13 Mev/nucleon and $\bar{D}_1 \bar{D}_2 D_3 \bar{D}_4$ (proton >175 Mev). The geometrical factors for the three coincidence modes are 5.4, 0.92, and 0.5-1.65 (see below) $\text{cm}^2\text{-ster}$, respectively. At energies above ~ 200 Mev, the last two coincidence modes become bidirectional. A detailed description of the telescope and the related electronics may be found in Fan et al. [*J. Geophys. Res.*, 73, 1552-1582, 1968] and Retzler and Simpson [*J. Geophys. Res.*, 74, 2149-2160, 1969].

The counting rates are prepared from quick-look data, and are subject to future revision when the final data tapes reach the University of Chicago. Times given are only approximate, (time accurate to ± 15 minutes), and the counting rates are accurate to $\sim 10\%$. When one of the two high-energy counting



Pioneer 6/7 Cosmic Ray Telescope

rates is at the quiescent level, a symbol Q is used instead of the actual rate. For the 0.6-13 Mev proton counting rate, the quiescent level is approximately 0.08-0.15 c/s. The two highest ranges exhibit a pronounced variation of the quiescent level with the solar cycle.

Pioneers 8 and 9 -- The cosmic ray proton count rates as observed on Pioneers 8 and 9 are provided through the cooperation of Dr. W. R. Webber and Dr. J. Lezniak of the University of New Hampshire.

Quick look data from telescopes "5" and "1+2" are supplied.

Telescope 5 is a wide angle, two element solid state telescope with an energy threshold of 14 Mev for protons and 0.6 Mev for electrons. The geometric factor is approximately 8.3 cm²-sterad during quiet times and 4.2 cm²-sterad during solar flare times.

Telescope 1+2 is a narrow-angle, five-element, solid-state telescope with a proton energy threshold of 64 Mev on Pioneer 8 and 42 Mev on Pioneer 9. The geometric factor of this telescope is 2.35 cm²-sterad.

INTERPLANETARY MAGNETIC AND ELECTRIC FIELDS (A.17, A.17a, A.18)

Pioneer 8 -- The Interplanetary (IP) Magnetic Field data from the NASA-Goddard Space Flight Center magnetometer on Pioneer 8 are being supplied by Franco Mariani of the University of Roma and N. F. Ness of Goddard. The data supplied are the absolute magnitude, /B/, (in gammas) and the solar ecliptic longitude, ϕ , (in degrees) of the field measured counterclockwise from the spacecraft-sun line, as viewed from the North Ecliptic Pole.

The instrument is a mono-axial fluxgate magnetometer. The sensor is mounted on one of three transverse booms 2.1 meters from the spin axis and at an angle of 54°45' to the spin axis.

Three samples are taken at equal intervals during one spacecraft rotation yielding three independent mutually orthogonal measurements defining the total vector magnetic field. The magnetometer incorporates an automatic inflight range switch between two dynamic range scales of ± 32 and ± 96 gammas for a resolution of ± 0.125 and ± 0.375 gammas. The accuracy of the instrument is limited by spacecraft associated magnetic fields and the sensor zero drift. A non-magnetic explosive-actuated indexing device is used to re-orient the fluxgate by 180° to establish its zero level.

Five bit rates are possible: 512, 256, 64, 16 and 8 bits/second. At the three higher rates, the average time interval between successive determinations of the field vector is 1.3, 1.4 and 1.75 seconds, respectively. A special purpose digital computer is included in the instrument to compute time averages of the field components when the spacecraft is operating at the low bit rates of 16 and 8.

The data supplied include the date, the Deep Space Network (DSN) coverage period, the observation time in UT, the magnitude and solar ecliptic longitude of the field, as described above.

The magnetic field data are sampled approximately every hour. Each hourly sample is an average over three consecutive vectors which are separated by 14 seconds or less, depending on the spacecraft bit rate.

The IP sector structure at the Pioneer 8 position can be inferred from the longitudinal angle: angles between 45 and 225 degrees are associated with outward sectors, and the remaining angles with inward sectors. It is recognized, however, that the field direction, at the time of observation, may not adequately represent the direction over a period of hours.

Pioneer 9 -- The Interplanetary (IP) Magnetic Field data from the NASA Ames Research Center magnetometer on Pioneer 9 are being supplied by Chas. P. Sonett and Davis S. Colburn. The data supplied are the magnitude, B , of the field in gammas and the solar ecliptic longitude, ϕ , of the field in degrees, measured from the spacecraft-sun line in a counterclockwise direction, as viewed from the North Ecliptic Pole. The instrument is a triaxial fluxgate magnetometer with onboard spin demodulation and use of appropriate filters to avoid aliasing errors. The filter time constant is adjusted to be proportional to the sampling interval. The sampling interval is 0.292, 0.583, 2.33, 9.33 and 18.7 seconds for 512, 256, 64, 16 and 8 bps, respectively. The digitization uncertainty in each component of the field is ± 0.2 gammas. The quick-look data are not corrected for sensor off-set in the component along the spin axis of the spacecraft. This, in general, gives an uncertainty in the field magnitude of less than one (1) gamma and does not affect the determination of the longitude, ϕ .

The data supplied include the date, the Deep Space Network (DSN) coverage period, the observation time in UT, the field magnitude and its solar ecliptic longitude, as described above.

The magnetic field data are sampled approximately every hour. Each hourly sample is an average over three consecutive vectors which are separated by 18.7 seconds or less, depending on the spacecraft bit rate.

The IP sector structure at the Pioneer 9 spacecraft can be inferred from the longitudinal angle: angles between 45 and 225 degrees are associated with outward sectors, and the remaining angles with inward sectors. It is recognized, however, that the field direction, at the time of observation may not adequately represent the direction over a period of hours.

Pioneers 8 and 9 -- The Interplanetary (IP) Electric Field data, as observed on Pioneers 8 and 9 on a real time basis, are provided through the cooperation of Dr. F. L. Scarf from the Space Sciences Department of the TRW Group. These IP Very Low Frequency (VLF) wave data consist of a sequence of narrow-band (400 Hz) signal amplitudes.

The table presents the date and Universal Time (UT) when the Electric Field Potential amplitudes (in millivolts) were read. The pass number indicates the total number of times, since launch, that each spacecraft has passed over the particular Deep Space Network tracking station at the observation time noted.

The real time 400 Hz data are selected to illustrate or characterize the activity during each pass and are being presented so that interested scientists can:

1. Attempt to correlate terrestrially-observed phenomena with variations noted in the IP Electric Field intensities at the spacecraft position.
2. Have access to simultaneous measurements of Plasma and E-field data on each spacecraft.
3. Study Solar Wind fluctuations and magnetic sectoring with the E- and B-field data on Pioneer 9.

Instrumental details of the Electric Field experiments are available in the following references: Pioneer 8: *J. Geophys. Res.*, 73, 6655, 1968 and Pioneer 9: *Cosmic Electrodynamics*, 1, 496, 1970.

I N F E R R E D I N T E R P L A N E T A R Y M A G N E T I C F I E L D

The table shows daily inferences of the polarity of the interplanetary magnetic field made from magnetograms produced by magnetometers at the Vostok Antarctic Station of the USSR and the Thule Geopole Station of the U.S. Air Weather Service. The inference relies on the discoveries of Mansurov [*Geomagn. Aeron.*, 9, 622-623, 1969] and Svalgaard [*Geophys. Pap. R-6*, 11 pp., Dan. Meteorol. Inst., Copenhagen, 1968] relating the variation of the polar cap magnetic field to the polarity of the interplanetary field. It was originally believed that the radial component (B_{XM} in Geocentric Solar Magnetospheric coordinate system) of the IP field determined the effect observed in the polar cap field, but recent evidence [Friis-Christensen, et al., *J. Geophys. Res.*, 77, 371, 1972] indicates the responsible component may be

BYM, the component in the ecliptic plane perpendicular to BXM. As long as the IP field remains in a normal Archimedes spiral, the variation in sign of BYM maps one-to-one with the variation in sign of BXM. The notation adapted for the table is that $BXM > 0$ ($BYM < 0$) is represented by the symbol A (away from the sun) and $BXM < 0$ ($BYM > 0$) is represented by the symbol T (toward the sun).

The effect is visible at Vostok in the first half of the Greenwich Universal Day and at Thule in the second half of the day. The inferences from Vostok are made at the Institute for Terrestrial Magnetism, Ionosphere and Radiowave Propagation (IZMIRAN), Moscow and are shown in the table as the first value (or set of values) each day. The inferences from Thule are made at the Space Environment Services Center, Boulder and shown as the second value (or set of values) each day. If two values are shown for a half day period, an apparent change of polarity occurred within that half day.

An asterisk along with an A or T indicates half-days when the effect was somewhat doubtful, but one polarity seemed predominant. An asterisk alone indicates half-days when no clear polarity effect could be discerned. A dash indicates half-days when missing data prevented inference of the polarity.

S O L A R P R O T O N E V E N T S

An unnumbered page with a diagonal slash across it will be included whenever provisional outstanding solar proton events have been reported during the month before month of publication. This will be prepared by the Space Environment Services Center of the Space Environment Laboratory. These sheets will be self-explanatory and are not to be used for research reference purposes, but are to be discarded when definitive data are published. They will merely provide some of the immediately available evidence when significant solar proton events have occurred in the previous month.

DATA FOR TWO MONTHS BEFORE MONTH OF PUBLICATION

TABLE OF CONTENTS

	<u>Page</u>
<u>Daily Solar Activity Centers</u>	
A.6 H α Synoptic Charts	20
Daily Charts Including:	
A.11f X-ray Spectroheliograms	20
A.9c 8.6 mm Spectroheliograms	21
A.3a Magnetograms	21
A.5 Calcium Plages	22
A.4 Daily H α Spectroheliograms	22
A.1 Daily Sunspot Drawings	22
A.6 H α Prominences	22
A.7b λ 5303Å Coronal Intensities	22
A.7c White-Light Corona	23
A.7d Solar EUV Spectroheliograms	23
A.7e NRL Solar XUV Coronagraphs	24
A.5a Individual Regions of Solar Activity Combining Calcium Plages, and Sunspots	24
A.5b Daily Calcium Indices	27
<u>Solar X-Ray Radiation</u>	
C.5,A.11 Daily/Hourly Averages and Outstanding Events	28
<u>Sudden Ionospheric Disturbances</u>	
C.6 SID Events	28
<u>Solar Radio Waves</u>	
C.4 Spectral Observations	32
C.3t 43.25, 80 and 160 MHz Selected Bursts	35
<u>Cosmic Rays</u>	
F.1 Table of Daily Average Neutron Counting Rates per Hour	35
F.1 Chart of Variations	37
<u>Geomagnetic Activity</u>	
D.1a Table of Indices Kp, Ci, Cp, Ap, aa	37
D.1ba Musical-note 27-day Recurrence Diagram	38
D.1 Daily Ap for Past Year	38
D.1g Table of Hourly Equatorial Dst Index	38
D.1d Principle Magnetic Storms	38
D.1f Sudden Commencements and Solar Flare Effects	39
<u>Radio Propagation Indices</u>	
B.51ca North Atlantic Quality Figures and Forecasts	39
B.52 Transmission Frequency Ranges - North Atlantic Path	40
G.53 Quality Indices on Transmissions from Canada to Germany	40

S O L A R A C T I V I T Y C E N T E R S
(A.1, A.3a, A.4, A.5, A.5a, A.5b, A.6, A.7, A.9c, A.11f)

H-alpha Synoptic Charts -- These charts of the entire solar surface show solar activity in terms of polarity of magnetic fields, filaments (cross-hatched), major sunspots (large dots), H-alpha plage (stipple), distinct neutral lines (solid lines), and estimated neutral lines (dashed lines).

Heliographic latitude is plotted vertically and solar longitude horizontally. Longitude is in terms of the mean rotation rate for sunspots (Carrington longitude). The dates when these longitudes pass the sun's central meridian appear at the top of the charts.

The charts are labeled with the serial number of the solar rotation as counted by Carrington, with the first rotation commencing November 9, 1853.

The positions of magnetic polarity reversal are inferred according to the techniques described by McIntosh [*Rev. Geophys. and Space Phys.*, 11, 837-846, 1972] and [*Solar Activity Observations and Predictions*, McIntosh and Dryer, ed., MIT Press, 1972]. The H-alpha structures that reveal these "neutral" lines are: filaments, filament channels, plage corridors, "iron-filing" pattern of fibrils adjacent to active centers, and arch-filament systems. The patterns are mapped by accumulating the positions of features on H-alpha filtergrams from several consecutive days. Seldom does a single photograph show the patterns in their complete form, owing to the transient nature of the filaments and the variable observing conditions.

Magnetic polarities are inferred from Hale's law: leader sunspots in opposite solar hemispheres have opposite polarities. Northern leaders possess negative polarity during even-numbered solar cycles, while southern leaders are positive. The current solar cycle is #20. The polarity rules will reverse with the first active centers of Cycle #21. The polarities of all areas on the sun are inferred by beginning with a leader sunspot, or the leading portion of a bipolar plage, and alternating polarities with each successive neutral line.

The H-alpha patterns mapped are the forms seen when the particular features were near W40 on the visible solar hemisphere. This bias toward the west enables a more realistic comparison with solar wind, particle, and magnetic-field data measured near the earth. Whenever a pattern undergoes a conspicuous change from the time of first visibility to the time when at W40, the former neutral-line position is depicted as a line with dots superimposed.

The charts published here are preliminary versions constructed as part of the real-time solar monitoring at NOAA's Space Environment Services Center in Boulder. In most cases, there has been corroboration with solar magnetograms made with photospheric spectral lines (Kitt Peak, Mt. Wilson, and Sacramento Peak). Some changes and additions will be necessary when more careful study of the filtergrams and magnetic-field data can be made. The date in the lower right corner is the date of last revision.

The mapping techniques include comparison with previous synoptic charts for maintenance of consistency and continuity. Constant use of the inferred magnetic-field data since 1967 has demonstrated their 90% accuracy when compared with magnetograph data.

Photographs or Charts -- On two pages per day are presented several photographs or charts of active solar centers recorded at optical and radio wavelengths. For each day the Carrington longitude, Lo, at 0000 UT, position angle, P, and center of sun, Bo, are given. Transparent Stonyhurst disks (regular or modified) are provided with this text to fit the size of the charts. Regular Stonyhurst disks have the longitude lines spaced in intervals of 10° east and west of central meridian. Modified Stonyhurst disks have the longitude lines spaced at days east and west of central meridian. With the 1973 Descriptive Text the large size transparencies were regular and the small size were modified. In this issue the large ones are modified and the small regular. Though a magnifying glass is needed to read detail, it is felt that the significant regions stand out on the scale used. *For those interested, larger sizes of these photographs or charts can be made available at cost through the World Data Center A for Solar-Terrestrial Physics.*

These data for each day are x-ray spectroheliograms; 8.6 mm spectroheliograms; solar magnetograms; calcium plage and sunspot tracings; H α filtergrams; white light, XUV and EUV spectroheliograms. The sunspot drawing also shows prominences and green line corona.

Details of these individual observations follow:

X-ray Spectroheliograms from OSO-7 -- The x-ray maps from the Goddard x-ray and EUV spectroheliograph on OSO-7 are now being published to replace those made by the University College London-Leicester University instrument on OSO-5, which ceased supplying data by the end of November 1972. OSO-7 began operations on 3 October 1971, so there is ample overlap in the two sets of maps to allow detailed comparisons between them, and thus long-term studies can continue without interruption.

The OSO-7 x-ray maps are made in the same "Large Raster" mode as that described in connection with the GSFC EUV map also published here. (See page 23.)

Each map has an overall field of view of about 60 arcmin on a side and is produced by a series of 64 consecutive parallel sweeps of the instrument package, each sweep tracing a line 60 arcmin long and spaced 57 arcsec from the previous line. The aperture of the x-ray spectroheliograph is nominally 20 x 20 arcsec (FWHM), as defined by a set of mechanical grid collimators. However, the effective resolution in the sweep direction is actually 75 arcsec due to the motion of the instrument package along the raster line during one data accumulation interval. (This sweep direction is identical to the TV scan direction labelled on the NRL OSO-7 pictures of the white-light corona.) Furthermore, since the line spacing is larger than the collimator response, there are strips 37 arcsec wide between raster lines which are missed by the x-ray detector. These two effects may cause some distortion of intensities of highly localized regions.

It takes 8.2 minutes to produce one full Large Raster; the time listed beside each map refers to the mid-point of the observation period. Each contour represents a factor of 2 increase in the detector response and is labelled in arbitrary units directly proportional to the surface brightness of the corona. The detector itself is a proportional counter which responds to radiation between 8 and 16Å. In this wavelength interval, the emission arises primarily from lines due to Mg XI, Mg XII, and Fe XVII ions; all of which are produced most efficiently at temperatures above 4×10^6 K. Therefore, these x-ray maps show only the hot components of the coronal enhancements overlying active regions. The position of the solar limb is derived from an H α monitor in the instrument and should be correct to 1 arcmin. Solar north is always located at the top of each map.

Specific quantities tabulated on each map include:

- Count: The output of the detector summed over the entire raster.
- Roll: The angle between ecliptic north and the perpendicular to the sweep direction, projected on the plane of the sky.
- P-TH: The angle between ecliptic north and solar north, projected on the plane of the sky.

The OSO-7 sweep direction is at an angle of Roll + (P-TH) -90° clockwise from solar north.

The tape recorder on OSO-7 failed in mid-May 1973. Some of EUV and x-ray maps are incomplete because the periods of direct contact with a tracking station is of short duration. The total counts given may also be low because of the incomplete coverage or high because of added background noise levels. The spacecraft is predicted to re-enter the earth's atmosphere in the summer of 1974.

Goddard experimenters making these observations from OSO-7 are Werner M. Neupert, Roger J. Thomas and Robert D. Chapman.

8.6 mm Spectroheliograms -- The 8.6 mm Solar Radio Mapping program is conducted at the AFCRL, Prospect Hill Radio Observatory, Waltham, Massachusetts. The geographic coordinates of the observation site are: latitude 42°23'18.6"N, longitude 71°15'16.8"W. The project is funded in part by the Laboratory Director's Fund.

The objective of the program is to study solar active regions by observing the physical phenomena associated with sunspots and solar flares at a wavelength of 8.6 mm. The flux on each map is calculated and is not corrected to 1 A.U. The contours on the maps are in 200°K intervals beginning at 4400°. These maps do not extend to the sun's limb. The data are presented in heliographic coordinates.

The 8.6 mm wavelength solar radio maps are collected between 0900 and 1300 hours local time each day, weather permitting. The antenna used for the solar observations is an elevation over azimuth mounted 29 foot circular paraboloid with a Cassegrain feed. The surface of the dish is made up of 30 honeycomb panels with aluminum skin and the secondary reflector is a 2 foot circular hyperboloid of solid spun aluminum. The antenna was designed to operate at 35 GHz with a gain: $66.5 \pm .5$ dB, a half power beamwidth: 0.07°, first side lobes: -18 dB, all side lobes beyond 1° cone: -55 dB and a pointing accuracy: $\pm .015^\circ$. The radiometer is a standard "Dicke" load comparison type operating at 34.5 to 35.5 GHz with an IF frequency of 131 MHz, a 3 dB noise bandwidth of 26 MHz, a switch rate of 97 Hz and integration time of 1 second.

Principal Investigators for the project are Mr. Vincent J. Falcone, Jr., Mr. Paul M. Kalaghan, and Mr. Larry E. Telford.

Magnetograms -- The Mount Wilson Observatory solar magnetograms are computer-plotter iso-gauss drawings. The polarities are indicated. "Plus" signifies the magnetic vector pointed toward the observer. The gauss levels are indicated. The observations are made with the magnetograph at the 150-foot tower telescope on Mount Wilson. The program is supported in part by the Office of Naval Research and the National Aeronautics and Space Administration. This instrument measures the longitudinal component of the magnetic field using the line $\lambda 5250.216$ Fe I. A solar magnetograph is basically a flux measuring instrument. It measures the total flux over the aperture which is being used. The magnetograph apertures are square (image slicer is used) and the raster scan lines are separated by the dimension of the aperture. This separation of the scan lines is given by the ΔY (DELTA Y) printed on the magnetogram. The units of ΔY are arc seconds. The DELTAX represents in the same units the distance along the scan line between points at which the data were digitized.

The scan is a boustrophedonic raster scan which extends for all scan lines beyond the disk. The data within about 12 arc seconds of the solar limb are not plotted. The scanning system is always oriented so that the scan lines are perpendicular to the central meridian of the sun. The cardinal points on the magnetogram refer to heliocentric coordinates so that the "N" and "S" define the rotation axis of the sun.

Because the magnetic field strength measured by the magnetograph is the product of the true field strength and the brightness of the image, the fields used to make the contours have been corrected for the brightness at each point. So effects of limb darkening and variable sky transparency have been corrected.

Effects due to weakening of the line profile in magnetic field regions have not been accounted for. In general the magnetic field strengths on the map are low by about a factor two because of these effects, but this varies somewhat with distances from the disk's center. For more details c.f. *Solar Physics*, 22, 402-417, 1972.

A number of errors can still be present. One of the most common of these is the zero setting of the magnetograph. At times there may be an obvious bias of the field over the whole disk toward one or the other polarity. This will tend to show very weak features of one polarity more readily than those of the other polarity. Occasionally for one reason or another a scan line may be skipped. In this case the isogauss lines will be drawn across the skipped line as if there were no scan line there. Other problems may arise from time to time. In general any feature which is present on only one day should be discounted as an artifact unless there is some particular reason to accept its reality.

Because of the difficulties with the zero offset from day to day, the polar fields will appear to vary. The polar fields can only be studied by comparing them with other weak-field regions observed on the same day.

Sometimes, because of the small scale of the reproductions, it is difficult to make out the details of the field distribution in some regions. *Large scale copies of the particular magnetograms may be obtained by writing to:*

World Data Center A for
Solar-Terrestrial Physics
NOAA
Boulder, Colorado, U.S.A. 80302

Calcium Plage Reports -- The contours are based on estimates made and reported on the day of observation. These data on calcium plage regions are as reported by the McMath-Hulbert Observatory of The University of Michigan supported by NOAA contract. They are the same regions which are summarized in the following section. Listed beside the drawings in each case are the quality of the day's observations and the initials of the observer for the day followed by a table of the plages by regions numbers, then area in millionths of the solar hemisphere and intensity, if area ≥ 3000 millionths or intensity ≥ 2.5 . When McMath-Hulbert Observatory has been unable to observe, available drawings supplied by the Solar Observatory at Catania, Italy are used. The areas will differ from the McMath-Hulbert areas since there is considerable subjectivity in the grouping of the bright calcium areas into regions. Each series should be homogeneous in itself.

H- α Spectroheliograms -- These H- α spectroheliograms are furnished by the solar patrol observatory in Boulder operated by the Space Environment Laboratory of NOAA. The flare patrol instrument is a 4 1/2 inch refractor with a half-angstrom Halle filter and effective focal length of 63 inches. Typical exposure times are one-tenth second. These photographs are supplemented by observations with a similar instrument at the U.S.A.F. Ramey AFB Observatory.

Sunspot Drawings -- The published sunspot drawings are prepared under the direction of P. S. McIntosh of the NOAA Space Environment Laboratory. Drawings and photographs from the NOAA Boulder Observatory are supplemented by drawings from the Sacramento Peak Observatory or photographs from the Culgoora Solar Observatory (C.S.I.R.O., Narrabri, N.S.W., Australia). In any case, the original material greatly exceeds the published copies in showing details of the sunspots. Sunspot groups are boxed according to a judgment of bipolar pairs based on spot group evolution and the structure of associated H- α plage. Serial numbers appearing adjacent to some of the sunspot groups are the last three digits in the McMath-Hulbert plage number with an alphabetic suffix indicating the relative ages of the groups. Usually a single number is placed with only the most important group within the plage.

H- α Prominences -- Drawings of prominences are added to the limb of the sunspot drawings by tracing detail from photographic prints made from the NOAA Boulder H α patrol films.

Coronal Emission -- Emission intensity values for each 5° interval together with peak values greater than 255 are presented adjacent to the sunspot drawing disks for each day that data are available for the $\lambda 5303$ (FeIV) coronal line. The measurements are expressed in millionths of an angstrom (10^{-6}\AA) of the continuum of the center of the solar disk (at the same wavelength as the line) that would contain

the same energy as the observed coronal lines [Billings, D. E., *A Guide to the Solar Corona*, Academic Press, p. 104, 1966]. The date of data presentation corresponds to the date of observation. The data are from a single station selected in the following priority: Sacramento Peak, Kislovodsk, Pic-du-Midi and Lomnický Štít. The Sacramento Peak data are reduced by the High Altitude Observatory of the National Center for Atmospheric Research. (Data from other coronal observatories will be included after detailed analyses facilitate direct comparisons.)

The data are presented for three intensity levels: 80-119, 120-199, and 200-255. Any values greater than 255 will be shown as a peak and its actual value given. The values will be centered on the appropriate 5° interval, overlapping on both side by 2½°. The three levels of intensity are indicated by arcs: the one nearest the disk represents the lowest level, the next arc the intermediate level, and the highest arc the highest level.

White Light Corona -- The photographs of the white light corona are "quick-look" reconstructions of data received daily from the Naval Research Laboratory coronagraph aboard OSO-7 (1971-083A). The corona is recorded from approximately 3 to 10 solar radii. The central dark portion of each photograph is an out-of-focus image of the coronagraph's external occulting disk, and the white circular spot shows the approximate size and position of the occulted sun. The image of the disk support is also out of focus and produces a broad shadow which extends radially outward. This shadow rotates slowly during the year as the spacecraft rolls about the solar direction, and is seen in the western half of each photograph at a position angle ranging from NW to nearly south. The coronagraph field is covered by a "concentric" polarizing filter which admits everywhere the vibration perpendicular to a solar radius. There are also two annular areas in the field, where the polarization direction of the filter is approximately radial. The outward decrease in brightness of the corona is compensated by a radial vignetting function in the coronagraph, so that the final picture has approximately uniform radial brightness. Thus, the pictures show the structure and location of streamers and equatorial bulge, and give a qualitative idea of polarization. The impression of overall brightness from day-to-day is not always reliable because of fluctuations in the reconstruction method.

The OSO-7 on-board tape recorder failed on May 18, 1973. After this date all coronal images have been recorded in separate 90° quadrants, during successive passes over ground stations. A quadrant is recorded at lower than normal resolution when a station pass is short. The published full photograph is a composite of the available quadrants, the first and last of which were taken at the times listed with the photograph.

Further information may be obtained from Richard Tousey or Martin J. Koomen at NRL.

Solar EUV Spectroheliograms -- The Goddard EUV Spectroheliograph on OSO-7 contains an optical system which is designed to record radiation from a small element of the solar disk at extreme ultra-violet wavelengths between 120Å and 400Å. The solar radiation is focussed by means of a Cassegrain telescope used at grazing incidence on a small aperture which acts as the entrance slit to a grating spectrometer. The aperture is fixed in one dimension to 20 arcsec but is selectable between 10 arcsec and 60 arcsec in the other. (10 arcsec by 20 arcsec is normally used.) Multiple exit slits and detectors placed along the focal curve of the spectrometer provide opportunities for simultaneous observation of the sun at several wavelengths, which can be varied by moving the detector mechanism along the focal plane. After selection of the desired wavelengths the entire instrument is moved back and forth by the spacecraft in a raster pattern to build up a "picture" of the sun point-by-point. In the "Large Raster" mode, used for the accompanying data, the size of the solar map is nominally 60 arcmin on a side. This is produced by 64 consecutive parallel sweeps, each sweep being 60 arcmin long and spaced 57 arcsec from the previous sweep.

The fixed 20 arcsec aperture is normal to the direction of the sweep. The selectable dimension, for which 10 arcsec is normally used, is parallel to the sweep direction. The resolution in this direction is however limited to about 75 arcsec, the amount of motion along a raster line during one data accumulation interval in the "Large Raster" mode. The time required for one Large Raster is 8.2 minutes. Because of the small aperture size, the raster line pattern in the "Large Raster" mode does not include all portions of the sun. There are strips 37 arcsec between raster lines which are not included in the scans. The omission may produce some distortion of intensities of highly localized regions. The spectrometer has been set to record a strong coronal emission line of Fe XV (fourteen times ionized iron) at 284.15Å.

A geometric scaling of isophotes (in arbitrary units directly proportional to the surface brightness of the corona) has been used to emphasize the large range of coronal brightness observed in this spectral line.

Specific quantities tabulated on each map include:

- Count: The output of the detector summed over the entire raster.
- Roll: The angle between ecliptic north and the perpendicular to the raster sweep direction, projected on the plane of the sky.
- P-TH: The angle between ecliptic north and solar north, projected on the plane of the sky.

Note that for some maps "Count" is appreciably higher than for adjacent maps. In such cases the observation was made with a larger (20 x 20 arcsec) aperture and is so indicated on the map. The solar limb is indicated by a circle on each map. This information is derived from an H α monitor in the instrument. Solar north is always located at the top of each map.

Goddard experimenters making these observations from OSO-7 are Werner M. Neupert, Roger J. Thomas and Robert D. Chapman.

NRL Solar XUV Coronagraphs -- The Naval Research Laboratory's extreme ultraviolet coronagraph on OSO-7 is no longer operating under the specifications with which it was launched. The bandwidth is no longer limited to 170-630Å and it is felt that information available from the coronagraphs is too little to warrant continued publication. The satellite is soon expected to re-enter the earth's atmosphere. A proposal, if accepted for funding, will result in a similar experiment being put into operation in mid-1976.

Individual Regions of Solar Activity -- The table provides a history of each active center visible on the solar disk using data from McMath-Hulbert Observatory (calcium plages under NOAA contract) supplemented by data from Catania for days of no data at McMath-Hulbert; Mt. Wilson Observatory (magnetic classification of sunspots); NOAA, Boulder (area, count and Brunner classification of sunspots) and Stanford University Observatory (intensity and flux of 9.1 cm radio emissions). The Greenwich date of central meridian passage of each region is given in the lead line for each region as well as prior rotation number.

After the year, month, and day the McMath-Hulbert calcium plage region number is repeated followed by the latitude, central meridian distance, and Carrington longitude of the center of the region on that day. The next two columns give the corrected area in millionths of a solar hemisphere, and the intensity of the region at time of measurement on that day, on a scale of 1 = faint to 5 = very bright, referring to the brightest part of the plage.

These data are based upon estimates made and reported on the day of observation. However, they have been compared with the re-evaluated data and all significant discrepancies have been corrected, either directly in the data or by means of footnotes. These data are from observations obtained and reduced by different observers on days of widely different observing quality. For the quality of the observation on each day and the identification of the observer see daily calcium maps. The McMath-Hulbert Observatory requests that special attention be paid to the quality of observation for the days in question and to the possible personal equation of the respective observers.

The sunspot data lists the Mt. Wilson* group number, the latitude, central meridian distance and Carrington longitude of each spot group and the magnetic classification and largest magnetic field strength measured in each group. The magnetic classifications are defined as follows:

- AP = αp All the magnetic measures in the group are of the same polarity which is that corresponding to the preceding spots in that hemisphere for that cycle.
- AF = αf All the magnetic measures in the group are of the same polarity which is that corresponding to the following spots in that hemisphere for that cycle.
- BP = βp A bipolar group in which the magnetic measures indicate that the preceding spots are dominant.
- B = β A bipolar group in which the magnetic measures indicate a balance between the preceding and following spots.
- BF = βf A bipolar group in which the magnetic measures indicate that the following spots are dominant.
- BY = βy A group which has general β characteristics but in which one or more spots are out of place as far as the polarities are concerned.
- Y = γ A group in which the polarities are completely mixed.

Statements will be added to the above classifications if the group is also of the "D = δ -configuration": spots of opposite polarity within 2° of one another and in the same penumbra.

The Mt. Wilson magnetic sunspot classifications are given for spot groups observed at Mt. Wilson. If a magnetic classification is based on magnetic measurements, that classification is enclosed in parentheses. When only half of the sunspot group is measured, a half parenthesis indicates which half was measured -- either the leader or the follower. A magnetic classification not enclosed in parentheses is determined from the appearance of the spot groups and the plage. A blank in the classification column indicate sufficient information was not available to make an intelligent determination of the magnetic classification. Prior to July 1966 the only magnetic classifications included in the lists were those for which there were magnetic measurements.

*The Mt. Wilson daily observations in monthly summary form may be obtained upon request from World Data Center A for Solar-Terrestrial Physics.

The largest magnetic field strength measured in each group is given. The number which appears under the column headed "H" is a coded representation of the largest magnetic field strength measured in the group. The field strength is only given to the nearest 500 gauss because it is felt that the uncertainties of measurement do not permit greater accuracy. These measurements are made with the line $\lambda 5250.216$ (Fe I). No correction is made for blending the Zeeman components. The code is as follows:

Code	Maximum Field Strength in Gauss	Code	Maximum Field Strength in Gauss
1	100- 500	6	2600-3000
2	600-1000	7	3100-3500
3	1100-1500	8	3600-4000
4	1600-2000	9	4100-4500
5	2100-2500	10	>4500

The area in millionths of a solar hemisphere, sunspot count and classification as observed at NOAA-Boulder are used to complete the sunspot information. Ramey or Manila sunspot data are substituted when available to fill gaps in Boulder data. The initial letter is used in the table to indicate the source of sunspot information.

The sunspot classification in column "C" is represented by three consecutive upper-case letters. It is the revised classification devised by P. S. McIntosh of NOAA. It consists of a modified Zürich Brunner class, the type of largest spot within the group, and the relative spot distribution or compactness of the group. This classification is included in the USSPS code, I.U.W.D.S. "Synoptic Codes for Solar and Geophysical Data, Third Revised Edition 1973", p. 108. The definitions of the classification and an illustration of the types of sunspots follow.

When possible separate bipolar sets of spots are identified by measured magnetic polarities, by the positions of spots relative to lines of polarity reversal inferred from structures on H-alpha filtergrams, and by the record of birth and evolution of spots. If these observations are not available, the following definitions identify most unipolar and bipolar spot groups: (see Figure and definitions to follow.)

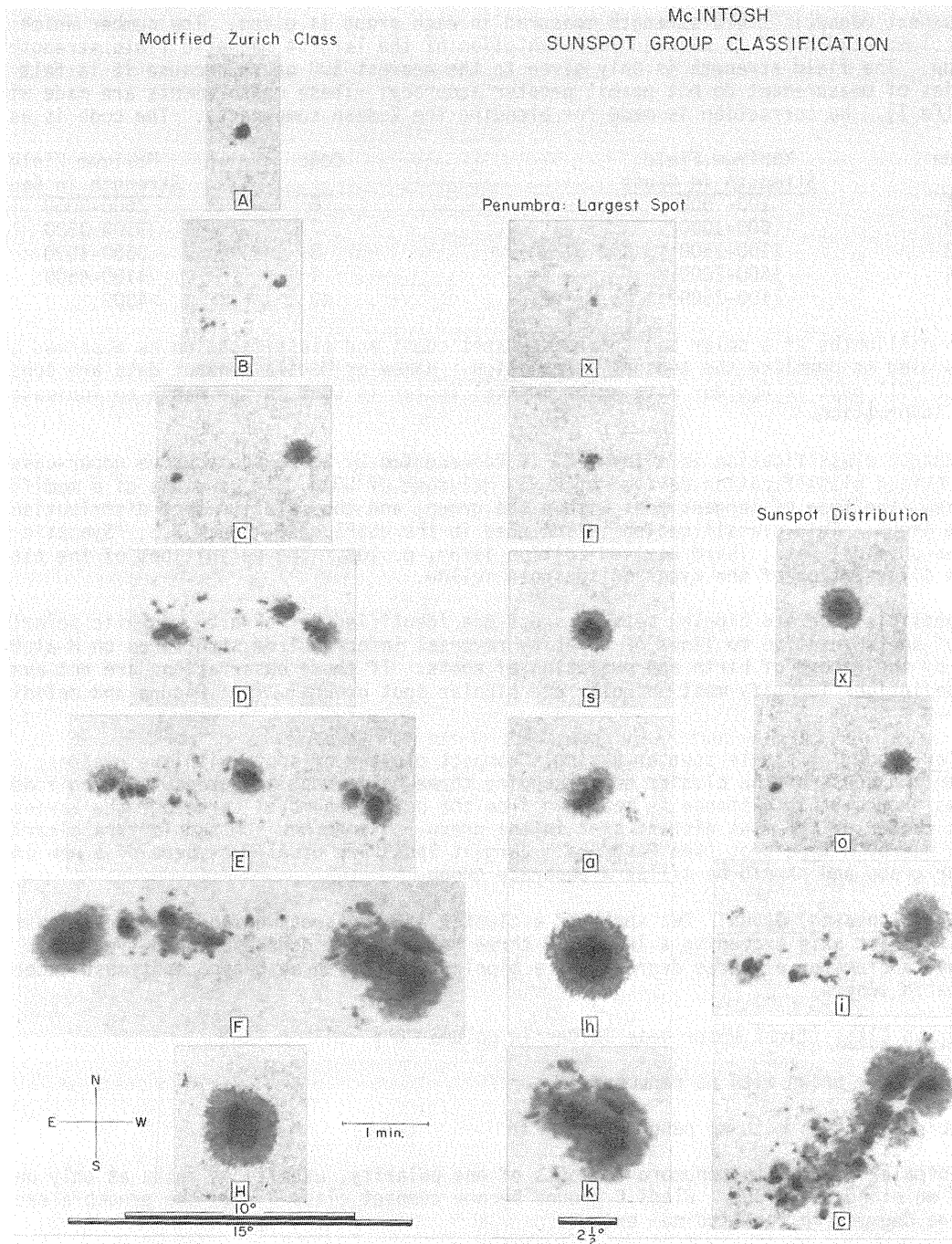
Unipolar Group: A single spot or a single compact cluster of spots with the greatest distance between two spots of the cluster not exceeding three heliographic degrees. In modified Zürich H-class groups, this distance is measured from the outer penumbral border of the largest spot to the center of the most distant spot in the group. Strong new spots which are clearly younger than a nearby h-type spot (see Penumbra: Largest Spot) are usually members of a new emerging bipolar group and should be called a separate group.

Bipolar (Elongated) Group: Two spots of a cluster of many spots extending roughly east-west with the major axis exceeding a length of three heliographic degrees. An h-type major spot can have a diameter of three degrees, so a bipolar group with an h-type spot must exceed five degrees in length.

Modified Zürich Class (first upper case letter in column "C")

- A A unipolar group with no penumbra.
- B A bipolar group with no penumbra.
- C A bipolar group with penumbra on spots of one polarity, usually on spots at only one end of an elongated group. Class C groups become compact class D when the penumbra exceeds five degrees in longitudinal extent.
- D A bipolar group with penumbra on spots of both polarities, usually on spots at both ends of an elongated group. The length does not exceed 10 degrees of heliographic longitude.
- E A bipolar group with penumbra on spots of both polarities and with a length between 10 and 15 heliographic degrees.
- F A bipolar group with penumbra on spots of both polarities and with a length exceeding 15 heliographic degrees.
- H A unipolar group with penumbra. The principal spots are nearly always the leader spots remaining from an old bipolar group. Class H groups become compact class D when the penumbra exceeds five degrees in longitudinal extent.

Note that Zürich classes G and J are missing in this revision. Class G groups are included in the definition of classes E and F, and class J groups are included in class H.



Penumbra: Largest Spot (second upper case letter in column "C")

- "x" No penumbra. The width of the gray area bordering spots must exceed three arc seconds in order to classify as penumbra.
- "r" The penumbra is rudimentary. It is usually incomplete, irregular in outline, as narrow as three arc seconds, brighter intensity than normal penumbra and has a mottled, or granular, fine structure. Rudimentary penumbra represents the transition between photospheric granulation and filamentary penumbra. Recognition of rudimentary penumbra will ordinarily require photographs or direct observation at the telescope.
- "s" Symmetric, nearly circular penumbra with filamentary fine structure and a spot diameter not exceeding $2\frac{1}{2}$ heliographic degrees. The umbrae form a compact cluster near the center of the penumbra. Also, elliptical penumbra are symmetric about a single umbra. Spots with symmetric penumbra change very slowly.

- "a" Asymmetric, or complex penumbra with filamentary fine structure and a spot diameter along a solar meridian not exceeding $2\frac{1}{2}$ heliographic degrees. Asymmetric penumbra is irregular in outline or clearly elongated (not circular) with two or more umbrae scattered within it. The example in the figure is transitional between "s" and "a". Asymmetric spots typically change form from day-to-day.
- "h" A large symmetric penumbra with diameter greater than $2\frac{1}{2}$ heliographic degrees. Other than size, it has characteristics the same as "s" penumbra.
- "k" A large asymmetric penumbra with diameter along a solar meridian greater than $2\frac{1}{2}$ heliographic degrees. Other than size, its characteristics are the same as "a" penumbra. When the longitudinal extent of the penumbra exceeds five heliographic degrees, it is almost certain that both magnetic polarities are present within the penumbra and the classification of the group becomes Dkc or Ekc or Fkc.

Sunspot Distribution (third upper case letter in column "C")

- "x" Single spot.
- "o" An open spot distribution. The area between leading and following ends of the group is free of spots so that the group appears to divide clearly into two areas of opposite magnetic polarity. An open distribution implies a relatively low magnetic field gradient across the line of polarity reversal.
- "i" An intermediate spot distribution. Some spots lie between the leading and following ends of the group, but none of them possesses penumbra.
- "c" A compact spot distribution. The area between the leading and following ends of the spot group is populated with many strong spots, with at least one interior spot possessing penumbra. The extreme case of compact distribution has the entire spot group enveloped in one continuous penumbral area. A compact spot distribution implies a relatively steep magnetic field gradient across the line of polarity reversal.

The first letter of the McIntosh classification is essentially the Brunner classification with the following exceptions:

McIntosh types:	Ero	and	Fro	=	Brunner class G
	Eso		Fso		
	Eao		Fao		
	Eho		Fho		
	Eko		Fko		
McIntosh types:	Hrx			=	Brunner class J
	Hsx				
	Hax				

N.B. For detailed research analyses these region tabulations should be used with caution.

Calcium Plage Index -- This table provides the daily calcium plage index based on the formula by Wesley R. Swartz, Ionosphere Research Laboratory, Pennsylvania State University as published in February 1971 text. The formula is re-expressed below:

$$Ca II_{index} = \left[\sum_i I_i A_i \cos \theta_i \cos \phi_i \right] / 1000$$

where the summation includes all the plages visible on the day.

I_i = intensity of plage i

A_i = corrected area of plage i in millionths of a solar hemisphere
(McMath-Hulbert Observatory data)

θ_i = central meridian distance of plage i in degrees

ϕ_i = latitude of plage i.

Values of this index for the period January 1, 1958 through January 31, 1971 appear in the Pennsylvania State University Ionosphere Research Laboratory Report 373(E), *The Solar Ca II Plage Index*, Wesley E. Swartz and Regan Overbeck, October 8, 1971.

SOLAR X-RAY RADIATION (A.11, C.5)

The data published consist of tables of hourly averages of x-ray flux in the 1 to 8Å and 8 to 20Å bands and a table listing x-ray flares detected. Because of the failure of the data storage system aboard the Naval Research Laboratory's SOLRAD 10 satellite (1971-058A) in June 1973, the SOLRAD 9 satellite (1968-17A) is again the primary data source. Once each minute data from the 0.5 to 3Å, 1 to 8Å, 8 to 16Å detectors are stored in the satellite memory. Therefore, a continuous record of the x-ray emission from the sun, except for gaps due to satellite night and charged particle interference, is available for these three bands. Data transmitted from SOLRAD 10 in real time are recorded whenever the satellite is within range of NRL's ground station, but the SOLRAD 10 data are no longer used in producing the hourly averages and flare summary. A complete description of the SOLRAD 9 experiments is given in NRL Report #6800 titled *The NRL SOLRAD 9 Satellites, Solar Explorer B, 1968-17A*. NRL Report #7408, titled *The SOLRAD 10 Satellite, Explorer 44, 1971-058A*, describes the SOLRAD 10 experiments. Robert W. Kreplin is the Scientific Program Manager for the NRL SOLRAD Project.

1 to 8Å Hourly Average Table -- The data from the 1 to 8Å ionization chamber are converted to a 1 to 8Å energy flux based on 2×10^6 K graybody solar emission spectrum [Kreplin, R. W., *Annales de Geophysique*, 17, 151, 1961]. The averages include data obtained during solar flares. Data contaminated by charged particle interference are excluded whenever possible. The values given for each hourly average are in units of 10^{-3} ergs/cm² sec, and the time scale is UT. The tabular entries are made with a shifting decimal point. Therefore, the values which may be expressed in the four spaces assigned to each entry range from .001 to 9999 times the basic unit, 10^{-3} ergs/cm² sec. Data for the 1 to 8Å band from SOLRAD 9 and SOLRAD 10 are virtually identical so normalization is not required.

8 to 20Å Hourly Average Table -- The data from the 8 to 16Å ionization chamber are converted to an 8 to 20Å energy flux based on a 2×10^6 K graybody solar emission spectrum. The averages include data obtained during solar flares. The 8 to 16Å ionization chambers are relatively unaffected by charged particle interference. The values given for each hourly average are in units of 10^{-2} ergs/cm² sec and the time scale is UT.

Data from all NRL 8 to 20Å experiments prior to the launch of SOLRAD 10 were reduced using detector efficiencies based on mass absorption coefficients calculated by a method described by Henke, et al., [J.A.P., 28, 98, 1957]. More recent mass absorption coefficients reported by Henke, et al., [Norelco Reporter, 14, 112, 1967] show values for aluminum, the window material of the 8 to 16Å detector, which significantly differ from the earlier values. Use of the later mass absorption coefficient values for aluminum gives energy fluxes 1.43 times those obtained using the older values. Only SOLRAD 10 data are routinely processed using the newer mass absorption coefficients. Therefore, 8 to 20Å flux values from SOLRAD 9 or any other NRL 8 to 20Å experiment flown prior to July 1971 should be multiplied by 1.43 to reflect the more recent mass absorption coefficients.

Table of Outstanding Events -- This table attempts to describe each detector solar x-ray flare by giving the starting date and time, the end time, and the peak energy flux and the time at which the peak energy flux occurs for the 0.5 to 3Å, 1 to 8Å and 8 to 20Å bands. The starting and ending times are arbitrarily determined as the time (UT) when the 1 to 8Å flux first rises above and subsequently drops below the 3×10^{-3} ergs/cm² sec level. In general, a flare will not be listed unless the 1 to 8Å flux remains above the 3×10^{-3} ergs/cm² sec level for more than four minutes. The peak flux values given for the 1 to 8Å and 8 to 20Å bands are based on a 2×10^6 K graybody solar emission spectrum, and the 0.5 to 3Å flux values are based on a 10×10^6 K graybody spectrum. The peak flux values given for the 0.5 to 3Å band are in units of 10^{-5} ergs/cm² sec, the 1 to 8Å peak flux values in units of 10^{-4} ergs/cm² sec, and 8 to 20Å peak flux values in units of 10^{-3} ergs/cm² sec. The 8 to 20Å values presented should be multiplied by 1.43 to reflect the more recent mass absorption coefficients for aluminum.

In all three tables the letter E following a value indicates that the true value is less than the listed value, and the letter A indicates that the true value is greater than the listed value.

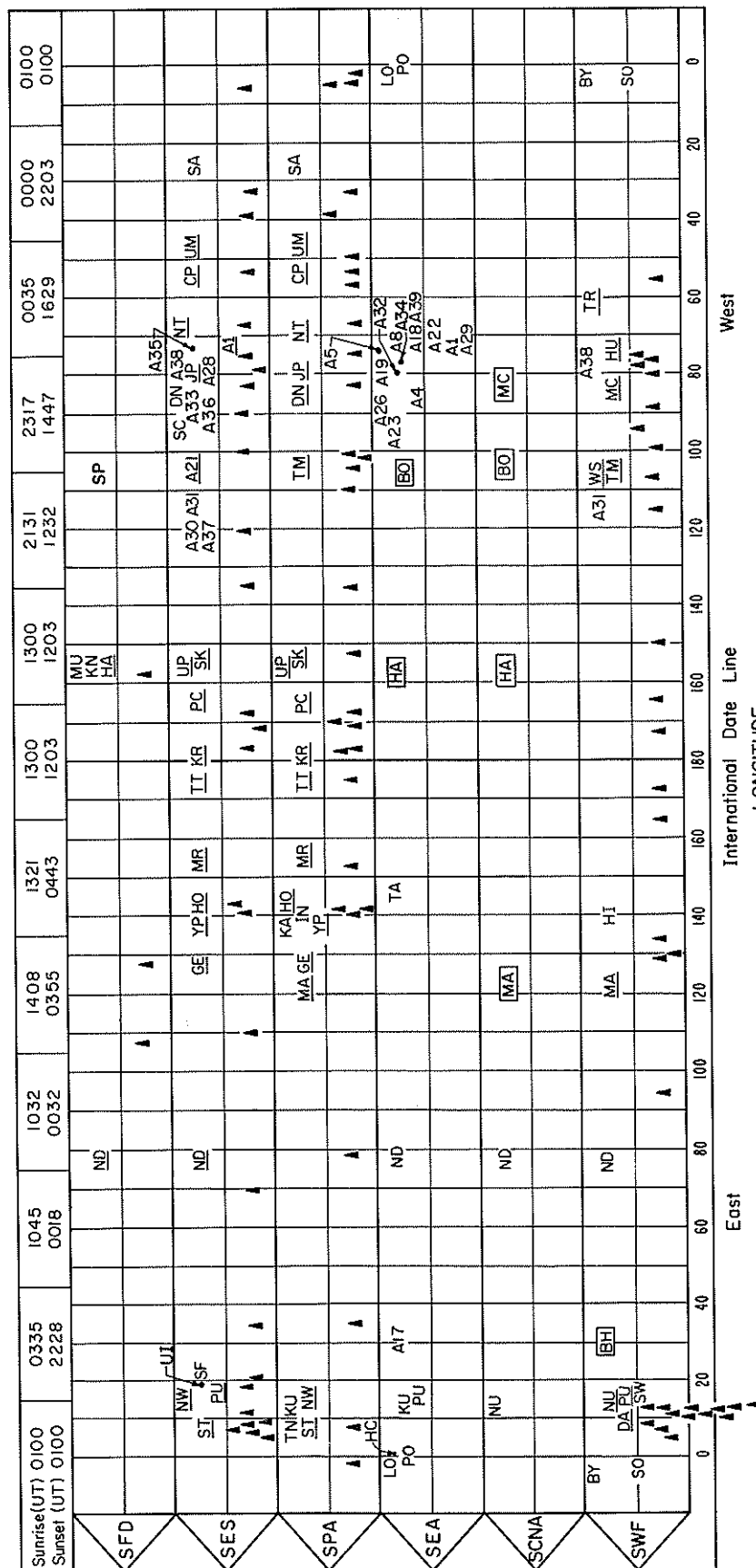
SUDDEN IONOSPHERIC DISTURBANCES (C.6)

Sudden ionospheric disturbances (SID) are presented in a table for two months before publication. There is one line per SID event, rather than as in the past years a line for each type of SID reported. This table gives the date, beginning, ending and maximum time in UT of each event; an importance rating;

STATION LIST FOR SUDDEN IONOSPHERIC DISTURBANCES TABLE

CODE	STATION LOCATION	SWF	SCNA	SEA	SES	SFD	SPA
BH	= BAHRAIN IS.	X					
BO	= BOULDER, COLORADO, USA		X	X			
BY	= BEARLEY, ENGLAND	X					
DA	= DARMSTADT, GFR	X					
HA	= HAWAII, USA		X	X		X	
HC	= HERSTMONCEAUX, ENGLAND			X			
HI	= HIRAIISO, JAPAN	X					
HU	= HUANCAYO, PERU	X					
IN	= INUBO, JAPAN						X
KA	= KASUAGI, JAPAN						X
KN	= KONA, HAWAII, HAWAII, USA					X	
KU	= KUHLLUNGSBORN, GDR			X			X
LO	= PRESTON, ENGLAND			X			
MA	= MANILA, PHILIPPINE ISLANDS	X	X				X
MC	= MCMATH-HULBERT OBS., MICHIGAN, USA	X	X				
MU	= HANA, MAUI, HAWAII, USA					X	
ND	= NEW DELHI, INDIA	X	X	X	X	X	
NU	= NEUSTRELITZ, GDR	X	X				
PO	= POITIERS, FRANCE			X			
PU	= PRAGUE, CZECHOSLOVAKIA	X		X	X		
SC	= ST. CLOUD, MINNESOTA, USA				X		
SF	= SOFIA, BULGARIA				X		
SO	= SOMERTON, ENGLAND	X					
SP	= SACRAMENTO PEAK, NEW MEXICO, USA					X	
SW	= ENKOPING, SWEDEN	X					
TA	= HOBART, TASMANIA			X			
TM	= TABLE MOUNTAIN (BOULDER, COLO, USA)	X					X
TN	= TORINO, ITALY						X
TR	= ST. AUGUSTINE, TRINIDAD, W. I.	X					
UI	= UPICE, CZECHOSLOVAKIA			X			
UM	= SAO PAULO, BRAZIL				X		X
WS	= WHITE SANDS, NEW MEXICO	X					
AMERICAN ASSOCIATION OF VARIABLE STAR OBSERVERS (AAVSO)							
A1	= VALLEY COTTAGE, NEW YORK, USA			X	X		
A4	= COLUMBUS, OHIO, USA			X			
A5	= RAMSEY, NEW JERSEY, USA			X			
A8	= HADDAM, CONNECTICUT, USA			X			
A17	= DURBAN, SOUTH AFRICA			X			
A18	= SCITUATE, MASSACHUSETTS, USA			X			
A19	= LATROBE, PENNSYLVANIA, USA			X			
A21	= LITTLETON, COLORADO, USA				X		
A22	= WELLESLEY, MASSACHUSETTS, USA			X			
A23	= ST. JOSEPH, MISSOURI, USA			X			
A26	= LOUISVILLE, KENTUCKY, USA			X			
A28	= MAYFIELD VILLAGE, OHIO, USA				X		
A29	= LEXINGTON, MASSACHUSETTS, USA			X			
A30	= SUNNYVALE, CALIFORNIA, USA				X		
A31	= MISSOULA, MONTANA, USA	X			X		
A32	= POMPTON PLAINS, NEW JERSEY, USA			X			
A33	= GLENNELLYN, ILLINOIS, USA				X		
A34	= PAEONIAN SPRINGS, VIRGINIA, USA			X			
A35	= BROOKLYN PARK, MINNESOTA, USA				X		
A36	= WORTHINGTON, OHIO, USA				X		
A37	= YAKIMA, WASHINGTON, USA				X		
A38	= ORMOND BEACH, FLORIDA, USA	X			X		
A39	= MANGROVE BAY, SOMERSET, BERMUDA			X			
LORAN-C SKYWAVE MONITOR STATIONS							
CP	= CAPE RACE, NEWFOUNDLAND				X		X
DN	= DANA, INDIANA, USA				X		X
GE	= GESASHI, OKINAWA				X		X
HO	= HOKKAIDO, JAPAN				X		X
JP	= JUPITER, FLORIDA, USA				X		X
KR	= KURE ISLAND				X		X
MR	= MARCUS ISLAND				X		X
NT	= NANTUCKET ISLAND, MASSACHUSETTS, USA				X		X
NW	= BO, NORWAY				X		X
PC	= PORT CLARENCE, ALASKA, USA				X		X
SA	= SANDUR, ICELAND				X		X
SK	= SITKINAK, ALASKA, USA				X		X
ST	= SYLT, GERMANY				X		X
TT	= ATTU, ALEUTIAN ISLANDS, USA				X		X
UP	= UPOLO POINT, HAWAII, USA				X		X
YP	= YAP ISLAND				X		X

MERIDIONAL POSITION OF SID STATIONS, BY TYPE



Presently active SID stations are shown above. The numbers across the top at 30° intervals indicate the earliest sunrise (top) and latest sunset (bottom) times in UT for the stations within ± 15° longitude. The times are based on the summer solstice (June 22). The small triangles throughout the chart indicate the midpoint of transmitting paths for SWF, SPA, SES, and SFD for only those stations that are underlined. The boxes around the 4 SCNA-SEA stations indicate similar equipment.

flare, if known. The selected times of beginning, ending and maximum are usually those of a sudden phase anomaly (SPA). The time that is chosen from the SPA reporting stations is selected by taking into consideration the amplitude of the event and the time of the associated flare, if known. In the table D = greater than, E = less than and U = approximate time indicated. The importance rating is obtained by subjective averaging of the importances reported by all stations for all the different types of SID. The importance rating is based on a scale of 1-, the least, to 3+, the most important. If SPA events are not available, shortwave fade out (SWF) events are used to determine the times. The degree of confidence of identifying the event is reported by the stations as a subjective estimate. This is then evaluated to decide whether the reported event is an SID or not. From the reports believed to be SID, a wide spread index is prepared signifying that the SID is geographically widespread. The index ranges from 1 (possible- single station) to 5 (definite- many stations). Some phenomena are listed if noted at only one location, if there has been a flare or other type of flare-associated effect reported for that time. In the flare column an * represents no flare patrol as yet available for time of event, and NF means no flare observed though there was a flare patrol at that time. Consideration is also given as to whether other reports are available from that longitude on that date. Below the table are listed the stations together with the type of SID reported which were analyzed to prepare the SID event table. A second table lists the number of SID for each day by the McMath region of the associated flare, if known.

The table on page 29 of this text gives the two-letter station code, the geographic location of the station and the type or types of SID information submitted. These data are made possible through the auspices of the International Ursigram and World Days Service, the U.S. Coast Guard, and private interested individual observers (AAVSO). Greater detail concerning the reporting stations can be found in "The Listing of Sudden Ionospheric Disturbances" by J. Virginia Lincoln [*Planet. Space Sci.*, 12, 419-434, 1964] and in earlier versions of this text.

The SID stations presently active are shown on the chart on page 30 by their longitude and by the type of SID recorded. The numbers across the top at 30° intervals indicate the earliest sunrise (top) and latest sunset (bottom) times in UT for the stations within ± 15° longitude. The times are based on the summer solstice (June 22). The small triangles throughout the chart indicate the midpoint of transmitting paths for SWF, SPA, SES, and SFD for only those stations that are underlined. (Many of the non-underlined SWF stations are commercial terminals, and the locations of the transmitters being recorded are not always known.) The world-wide coverage of SID effects is indicated by the density of the triangles, and will show in which parts of the world the ionosphere is studied for SID effects. The boxes around the five SCNA stations note that those stations record cosmic noise absorption with the same equipment; i.e., recorders designed by Robert Lee of the High Altitude Observatory, Boulder, Colorado.

N.B. The detailed data as formerly published are available at cost of reproduction from World Data Center A for Solar-Terrestrial Physics, NOAA, Boulder, Colorado 80302.

SID, sudden ionospheric disturbances (and GID, gradual ionospheric disturbances) may be detected in a number of ways: shortwave fadeouts (SWF), increases in cosmic absorption (SCNA), enhancement or decrease of low frequency atmospherics (SEA or SDA), sudden phase anomalies at VLF (SPA), sudden enhancements at VLF (SES), sudden phase anomalies at LF (SPA and SFA), and sudden frequency deviations (SFD).

SWF -- SWF events are recognized on field-strength recordings of distant high-frequency radio transmissions.

In the coordinated program, the abnormal fades of field strength not obviously ascribable to other causes, are described as shortwave fadeouts with the following further classification:

- S-SWF (S) : sudden drop-out and gradual recovery
- Slow S-SWF (SL) : drop-out taking 5 to 15 minutes and gradual recovery
- G-SWF (G) : gradual disturbance: fade irregular in either drop-out or recovery or both.

SCNA-SEA -- Sudden ionospheric disturbances recognized on recorders for detecting cosmic absorption at about 18 MHz are known as SCNA, or recognized on recorders for detecting enhancements of low frequency atmospherics at about 27 kHz are known as SEA.

SPA and SES -- Sudden phase anomalies (SPA) are observed as a phase shift of the downcoming sky-wave on VLF recordings or on pulse measurements on LF recordings. An estimate of the intensity can be obtained in terms of the degree of phase shift [see Chilton, C. J. et al., *J. Geophys. Res.*, 68, 5421-5436, 1963]. The length of path and amount of sunlight on the path must of course be considered.

Sudden enhancements of signal strength (SES) are observed on field-strength recordings of extremely stable VLF transmissions.

SPA recorded by LF pulse observations over a one hop propagation path yield information more indicative of the ionospheric changes occurring at the mid-point of the path, rather than over the entire path. LF phase observations, reported in degrees, represent an increase in sensitivity over VLF observations. The phase sensitivity is directly proportional to the ratio of the frequencies for identical paths. However, since the height of energy deposition is related to the type of flare x-rays emitted, the LF

measurements in conjunction with the VLF measurements will tend to indicate the x-ray intensity range. Since the LF signal can apparently be reflected from either of two layers within the D-region [Doherty, R. H., *Radio Science*, 2, 645-651, 1967], phase retardations as well as phase advances may occur during an SID at LF.

The amplitude of the low frequency pulse observations made at Loran stations normally changes during an SID. This change is usually, but not always, in the direction of a signal enhancement (SES). The height of signal absorption is below the height of signal reflection. LF amplitude observations along with the LF and VLF phase observations for any one event tend to indicate the x-ray intensities associated with that event. Amplitude changes are reported in dB to the nearest dB of voltage change. Since 6 dB represents doubling of the received signal and 20 dB represents a ten fold change in amplitude, it is obvious that many SIDs produce large effects in LF propagation.

LF-SPA and SES measurements are observed by LF Loran-C stations. These stations record pulse measurements on 100 kHz. As part of the Loran-C sky-wave monitoring program, stations within each chain transmit to one another.

See table on page 29 for code letters and locations of Loran-C stations.

SFA -- On LF amplitude recordings on paths about 1000 km long, sudden phase anomalies of the type known as SFA can be detected. These are events recognized by indirect phase measurements made evident by the one-hop sky-wave interfering with the ground wave.

SFD -- A sudden frequency deviation (SFD) is an event where the received frequency of an HF radio wave reflected from the ionosphere increases suddenly, peaks, and then decays back to the transmitted frequency. Sometimes several peaks occur and usually the frequency deviation takes on negative values during the decaying portion of an SFD. The peak frequency deviation for most SFDs is less than 0.5 Hz. The start-to-maximum time is typically about 1 minute. SFDs are caused by sudden enhancements of ionization at E and F1 region heights produced by impulsive flare radiation at wavelengths from 10 - 1030 Å. A more complete discussion of SFDs can be found in "Contribution of X-Ray and EUV Bursts of Solar Flares to Sudden Frequency Deviations", by R. F. Donnelly, [*J. Geophys. Res.*, 74, 1873-1877, 1969].

S O L A R R A D I O W A V E S

S P E C T R A L O B S E R V A T I O N S (C.4)

Solar spectral events from Fort Davis (Texas), Culgoora (Australia), Boulder (Colorado), Sagamore Hill (Massachusetts), Weissenau (GFR), Dürnten (Switzerland) and Dwingeloo (Netherlands) are presented in a combined table. The contents of the table are described below:

Greenwich date

Observing periods during day (UT) -- aligned with first burst from observatory

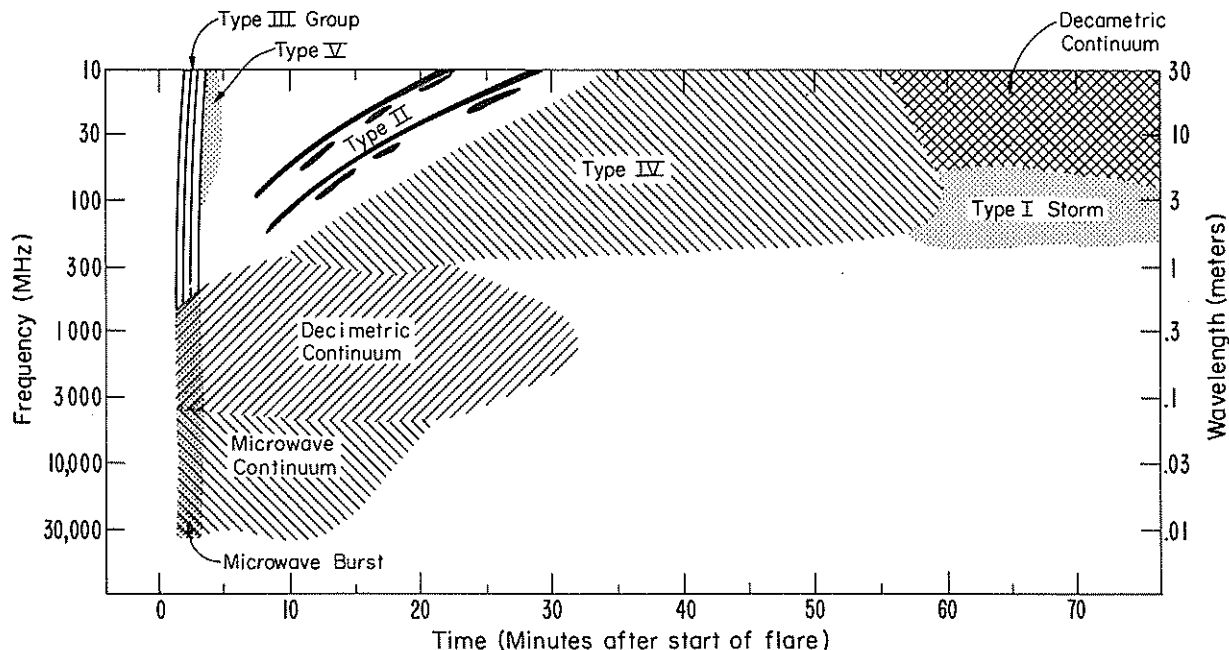
Station -- HARV = Fort Davis, CULG = Culgoora, BOUL = Boulder, SGMR = Sagamore Hill,
WEIS = Weissenau, DURN = Dürnten and DWIN = Dwingeloo.

Burst indicated in wavelength band by beginning and ending times in UT together with an indication of intensity on a 1 to 3 scale, 3 the most important. Symbol "E" is used for an event in progress before the time given and "D" for one that ends after the given time.

Spectral type --
 I = storm bursts
 II = slow drift bursts
 III = fast drift bursts*
 IV = prolonged continuum
 V = brief continuum (normally following type III bursts)
 CONT = continuum in close association with type III burst storms, often with reverse drift bursts and often, but not always, associated with noise storms on metric wavelengths (used by BOUL and SGMR)
 UNCLF = unclassified activity

See J. P. Wild, S. F. Smerd and A. A. Weiss, *Annual Review of Astronomy and Astrophysics*, 1, 291, 1963 for description of types I through V.

*The full generic name is used at the decimeter wavelengths, unless the burst is clearly the high-frequency extension of a meter-wave type III burst.



The schematic diagram above illustrates a typical dynamic spectrum which might be produced by a large flare (Importance 2B and larger). Various flares produce many variations to this "typical spectrum". The nomenclature for the various burst components is often confusing. Alternate names for some components are:

Microwave continuum: Type IV_u, Type B (Post Burst), or Type C (Gradual Rise and Fall)

Decimetric Continuum: Type IV dm

Type IV: IV_m A, Flare continuum (a stationary early phase), moving type IV (if motion is observed), IV_m B, Storm continuum (a late stationary phase).

Type I storm: Noise Storm

Symbols appended to spectral type:

B = Single burst	U = U-shaped burst of Type III
G = Small group (<10) of bursts	RS = Reverse slope burst
GG = Large group (>10) of bursts	DP = Drifting pairs
C = Underlying continuum (particularly with type I)	DC = Drifting chains
S = Storm in the sense of intermittent but apparently connected activity	H = Herringbone
N = Intermittent activity in this period	W = Weak activity
	P = Pulsations

The bursts are divided into dekameter, meter, decimeter and centimeter wavelength ranges. For the reporting stations listed below, these ranges cover approximately the frequency bands 10-30, 30-300, 300-3000, and greater than 3000 MHz.

Weissenau Radio Astronomy Observatory, Astronomical Institute of Tübingen University -- This research work is supported by the University of Tübingen, Baden-Württemberg, GFR. Observations were started in August 1966. Instrumental descriptions were given by Urbarz, *Solar Phys.*, 7, 147-152, 1969; Urbarz, *Information Bulletin of Solar Radio Observations*, No. 25, 8-10, 1969; Kraemer, *Kleinheubacher Berichte*, 13, FTZ Darmstadt, 165-168; Urbarz, *Z. Astrophys.*, 67, 321-338, 1967.

A 35 mm film is used with a 0.2 mm/s feed, the sweep rate is 4 per sec. The number of resolution elements of recorded events is about 100 per octave on film.

In 1971 the ratio of the number of type III bursts reported at Weissenau to those reported at Ft. Davis and Culgoora, respectively, was 1:2.5 and 1:3.5. It is concluded that the same ratios hold for

minimum detectable fluxes on the film recordings. Typical values of minimum detectable flux on channels 1, 3, 4, 5 and 6 are about 100 flux units and on channel 2 about 600 flux units ($10^{-22}\text{Wm}^{-2}\text{Hz}^{-1}$).

Harvard Radio Astronomy Station, Fort Davis, Texas -- Summaries are presented of solar radio bursts recorded in the frequency range 10-4000 MHz. The equipment used at the Station has been described by Thompson [*Astrophys. J.*, 133, 643, 1961] and by Maxwell [*Solar Physics*, 16, 224, 1971]. At 100 MHz the intensity ranges listed as 1, 2, and 3 correspond approximately to 550, 50500, and $>500 \times 10^{-22}\text{Wm}^{-2}\text{Hz}^{-1}$.

Culgoora Solar Observatory, Australia -- The observations at C.S.I.R.O. Solar Observatory, Culgoora, N.S.W., Australia ($30^{\circ}18'56''\text{S}$, $149^{\circ}33'40''\text{E}$) are made by the C.S.I.R.O. Division of Radiophysics, Epping, N.S.W. Summaries are presented of solar radio bursts in the frequency range 8-8000 MHz. For a description of the equipment see K. V. Sheridan, *Proc. Astron. Soc. Australia*, 1, 58, 1967. The intensity scale is qualitative.

Astro-geophysics Department, University of Colorado -- Data are presented on solar radio emission recorded at Nederland near Boulder, Colorado in the spectral range 7.6 to 80 MHz. This range is broken into three subranges; each is swept in 0.5 seconds. The collecting area of the antennas is approximately 1000 square meters, in two corner reflectors forming an interferometer pair. Observations are taken routinely throughout the Boulder observing day from about 1400 UT to 2400 UT. On the low-frequency side, strong bursts are frequently limited by external reflection of the wave above the ionosphere; weaker bursts are obscured by ionospherically reflected telecommunications stations at frequencies lower than about 20 or 25 MHz, and by television stations near 54 MHz and near 68 MHz. The equipment is described by R. H. Lee and J. W. Warwick, *Radio Science*, 68D, 807, 1964.

Examples taken with this equipment are published in J. W. Warwick, *Solar System Radio Astronomy*, (J. Aarons, ed.), Plenum Press 1967. Intensities are on a rough scale from 1- to 3+, crudely convertible to flux densities as follows:

1- to 1+;	$5 \times 10^{-22} < S < 2 \times 10^{-21}$
2- to 2+;	$2 \times 10^{-21} < S < 8 \times 10^{-21}$
3- to 3+;	$8 \times 10^{-21} < S \leq 3 \times 10^{-20}$

Above about $3 \times 10^{-20}\text{Wm}^{-2}\text{Hz}^{-1}$, the equipment saturates and does not indicate relative intensities satisfactorily.

Bursts lying exclusively above 40 MHz are reported as metric band events and those lying exclusively below 40 MHz are reported as dekametric band events. Most bursts are observable in both bands and are so reported.

In the summer of 1970 the radio observatory was moved from north of Boulder to a site two miles south of Nederland, Colorado. Geographic coordinates of the site are $39^{\circ}57'\text{N}$ $105^{\circ}31'\text{W}$. Operation of the corner reflectors was resumed October 29, 1970.

Sagamore Hill Radio Observatory -- Spectral measurements of dekameter wavelength Type II, III, IV and V radio emission are made at Sagamore Hill on a patrol basis. The patrol has been in operation since September 1965. A special purpose radiometer sweeps the 24-48 MHz frequency range at a rate of 1 sweep per second (prior to July 12, 1970 the range was 19-41 MHz). Two semi-bicone stationary antennas, spaced 300 meters apart on an E-W line to form the interferometer, are used with the spectral receiver.

With this array, positive identification of any solar event is enhanced by the resultant fringe pattern on the spectrogram. (The bicone antennas are a D. Gaunt design.)

All raw data are recorded on a Statos-V x, y, z Electrostatic Recorder (Model 500) for real time readout. An improved solid state sweep frequency radiometer providing up to 10 dB greater sensitivity than the original instrument is now in routine operation at Sagamore Hill. A similar instrument with the same frequency interval is also in service at the Manila Observatory, Quezon City, Republic of the Philippines.

Although the International Council of Scientific Unions in *IQSY Instruction Manual*, No. 2, Solar Activity (July 1963) specifies the classification of sweep frequency spectral events, it fails to suggest a quantitative intensity designation for events other than 1 = weak, 2 = moderate and 3 = strong. Nor is there any uniformity among observatories in interpreting the intensity levels. The reason for this stems from the fact that equipments and antenna systems at different stations are different, having different gains, different dynamic ranges and saturate at different levels. With the 24-48 MHz equipment at Sagamore Hill:

Intensity 1 = 8 to 80 flux units
Intensity 2 = 80 to 1600 flux units
Intensity 3 = >1600 flux units

where 1 flux unit = $10^{-22}\text{Wm}^{-2}\text{Hz}^{-1}$.

Dürnten Spectrograph, Switzerland -- The Dürnten spectrograph has been constructed by means of the Swiss National Science Foundation. It is located at Dürnten (47°17'N, 8°51'E) near Zürich, Switzerland. The film registration now covers a frequency range from 150-1000 MHz in one continuous sweep. The sweep rate is normally set at 4 Hz. The threshold intensity I_{th} amounts to about 110 ± 30 flux units between 100 and 200 MHz. Between 200 and 1000 MHz the threshold intensity is linearly related to the frequency by the expression $I_{th} = 0.5f \pm 0.2f$. Saturation occurs roughly at $I = 2 I_{th}$. Intensities are indicated according to the following intensity levels:

Intensity 1 = not saturated
Intensity 2 = nearly saturated
Intensity 3 = clearly saturated

For more detailed description of the instrument see: Tarnstrom, G. L., *Astr. Mitt. Eidgen. Sternwarte Zürich*, No. 3]7, 1973.

Culgoora Radioheliograph at 43.25, 80 or 160 MHz -- The radioheliograph at the CSIRO Solar Observatory, Culgoora (Australia) is a circular array of 96 paraboloid reflector aeriels equally spaced around a circle of 3 km diameter. It records 2 two-dimensional pictures of the Sun each second: one in the left-handed, the other in the right-handed sense of circular polarization [J. P. Wild, editor, *Proc. IREE (Aust.)*, 28, 277, 1967]. Originally the heliograph operated at 80 MHz; it has been converted to time-sharing operation at 43.25, 80 and 160 MHz covering fields of view of $2^\circ \times 1.6^\circ$, $2^\circ \times 1.6^\circ$ and $1^\circ \times 0.8^\circ$ with half-power beamwidths at zenith of 7.4', 3.7' and 1.9', respectively, [K. V. Sheridan, N. R. Labrum and W. J. Payten, *Proc. IEEE*, 61, 1312, 1973]. For the 43.25 MHz frequency an array of 48 corner reflector aeriels set on a circle of 2.77 km diameter has been built just inside the main radioheliograph array. At this frequency only one sense of linear polarization is received.

The heliograph pencil beam can track the Sun for 6 hours and 40 minutes centered on local noon. The mechanical movement of the aeriels is limited to 4 hours and 48 minutes (slightly less near the summer and winter solstices) so that the Sun drifts into and out of the broad aerial beams during the first and the last hour of observation. The normal observing hours are approximately 2300 to 0500 UT. The necessity to provide time for maintenance and development has limited observations to about 2/3 of all days since the end of 1967.

The events selected for listing in the Table may be: small, isolated events during periods of little activity; daily samples during prolonged storms; or outstanding events during active periods. Source positions are given by their central distance in units of the Sun's optical radius, R_0 and their position angle; the latter is the angle of 0° to 360° measured eastward from the north point of the solar disk (i.e., from celestial north). The apparent projected positions and the polarization listed here are taken from the visual analogue display of the taped, digital heliograph data; the expected relative accuracy is about $0.1 R_0$ in distance and 10° in PA. The polarization is described qualitatively as weak [l or r] or strong [L or R] circular polarization. The intensity is given on a scale 1 to 3, with the corresponding flux densities, S , very approximately in the range:

- 1 : $S < 2 \times 10^{-21} \text{ Wm}^{-2} \text{ Hz}^{-1}$
- 2 : $2 \times 10^{-21} < S < 2 \times 10^{-20} \text{ Wm}^{-2} \text{ Hz}^{-1}$
- 3 : $S > 2 \times 10^{-20} \text{ Wm}^{-2} \text{ Hz}^{-1}$

Storms which are mostly of intensity 1 will not normally be listed. The positions may be affected by unknown amounts of ionospheric refraction; this effect is more pronounced the lower the frequency. If refraction errors are suspected this will be noted in the "remarks" column of the Table.

C O S M I C R A Y S (F.1)

Tabulated Observations -- The table presents the daily (UT) average counting rates per hour (scaled) for nine high counting rate neutron monitors: Thule, Alert, Deep River, Calgary, Sulphur Mountain, Kiel, Climax, Dallas and Tokyo. These monitors have different values of magnetic cutoff rigidity, while their asymptotic cones of acceptance "look" approximately in the equatorial plane in essentially the same direction in space. The nine sets of data can therefore be used to estimate the rigidity dependence of fluctuations which occur in the primary cosmic radiation.

The characteristics of the nine stations are given below; the data have been corrected applying the listed barometric coefficients to the listed mean station pressures.

Station	Thule	Alert	Deep River	Calgary	Sulphur Mt.	Kiel	Climax	Dallas	Tokyo
Geog. Lat., N.	76°35'	82°31'	46°06'	51°05'	51°12'	54°18'	39°22'	32°59'	35°45'
Geog. Long., E.	291°35'	297°40'	282°30'	245°52'	244°24'	10°06'	253°49'	263°16'	139°43'
Cutoff, GV	0.00	0.00	1.02	1.09	1.14	2.29	3.03	4.35	11.61
Altitude, m	260	66	145	1128	2283	54	3400	208	20
Detector type	NM 64	NM 64	NM 64	NM 64	NM 64	NM 64	IGY	NM 64	NM 64
Scaling factor	100	100	300	100	100	100	100*	120	128
Baro. coeff., % mm Hg	1.00	.987	.987	1.0155	1.0085	.961	.943	.971	.844
Mean press. mm Hg	730	752	747	671	582	755	504	746.3	760.5

* From January 1, 1966.

The Climax, Colorado, U.S.A., neutron monitor, station B305, data are communicated by J. A. Simpson and G. Lentz of the Enrico Fermi Institute for Nuclear Studies, University of Chicago. The instrument is a standard Chicago type neutron monitor, utilizing 12 BF₃ counter tubes. The station has a mean barometric pressure of 504.0 mm Hg. For a more detailed description of the neutron intensity monitor and its associated electronics see J. A. Simpson, *Annals of the IGY, Vol. IV, Part VII, 351-373, 1957*. The publication of these data in this monthly series began September 1960. *Earlier data, beginning June 1957, are available in bihourly form at the World Data Center A for Solar-Terrestrial Physics.*

The Dallas, U.S.A. neutron monitor follows the IQSY design described by Carmichael [IQSY Instruction Manual No. 7]. The Dallas reference pressure was 1000 mb until 6 August 1965, being changed from that date to 995 mb. The attenuation length used in the pressure correction is 137.2 mb. The data have not been corrected for the minor changes (<1%) in efficiency of monitor which inevitably occur over any appreciable period of time. The monitor is operated by Edwin P. Keath of the University of Texas at Dallas (formerly the Southwest Center for Advanced Studies), Dallas, Texas. The Dallas monitor commenced operation on 1 December 1963. *Hourly mean data are routinely distributed to the scientific community and the World Data Center A for Solar-Terrestrial Physics, by the Cosmic Ray Laboratory, The University of Texas at Dallas, P. O. Box 30365, Dallas, Texas, U.S.A., 75080.* The monitor at Churchill, previously operated by the same group, ceased operation in September 1973.

The Deep River, Ontario, Canada, neutron monitor, Station B211, follows the IQSY [IQSY Instruction Manual No. 7]. Publication of the daily rates in this series began in January 1966 but a chart of hourly values from Deep River, described below has been published herein since January 1959. Until December 31, 1972 the station was operated and maintained by Atomic Energy of Canada Ltd., but on January 1, 1973 the National Research Council of Canada took over the responsibility for maintenance of the station. *The original data can be obtained from National Research Council of Canada, Ottawa, Ontario, Canada, K1A 0R6, or from any of the World Data Centers.*

The 18-NM-64 neutron monitor located at Alert, North West Territories, Canada, is unique because its asymptotic cone of acceptance in space is less than 10° wide and is aligned with 7° of the spin axis of the earth. Hence, unlike the stations whose cones of acceptance rotate with the earth approximately in the plane of the ecliptic, Alert always "looks" into a fixed cone directed northwards. It experiences negligible periodic diurnal intensity variation.

The monitor at Alert was provided by Atomic Energy of Canada, Ltd., and housed in a building provided by National Research Council of Canada. Until December 31st, 1972, the monitor was maintained by A.E.C.L., but since January 1st of 1973 this has become the responsibility of the National Research Council. Day-to-day operation is by courtesy of the Canadian Meteorological Service.

The two high counting rate neutron monitors at Sulphur Mountain and Calgary have values for magnetic cutoff rigidity comparable to the Deep River monitor. Their asymptotic cones of acceptance "look" approximately in the equatorial plane in essentially the same direction in space.

The data, beginning January 1971, from Sulphur Mountain and Calgary Super neutron monitors are communicated by D. Venkatesan and T. Mathews of the Department of Physics, University of Calgary, Calgary 44, Alberta, Canada. The stations have mean barometric pressures of 766 mb, and 883 mb., respectively. The barometric coefficients used to correct the data are 0.7665%/mb and 0.7718%/mb, respectively. *Hourly mean data from both installations are routinely distributed to the scientific community and the World Data Center A for Solar-Terrestrial Physics, Boulder, Colorado. The data began March 1963 for Sulphur Mountain and January 1964 for Calgary, and are available at the World Data Center. The stations were set up by B. G. Wilson (now at Simon Fraser University, Burnaby, British Columbia).*

The Thule nucleonic intensity detector, of standard IQSY design, is located at AFCRL Geopole Station, Greenland: latitude 76°36'N, longitude 68°48'W, altitude 260m, geomagnetic threshold rigidity essentially zero. The data are communicated by Martin A. Pomerantz, Bartol Research Foundation, Swarthmore, Pa. 19081.

The scaling factor is 100. The plots represent percentage deviations from the monthly mean intensity. The data are corrected to the standard station atmospheric pressure, 730 mm of Hg, with the barometric coefficient — 1.00% per mm of Hg, as determined by regression analysis for the year 1972. Any changes in either the atmospheric attenuation length or in the sensitivity arising from long term drifts are applied retrospectively before the final hourly mean data are routinely distributed to the World Data Centers and to the scientific community.

Two other monitors, at Kiel and Tokyo, have asymptotic cones of acceptance much different from those given above. Therefore, they can be used to distinguish between UT-dependent and LT-dependent time variations. Higher cutoff rigidities also aid further estimation of rigidity dependence. The publication of these data begin with the December 1973 data.

The data from both 18-NM-64 neutron monitors are routinely submitted to World Data Center A, B, C1 and C2 for Cosmic Rays as well as to listed researchers. Kiel data has been available since September 1964 and Tokyo (or Tokyo-Itabashi) data since January 1970. The data are communicated to *Solar Geophysical Data* by M. Wada after receiving the Kiel data from O. Binder.

Charts -- Variations of cosmic ray intensity are depicted in chart form for seven of the above stations. One chart depicts the variations of cosmic ray intensity recorded by the IQSY design 48-NM-64 neutron monitor at Deep River, Ontario, Canada. Through December 31, 1972, these data were submitted by J. F. Steljes of Atomic Energy of Canada, Ltd., Chalk River, Ontario. On January 1, 1973, this responsibility was transferred to Margaret D. Wilson of the National Research Council of Canada, Ottawa, Canada. The vertical scale lines mark the days of the month in Universal Time: the horizontal scale lines are at intervals of 5% based upon 1.846×10^6 counts per hour (after barometric correction) arbitrarily taken as 100%. The charts have been published from January 1959, publication beginning in the November 1960 issue. From January 1959 to April 1962 a smaller monitor was used and the 100% counting rate was 0.0555×10^6 counts per hour. From May 1962 to January 1965 the monitor was of intermediate size and the 100% counting rate was 0.555×10^6 counts per hour. A preliminary barometric coefficient was used from May 1962 to October 1962; in the March 1963 issue final revised charts were published for these six months using a better value of the barometric coefficient.

Beginning with the chart for July 1966 the variations of cosmic ray intensity as recorded by the IQSY design 18-NM-64 neutron monitor at Alert, Canada, have been presented. The Alert graph is normalized so that 100% is 0.6678×10^6 counts per hour.

The charts also depict the variations of cosmic ray intensity as recorded by the Sulphur Mountain and Calgary monitors. The vertical scale lines mark the days of the month in Universal Time; the horizontal scale lines are at intervals of 5% based upon 0.8827×10^6 counts per hour (after barometric correction) arbitrarily taken as 100% for Sulphur Mountain and 1.1767×10^6 counts per hour (after barometric correction) arbitrarily taken as 100% for Calgary.

The charts depicting variation of cosmic ray intensity at Thule, Kiel and Tokyo are deviations from the monthly mean.

G E O M A G N E T I C A C T I V I T Y (D.1)

Kp, Ci, Cp, Ap, aa, and Selected Quiet and Disturbed Days -- The data in the table are: five quietest days (QQ), ten quietest days (QQ or Q), and five most disturbed days of the month (D) adjacent to date; three-hour range indices Kp; international character figure, Ci; character figure, Cp (standardized Ci); daily "equivalent amplitude", Ap; and aa indices.

The data are made available by the Permanent Service of Geomagnetic Indices of IUGG: Association of Geomagnetism and Aeronomy through Commission IV: Magnetic Activity and Disturbances. The Meteorological Institute, De Bilt, The Netherlands, collects the data from magnetic observatories distributed throughout the world, and compiles the Ci and selected days data. The Institute für Geophysik, Göttingen University, computes the planetary and equivalent amplitude indices.

Kp is the mean standardized K-index from 13 observatories between geomagnetic latitudes 47 and 63 degrees. The scale is 0 (very quiet) to 9 (extremely disturbed), expressed in third of a unit, e.g., 5- is 4 and 2/3, 5o is 5 and 0/3, and 5+ is 5 and 1/3. This planetary index is designed to measure solar particle-radiation by its magnetic effects, specifically to meet the needs of research workers in the other geophysical fields.

The Ci-figure is the arithmetic mean of the subjective classification by observatories of each day's magnetic activity on a scale of 0 (quiet) to 2 (storm).

The Cp-figure is a standardized version of the Ci-figure and is derived from the indices Kp by converting the daily sum of ap into the range 0.0 to 2.5.

Ap is a daily index of magnetic activity on a linear scale rather than on the quasi-logarithmic scale of the K-indices. It is the average of the eight values of an intermediate 3-hourly index "ap", defined as approximately one-half the average gamma range of the most disturbed of the three force components, in the three-hour interval at standard stations; in practice, ap is computed from the Kp for the 3-hour interval. The extreme range of the scale of Ap is 0 to 400. Values of Ap (like Kp and Cp) have been published for 1932 to 1961 in *IAGA Bulletin No. 18* by J. Bartels. Yearly compilations of these data, as well as Ci and selected days, are published in the series of *IAGA-Bulletin No. 32 (the continuation of IAGA Bulletin No. 12)*. These Bulletins are available from the IUGG Publications Office 39, Rue Gay Lussac, Paris (V). These indices are also available at the World Data Centers.

The aa indices are the continuation of the series beginning in the year 1868. A full description of these indices is given in the *IAGA Bulletin 33*, which contains them for the years 1868-1967. Descriptions are also given (especially comparisons with am, ap, or Ci indices) in two short papers [*Ann. Geoph. 27*, 62-70, 1971, and *J. Geophys. Res.*, 77, 6870-6874, 1972]. aa values for 1968-1973 will soon be published in IAGA Bulletin 32 series.

Briefly, such three-hourly indices, computed from K indices of two antipodal observatories (invariant magnetic latitude 50°), provide a quantitative characterization of the magnetic activity, which is homogeneous through the whole series. Half-daily and daily values give an estimation of the activity level very close to that obtained with am indices. Values are in gammas and correspond to the activity level at a magnetic latitude of 50°. The aa indices are computed for:

N = daily values for the Northern hemisphere,
S = daily values for the Southern hemisphere,
M = half-daily values of aa indices for the
Greenwich day.

Letters C and K refer to a classification of the quiet days of the month (C = really quiet, K = quiet but with slightly disturbed three-hourly intervals). The letters on the left refer to the 24 hour Greenwich day, on the right to a period of 48 hours centered on the Greenwich noon.

The magnetically quiet and disturbed days (D & Q) are selected in accordance with the general outline in *Terr. Mag.* (predecessor to *J. Geophys. Res.*) 48, 219-227, 1943. The method in current use calls for ranking the days of a month by their geomagnetic activity as determined from the following three criteria with equal weight: (1) the sum of the eight Kp's; (2) the sum of the squares of the eight Kp's; and (3) the greatest Kp.

Chart of Kp by Solar Rotations -- Monthly a graph of Kp is given for eight solar rotations, furnished through the courtesy of the Geophysikalisches Institut of the University of Göttingen. Annually a graph of the whole year by solar rotations is included. From time to time another 27-day rotation chart depicting the daily geomagnetic character figure, C9, is presented. C9 is obtained from Cp by reducing the Cp-values to integers between 0 and 9 according to the key given in the charts.

The activity indices are described by J. Bartels in *Annals of the IGY, Vol IV*, 227-236, London, Pergamon Press, 1957. Below the chart of Kp a table of Ap indices for the last 12 months is presented so that trends in magnetic activity can be easily followed.

Provisional Hourly Values of the Equatorial Dst Index -- The equatorial Dst index at given UT represents magnetic field variations at the dipole equator on the earth's surface, averaged over local time, that are caused mainly by the magnetospheric equatorial currents including the cross-tail current. The reference level of Dst is such that Dst is statistically zero on the days internationally designated as quiet days.

Provisional hourly Dst data are based on hourly values of the horizontal component from four magnetic observatories: San Juan, Honolulu, Kakioka, and Hermanus. These provisional hourly values are replaced by a more definitive annual set of the Dst index at the end of each year. The provisional hourly values are calculated and forwarded for publication by M. Sugiura, NASA-Goddard Space Flight Center, Greenbelt, Maryland 20771 and D. J. Poros, Computer Sciences Corporation, Silver Spring, Maryland 20910.

Principal Magnetic Storms -- Finally a table presents the principal magnetic storms for the month as reported by several observatories through cooperation with the International Association of Geomagnetism and Aeronomy. These are the data formerly published in the *Journal of Geophysical Research*. They are now, however, grouped by the storm rather than by station. The geomagnetic latitude of the station is indicated. The beginning time is given to the hour and minute in UT. The ending time is given only to the nearest hour. This is the time of cessation of reasonably marked disturbance movements in the trace. More specifically, the time when the K-index measure has diminished to 2 or less for a reasonable period.

The type of sudden commencement, if any, together with its magnitude in each element D, H, or Z is next in the table: sc = sudden commencement; sc* = small initial impulse followed by main impulse (in this case the amplitude is that of the main pulse only, neglecting the initial brief pulse); dots in these columns represent a storm with gradual commencement; dashes indicate no data entries. Signs of amplitudes of D and Z are taken algebraically; D reckoned positive if toward the east and Z reckoned positive if vertically downward. In the next columns the day and the three-hour periods on that day when the K index reached its maximum are given. Finally, in the last three columns the maximum ranges in D, H and Z during the storm are given. For each date the data are listed in north-to-south geomagnetic latitude order. The table below gives the abbreviation used for the observatory names.

GEOMAGNETIC OBSERVATORIES

<u>Code</u>	<u>Station</u>	<u>Geomag. Latitude</u>	<u>Code</u>	<u>Station</u>	<u>Geomag. Latitude</u>
AA	Addis Ababa	5.3N	HU	Huancayo	0.6S
AL	Alibag	9.5N	HD	Hyderabad	7.6N
AM	Amberley	47.7S	IR	Irkutsk	41.0N
AN	Annamalainagar	1.5N	KG	Kerguelen	56.5S
AP	Apia	16.0S	MB	M'Bour	21.3N
BD	Boulder	48.9N	NE	Newport	55.1N
CO	College	64.6N	PM	Port Moresby	18.7S
EB	Ebro	43.9N	SJ	San Juan	29.9N
FR	Fredericksburg	49.6N	SI	Sitka	60.0N
GN	Gnangara	43.2S	TO	Toolangi	46.7S
GU	Guam	4.0N	TV	Trivandrum	1.1S
HR	Hermanus	33.7S	TU	Tucson	40.4N
HO	Honolulu	21.1N	WI	Witteveen	54.2N

Sudden Commencements and Solar Flare Effects -- These reports are provided by A. Romaña for the Permanent Service of Geomagnetic Indices of IUGG, Association of Geomagnetism and Aeronomy, Commission IV: Magnetic Activity and Disturbances. The sudden commencements (s.s.c.), sudden impulses (s.i.) and solar flare effects (s.f.e.) are from magnetograms of the world-wide network of magnetic observatories. The stations, together with their abbreviations, are given in IAGA Bulletin No. 20 of the International Union of Geodesy and Geophysics as well as the series IAGA Bulletin No. 32 which contain the yearly compilations of these data. These reports have been published quarterly in *Solar-Geophysical Data* beginning with data for January 1966. Previous to that time they were published periodically in the *Journal of Geophysical Research*.

Beginning with December 1970 these data are based on fewer reports and, thus, will differ slightly in detail from the similar data published previously. The decision to publish this less complete report was made in order to make the data available more rapidly. The table gives date and UT time of event with stations by two letter abbreviations grouped by quality A, B, or C.

RADIO PROPAGATION QUALITY INDICES (B.51)

One can take as the definition of a radio propagation quality index: the measure of the efficiency of a medium-powered radio circuit operated under ideal conditions in all respects, except for the variable effect of the ionosphere on the propagation of the transmitted signal. The indices given here are derived from monitoring and circuit performance reports, and are the nearest practical approximation to the ideal index of propagation quality.

Quality indices are expressed on a scale that ranges from one to nine. Indices of four or less are generally taken to represent a significant disturbance. (Note that for geomagnetic K-indices, disturbance is represented by high numbers.) The adjectival equivalents of the integral quality indices, known as the CRPL quality figure scale, are as follows:

1 = useless	4 = poor-to-fair	7 = good
2 = very poor	5 = fair	8 = very good
3 = poor	6 = fair-to-good	9 = excellent

The forecasts are expressed on the same scale.

The quality figures represent a consensus of experience with radio propagation conditions. Since they are based entirely on monitoring or traffic reports, the reasons for low quality are not necessarily known and may not be limited to ionospheric storminess. For instance, low quality may result from improper frequency usage for the path and time of day. Although, wherever it is reported, frequency usage is

included in the rating of reports, it must often be an assumption that the reports refer to optimum working frequencies. It is more difficult to eliminate from the indices conditions of low quality for reasons such as multipath or interference. These considerations should be taken into account in interpreting research correlations between the Q-figures and solar, auroral, geomagnetic or similar indices.

North Atlantic Radio Path -- The quality figures are compiled by the Telecommunication Services Center, Office of Telecommunications, at Boulder, Colorado from radio traffic data for North Atlantic transmission paths closely approximating New York-to-London. These are reported by the Canadian Broadcasting Corporation, International Telephone and Telegraph, Radio Corporation of America, U. S. Coast Guard, and Federal Communications Commission.

The original reports are submitted on various time intervals. The observations for each 6-hour interval are averaged on the original scale. These 6-hour indices are then adjusted to the 1 to 9 quality-figure scale by a conversion table prepared by comparing the distribution of these indices for at least four months, usually a year, with a master distribution determined from analysis of the reports originally made on the 1 to 9 quality-figure scale. A report whose distribution is the same as the master is thereby converted linearly to the Q-figure scale. The 6-hourly quality figure is the mean of the reports available for that period.

The 6-hourly quality figures are given in this table to the nearest one-third of a unit, e.g. 5.0 is 5 and 0/3; 5- is 4 and 2/3; 5+ is 5 and 1/3. Other data included are:

- (a) Whole-day radio quality indices, which are averages of the four 6-hourly indices.
- (b) Short-term forecast, issued every six hours by the Telecommunication Services Center. These are issued one hour before 02^h, 08^h, 14^h, and 20^h UT and are applicable to the period 1 to 7 hours ahead.
- (c) Weekly Radio Telecommunication Forecasts (WF) are issued once a week and are applicable to 1 to 7 days ahead for HF radio propagation conditions on typical high latitude paths passing through or near the auroral zone. They are scored against the average of the whole day North Atlantic quality figures. They are modified as necessary by a supplemental forecast.
- (d) Half-day averages of the geomagnetic K indices measured by the Fredericksburg Magnetic Observatory of the NOAA Environmental Research Laboratories, K_{Fr}.

North Pacific Radio Area -- A local tape-recorded service, telephone (area code 907) 753-9228 is operated at the Anchorage NOAA station giving a statement of current magnetic conditions, a forecast of geomagnetic conditions for the coming day, current ionospheric conditions, HF radio propagation conditions for the past 24 hours and predicted conditions for the next 24 hours.

Transmission Frequency Ranges -- The North Atlantic path (Lüchow (53.0°N, 11.2°E) - Halifax) is represented by five frequencies, 6.425, 8.542, 12.813, 17.084 and 22.378 MHz, recorded continuously. They are shown in a series of diagrams one for each day. The heavy solid lines represent field strength ≥ -12 dB above 1 μ V/m (transmitter power reduced to 1 kW). Observed field strengths between -12 dB and -40 dB above 1 μ V/m are shown by the fine line. These diagrams are based on data reported by the German Post Office through the Fernmeldetechnisches Zentralamt, Darmstadt, Federal Republic of Germany.

Radio Propagation Quality Indices are calculated from the records of five frequencies of the circuit Lüchow-Halifax (Germany-Canada). As the ionospheric propagation parameters quasi-MUF, -LUF are not known from these five frequencies alone, but there is a certain positive correlation between the width of the frequency transmission range and the mean field strength F in the calculations, the "band characteristic figure (BK)" is used:

$$BK = F.$$

From this the relative band characteristic figure is formed as the ratio

$$BK_r = \frac{\overline{BK}}{BK_{rot}}$$

with \overline{BK} = average of BK over a day or night period, respectively, for the respective propagation path, BK_{rot} = average of BK over the preceding 27 days (=1 solar rotation). Positive phases related to the 27-day running average are then defined by $BK_r > 1$ and disturbances by $BK_r < 1$, while $BK_r = 1$ corresponds to normal conditions. The BK_r values are multiplied by 6 (the corresponding normal value on the forecasting scale 1-9) in order to form values which are more comparable to the forecasts. These propagation quality

indices $G = 6 \cdot BK_p$ are tabulated for the daytime and nighttime periods of the circuit Canada-Germany. Here "day" means the period during which the day frequencies can normally be used in the direction concerned, and "night" the period during which the night frequencies can be used. These periods are determined by sunrise and sunset at both terminals of the circuit. The indices are evaluated to the nearest fifth of a unit. See B. Beckmann, "Positive Phases and Disturbance of the Ionospheric Wave Propagation in Comparison with Solar-Terrestrial Events", Paper No. 25, *AGARD Conference Proceedings No. 49, Ionospheric Forecasting*, edited by Vaughn Agy, Institute for Telecommunication Sciences, Office of Telecommunications, Boulder, Colorado 80302, U.S.A., 1970.

DATA FOR SIX MONTHS BEFORE MONTH OF PUBLICATION

TABLE OF CONTENTS

	<u>Page</u>
<u>Solar Flares</u>	
C.1ba Standardized Data and Individual Reports	44
C.1e Flare Index	44
C.1d No-Flare-Patrol Graph	45
<u>Solar Radio Waves</u>	
C.3 Outstanding Occurrences at Fixed Frequencies	45
<u>Solar X-Ray Radiation</u>	
A.11ab Naval Research Laboratory -- Explorer 37	53
<u>Solar Proton Monitoring</u>	
A.12ab,A.12aa Explorer 43	53
D.1e <u>Magnetograms of Geomagnetic Storms</u>	57

SOLAR FLARES (C.1ba, C.1e, C.1d)

Confirmed and Unconfirmed -- Beginning with flare data for January 1968, the flare reports published in the sixth month after observation are divided into two tables as described below. In one of the tables is collected the most homogeneous and reliable flare data. The remaining data appear in the second table. (See pages 8 and 9 of this text for description of the column headings).

This change has been made possible through close cooperation with G. Olivieri, Observatoire de Paris, 92 Meudon, France, who prepares the flare listing for the *IAU Quarterly Bulletin on Solar Activity* (QBSA). The cooperation of NOAA with the Meudon Observatory involves effective sharing of the work and responsibilities in preparing the flare compilations for publication in these monthly *Solar-Geophysical Data* reports and in the *IAU Quarterly Bulletin on Solar Activity*. Data analysis programs have been prepared at Meudon by R. Servajean and at Boulder by C. Sawyer and C. McLellan. The data appearing in these reports will thus be coordinated with the data appearing in the QBSA.

Raymond Michard of Meudon developed the filtering technique for determined "confirmed" flares based on a comparison of reports from the station, or stations, which see a flare (positive reports) and stations who do not see it, although observing at the same time (negative reports).

Both types of reports are weighted according to the observing technique in use at each station and according to the continuity of its patrol at the supposed time of the event. For a reported flare to be rejected from the QBSA, the total weight of negative reports should exceed the total weight of positive reports by a factor larger than two. However, the flare events reported by at least 3 stations are accepted without any filtering. Negative reports are weighted depending on whether or not they contain the maximum. Also visual stations are given only half weight.

The first table, entitled "Confirmed", contains the flares that will be published in the *Quarterly Bulletin* with mean parameters that will differ slightly from those in *Solar-Geophysical Data*, and in addition contains the subflares confirmed by the NOAA grouping program. These latter are indicated by two minus signs preceding the brightness letters. The second table, entitled "Unconfirmed", contains all of the remaining individual observatory reports and the corresponding group reports. When this program was first started, the second table was entitled "Small or Unconfirmed" since it then contained the "Confirmed" subflares that were faint or of less than 1 heliographic square degree as well as the "Unconfirmed" events.

Reports of the same flare from different observatories are listed together, and headed by the summary "group report" (GRP) that gives average values for each quantity. The principal criteria for grouping reports together are position and time of maximum. Each maximum time reported by at least two observatories forms the basis of a separate group description, but a single group number is assigned to several group reports when they describe successive maxima of a single flare. The maximum reported by the largest number of observatories appears first. The mean importance of secondary maxima is marked with an asterisk.

On the Group line under "Remarks" are given the number of observatories reporting the maximum, the number of values entering the average importance, the number entering the average measured area and the number of observatories patrolling the sun at time of maximum. In cases of multiple maxima the "Remarks" apply only to that maximum with which the entry appears and not to the entire flare event. A line of explanation has been added before each flare event having more than one maxima. The total number of stations reporting at least one maximum of the event is given. The number of stations observing at the time of the principal maximum, but not reporting the event, is given in the second statement. For some months, the averages are obtained by correcting each reported value of importance and of measured area by an amount that depends on the reported value, the position of the flare on the solar disk, and the reporting observatory. Grouping and averaging are done by an electronic computing machine. The rules have been changed from time to time, so these data are not completely homogeneous.

Intervals when no observatory reported patrol observations are listed chronologically in the table. Discrepancies noted by the grouping program that might indicate an error in the report are listed at the end of the table, and the reported value questioned is marked by an asterisk to the left of the report in question.

Flare Index -- The daily flare index, calculated from the confirmed flares, is defined as

$$I_f = \frac{7600}{T^*} \sum A_d^2$$

where individual flare areas A_d are measured in square degrees and T^* is the effective observing time in minutes. Only those confirmed flares of greater than 1 square degree in area, as included in the *IAU Quarterly Bulletin on Solar Activity*, are used in calculating the flare index. I_f corresponds closely to the flare index developed at the High Altitude Observatory to measure the integrated intensity of

flare radiation. The flare areas are not corrected for geometric foreshortening, so the definition of I_f places great weight on large flares, located near the center of the sun's disk. Characteristics of the index I_f are discussed in more detail in the paper by C. Sawyer "Daily Index of Solar Flare Activity" [*J. Geophys. Res.*, 72, 385, 1967].

The table lists the date, index and actual hours of observation included in the calculation and follows the table of Confirmed Solar Flares.

A regional flare index is described in the text for the data for seven months before month of publication on page 61.

Patrols -- Following the tables a graph of the intervals of no flare patrol observation for all the observatories included in the total patrol is given. The graph is divided into visual and cinematographic patrols. (See page 9 for more detail.)

S O L A R R A D I O W A V E S (C.3)

Outstanding Occurrences -- There have been many requests to publish not only the data from the western hemisphere but also the data from the whole world. Data flow to World Data Center A for Solar-Terrestrial Physics is such that all these data are only available for publication in the sixth month after observation. Therefore, beginning with data for January 1969, all of the outstanding occurrences at fixed frequencies, reported world-wide, are published in these reports *Solar-Geophysical Data, Part II*.

In the table bursts reported from different observing stations are joined by brackets when they occur near the same time. Each set of brackets may not always include all of the solar event. The frequency in MHz precedes the abbreviated station name. Following the name is given the type of event. For each event start and maximum phase in UT, duration in minutes, and peak and mean flux densities in $10^{-22} \text{Wm}^{-2} \text{Hz}^{-1}$ are listed. From time-to-time illustrations of selected outstanding bursts will be included.

The key for identifying type of event is as below:

1 = Simple 1	22 = Simple 3F	32 = Absorption
2 = Simple 1F	23 = Simple 3AF	40 = Fluctuations
3 = Simple 2	24 = Rise	41 = Group of Bursts
4 = Simple 2F	25 = Rise A	42 = Series of Bursts
5 = Simple	26 = Fall	43 = Onset of Noise Storm
6 = Minor	27 = Rise and Fall	44 = Noise Storm in Progress
7 = Minor +	28 = Precursor	45 = Complex
8 = Spike	29 = Post Burst Increase	46 = Complex F
20 = Simple 3	30 = Post Burst Increase A	47 = Great Burst
21 = Simple 3A	31 = Post Burst Decrease	48 = Major
		49 = Major +

The code name used in this publication to identify the station, its alternate station names if appropriate, the geographic coordinates, and frequencies in MHz on which the station reports are presented in the table on page 47.

Reports will normally be received from all of these stations. Details of some of the observatories are published here as an indication of the equipment and description of burst types used.

From time-to-time selected solar noise bursts are illustrated.

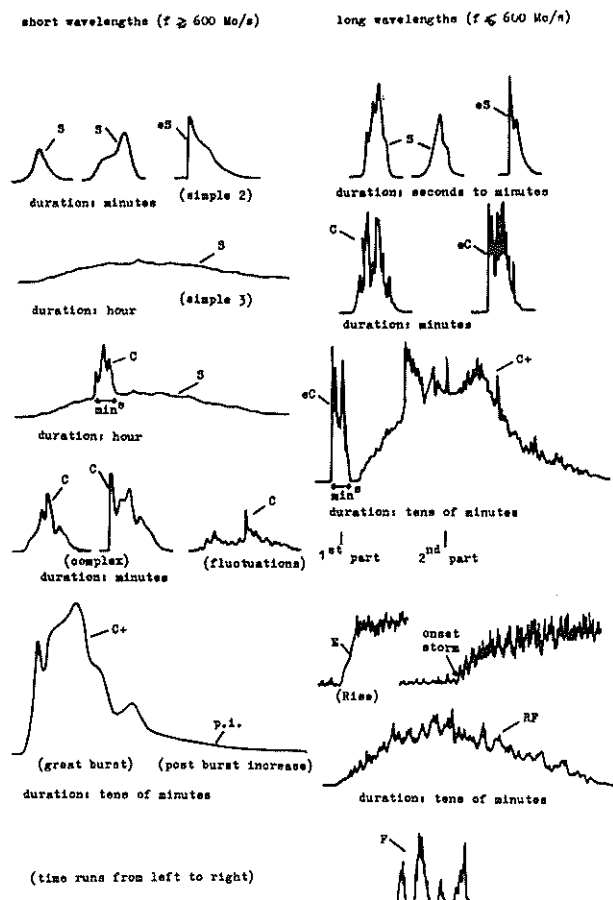
Details of Observatories -- 35000, 15400, 8800, 4995, 2695, 1415, 606, 410 and 245 MHz, Sagamore Hill -- The Sagamore Hill Solar Radio Observatory (42°37'54.36"N; 70°49'15.15"W) of the Air Force Cambridge Research Laboratories began operating a fixed frequency solar patrol at 8800, 4995, 2695, 1415 and 606 MHz in 1966. The patrol was extended to 15400 MHz in 1967, to 35000 and 245 MHz in 1969, and to 410 MHz in early 1971. Certain portions of the project were funded by the AFCRL In-House Laboratory Independent Research Fund. The observational part of the program is carried out with the help of the Air Weather Service which maintains a detachment at Sagamore Hill for this purpose.

High accuracy of the background sun is stressed at all frequencies. It is felt that accuracies of between ± 3 to 10% are being routinely met. (A recently completed study on solar absolute calibration employing all available data and special tests [Tanaka, H., et al., "Absolute calibration of solar radio flux density in the microwave region," *Solar Physics*, 29, 243-262, 1973] seems to suggest that flux densities reported by observers of the lower to mid-centimeter wavelength range have been consistently high by perhaps 10%. The Sagamore Hill group prefers to continue its present data calibration through at least sunspot minimum, before suggesting any corrections to its published data). The patrol provides data on the spectra of bursts which are studied for an explanation of causative mechanisms involved. To provide valid flux measurements, low resolution antenna systems are employed as required. To this end, four separate multi-frequency solar tracking antenna systems with five parabolas are employed as follows:

245 MHz	28-ft parabola
410 MHz	
606 MHz	28-ft parabola
1415 MHz	
2695 MHz	8-ft parabola
4995 MHz	
8800 MHz	
15400 MHz	3-ft parabola
35000 MHz	1.5-ft parabola

In some instances, notably at 1415, 4995 and 8800 MHz, necessary beam broadening is effected by feed design and under illumination. Corrections are employed to convert apparent quiet sun fluxes to true fluxes when required.

All receivers are essentially "Dicke" radiometers. Several different configurations are used; systems at 2695 MHz and above operate in a dual sideband mode where the local oscillator setting is designated as the nominal operating frequency. In these instances, the I.F. bandwidth is about 8 MHz. The system at 1415 MHz operates in a single sideband mode with the addition of a passive R.F. filter. The I.F. bandwidth is 8 MHz and the L.O. is set at 1445 MHz. Systems at 245, 410 and 606 MHz operate in a single sideband mode with an I.F. bandwidth of 1 MHz to cope with local interference and T.V. encroachment. All systems except that at 35 GHz operate with an I.F. of 30 MHz. The 35 GHz system uses 60 MHz.



Classification of distinctive events.

Solar Radio Observatories
(Fixed Frequency Observations)

CODE NAME	STATION	ALTERNATE NAME	GEOGRAPHIC		FREQUENCIES REPORTED (MHz)
			LAT	LONG	
ABST	Abastumani		42N	43E	221
ARCE	Arcetri		44N	11E	9285, 2830, 1420
BERL	Berlin-Adlershof		52N	13E	9500, 3000, 1490
BERN	Berne		47N	07E	10500
BORD	Bordeaux	Floriac	44N	01W	930
BOUL	Boulder		40N	105W	18 (Univ. of Colo.) 4995, 2695, 1420, 245 (NOAA)
CANR	Canary Island		28N	15W	4995, 2695, 1420
CRIM	Simferopol	Crimea	44N	34E	3100
CRON	Carnarvon		25S	114E	4995, 2695, 1420
DWIN	Dwingeloo		53N	06E	315, 283
GORK	Gorky	Zimenki	56N	44E	9100, 2950, 950, 650, 200, 100
HARS	Harestua	Blindern	60N	10E	225
HIRA	Hiraiso		36N	140E	500, 200, 100
HUAN	Huancayo		12S	75W	9400
IRKU	Irkustsk	Siberian IZMIR	52N	104E	9750
IZMI	Moscow IZMIRAN	Krasnaja Pakhra	55N	37E	210
KIEL	Kiel		54N	10E	1420, 420, 240
KIEV	Kiev		50N	30E	550, 204
KISV	Kislovodsk		43N	42E	15000, 6100
MANI	Manila		14N	121E	8800, 4995, 2695, 1415, 606
MCMA	McMath-Hulbert		42N	83W	18
ONDR	Ondrejov		49N	14E	9400, 808, 536, 260
OTTA	Ottawa ARO	Algonquin	45N	78W	2800
PENN	Penn. State Univ.		41N	78W	10700, 2700, 960
PENT	Penticton		49N	119W	2695
POTS	Potsdam	Tremsdorf	52N	13E	510, 234, 113, 23
SANM	San Miguel		34S	58W	408
SAOP	Sao Paulo		22S	46W	7000
SGMR	Sagamore Hill		52N	72W	35000, 15400, 8800, 4995, 2695, 1415, 606, 410, 245 71000, 37000, 19000, 9400, 2800
SLOU	Slough		51N	00E	
TOKO	Tokyo	Mitaka	35N	139E	17000, 612
TRST	Trieste		46N	14E	408, 237
TYKW	Toyokawa		34N	137E	9400, 3750, 2000, 1000
UCCL	Uccle	Humain	50N	04E	600
UPIC	Upice		50N	16E	30
VORO	Voroshilov	Ussurisk	43N	132E	208

Principal flux calibrations using Argon lamps in all instances except 15.4 and 35 GHz are made at about 1700 UT (meridian transit) each day, although morning and afternoon calibrations are also made. The systems below 2695 MHz were calibrated originally against the known flux of Cassiopeia A. Recalibrations are made as believed necessary. The 2695 MHz system was calibrated originally against Ottawa (2800 MHz) and Penticton (2700 MHz). Relative accuracies are maintained. Frequencies of 4995, 8800 and 15400 MHz were calibrated originally against the accurately known brightness temperature of the full moon. Procedures were repeated at 4995 and 8800 MHz in 1971.

The 35 GHz system is operated only for burst recordings. Since the variation of the S.V.C. is small at 35 GHz, it is assumed that the whole sun flux density is about 2000 flux units ($fu = 10^{-22} W m^{-2} Hz^{-1}$). Bursts are then calibrated as a percentage of the quiet sun signal and variational propagation conditions can be ignored. All flux data reported, both the daily flux and burst components, are adjusted to 1 A.U. Corrections are also made for average vertical atmospheric attenuations as follows:

15400 MHz	0.085 dB
8800 MHz	0.070 dB
4995 MHz	0.055 dB
2695 MHz	0.051 dB
1415 MHz	0.05 dB
606 MHz	0.045 dB

To "capture" and calibrate all bursts as accurately as possible at least two and sometimes three recording and radiometric audio channels are employed. Bursts are first calibrated assuming receiver linearity and then adjusted from correction curves periodically revised and/or from peak calibration matching of signal generator output referred to calibrated Argon lamps.

All 606 MHz data must be multiplied by 0.91 as determined in 1966 for most probable absolute values.

Outstanding occurrences are listed according to the morphological classification of bursts as described in the *IQSY Instrument Manual No. 2*, Solar Activity (July 1963) and by the Ottawa classification of 10.7 cm bursts, conventionally extended to all centimeter wavelength bursts.

A summary of several corrections appropriate for the data before 1972 and previously listed in various issues of *Solar Geophysical Data* and *Descriptive Texts* was given in the Number 330 (Supplement) of February 1972.

10700, 2700 and 960 MHz Pennsylvania State University -- The Pennsylvania State University Radio Astronomy Observatory (PSURAO) is conducting a daily solar patrol at 10.7 GHz, 2.7 GHz, and 960 MHz. The purpose of the patrol is to obtain correlated flux density measurements with special emphasis on solar bursts.

The antennas for the three radiometers are mounted on a single polar tracking mount located on the roof of the observatory. The 10.7 and 2.7 GHz radiometers use 1 meter and 1.83 meter parabolic reflecting antennas, respectively, fed with horns matched to wave guides. The 960 MHz radiometer uses a dipole fed 1.8 meter parabolic reflecting antenna.

The radiometers operating at 10.7 GHz, 2.7 GHz and 960 MHz are switched superheterodyne receivers. The I.F. frequencies are 30 MHz with 8 MHz I.F. bandwidths. Both signal and image channels are used. The sensitivities of these radiometers are 2.0 fu at 10.7 GHz; 0.7 fu at 2.7 GHz; and 0.4 fu at 960 MHz [$fu = 10^{-22} W m^{-2} Hz^{-1}$].

The outputs of the radiometers are recorded on a 6 channel Sanborn recorder at a rate of 0.5 cm/min. All frequencies are recorded at two gains differing by a factor of about ten. All recordings are linear.

Eight pieces of information are usually given for distinct events. These are the date, frequency, time of start, time of maximum flux density, duration, maximum flux density, mean flux density and event type.

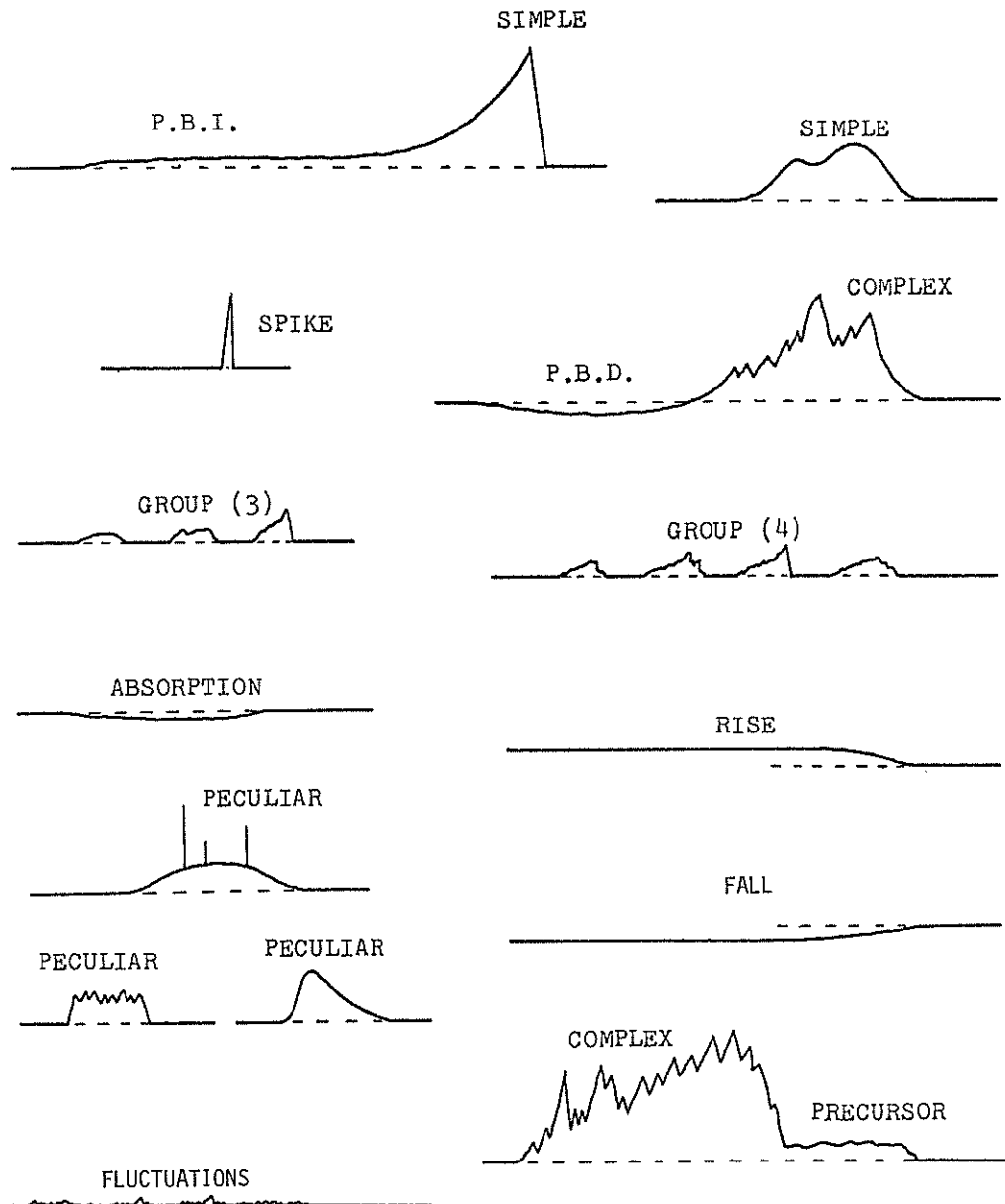
The time of start of the event is the time at which a visual inspection of the analog record indicates that a distinct change in flux density begins. The time of maximum flux density is also determined by a visual inspection of the record. These times are usually given to the nearest tenth of a minute.

The duration is the time interval between the start of the event and the moment that significant activity ends. This time interval is usually given to the nearest tenth of a minute but never to more than three significant figures.

The peak flux density is the highest level, over and above the pre-event flux density level, that is observed during the event. No adjustment for the varying earth-sun distance or absorption in the atmosphere is made. The mean flux density is the time average of the flux density during the event. These are reported to the nearest tenth of a solar flux unit [$fu = 10^{-22} W m^{-2} Hz^{-1}$], but never to more than three significant figures.

A "D" appearing after any number means that the exact value is greater than the preceding number, while an "E" means that it is less than the preceding number.

EXAMPLES PENNSYLVANIA STATE UNIVERSITY



Note: Time increases from right to left on all figures.

The classification system used by PSURAO has evolved from the one given by the *IQSY Instruction Manual No. 2 Solar Activity*. This evolution has been strongly influenced by the scheme given by Covington elsewhere in this publication. Each event is classified according to its appearance on the record only. No attempt at interpreting the physics of an event is used in its classification.

Events which are made up of smooth changes in flux density, i.e., are uncomplicated in appearance, are called SIMPLE. For frequencies greater than 600 MHz, three kinds of SIMPLE events are recognized. SIMPLE 1 events have a peak flux density (f_u) and duration (min) both less than 10.0. SIMPLE 2 events have a peak flux density (f_u) greater than both the duration (min) and 10.0, while SIMPLE 3 events have a duration (min) greater than both the peak flux density (f_u) and 10.0. For frequencies less than 600 MHz, the above distinctions are not made.

Events which show rapid changes in flux density with several prominent peaks are called COMPLEX. In practice there are not two distinct types, SIMPLE and COMPLEX; events form a continuum between the two.

An event which would normally be classified as either SIMPLE or complex, but has a peak flux density of 500 fu or more, is called a GREAT BURST.

Events which would otherwise be classified as either SIMPLE or COMPLEX, but which show some feature not usually observed, are classified PECULIAR (in the published table the key code is left blank). An example of such a feature is an unusually fast drop from an enhanced flux density level to the pre-event level, at the end of the event. Such events appear to be the mirror image of normal events.

A distinct enhancement of the flux density level immediately preceding a more intense event is called a PRECURSOR. The duration reported is the time interval from the start of the enhancement to the start of the more intense event.

An enhanced flux density level immediately following a more intense event, with a gradual decrease to the pre-event level, is called a post burst increase, P.B.I. A diminished level following a more intense event, with a gradual rise to the pre-event level, is called a post burst decrease, P.B.D.

An event which shows a rapid rise to a single peak, followed by a rapid fall to the pre-event level, with a duration of about one minute or less, is called a SPIKE. No mean flux density is given.

A series of distinct events between which the flux density returns to the pre-event level is called a group of bursts or GROUP. The individual events may be SIMPLE, COMPLEX, PECULIAR or SPIKE, and are usually of short duration, 5 minutes or less. This type is used to label events which, if handled individually, would occupy more space than their importance warrants. The interval of time from the start of the first event to the end of the last event of the GROUP is reported as the duration. The peak flux density of the GROUP and its associated time are given, but no mean flux density is computed.

A series of irregular changes in the flux density level, with no distinct grouping into individual events, is labelled FLUCTUATIONS. Only the time of start and the duration are reported.

A gradual decrease of the flux density with a subsequent return to the pre-event level is called an ABSORPTION.

Occasionally there is observed a somewhat distinct change in the flux density level with no observed return to the pre-event level. If the change is a rise in level, the event is called a RISE, while a change in the opposite direction is called a FALL. No duration or mean flux density is given.

Examples of the records of these events are given on page 49.

2800 MHz Ottawa (ARO) and 2695 MHz Penticton (DRAO) -- Enhancements of the solar radio flux from a slowly varying or a constant level during the day are listed separately as outstanding events or bursts on the basis of the classification described by Covington [*J. Royal Astron. Soc., Can.*, 45, 1951; and Paper 28, *Paris Symposium on Radio Astronomy*, 1959]. The events are from the Algonquin Radio Observatory (45°57'N, 78°03'W) and from the Dominion Radio Astrophysical Observatory (DRAO) at Penticton, B.C. (49°19'N, 119°37'W). From the beginning, the solar radio noise enhancements at 2800 MHz have been described by type names that are indicative of the general structure found from visual inspection of the records as well as by numerical values of maximum burst intensity and duration. It has been found that these types also have application for bursts observed throughout the microwave region. Recent records of solar noise bursts observed simultaneously at the two widely separated stations of A.R.O. and D.R.A.O. have led to the recognition of new variations which are sufficiently unique to be regarded as new types of bursts. Even though these events occur infrequently, they are needed in any morphological description of burst profiles and are probably associated with unique physical processes in the solar atmosphere. A summary of the burst types in use as of May 1, 1969 is provided on page 52.

The peak intensity of the microwave event ranges from a threshold value of 1 to 3 flux units to several thousand flux units, while the duration varies from a fraction of a minute to several hours. The threshold level depends upon such factors as residual receiver noise and the interference patterns produced at sunrise and sunset by the direct solar ray and one reflected from the earth. Most of the microwave events are single events with various flux variations or profiles. A large proportion show a simple smooth rise to a single peak followed by a slow decay to the pre-existing undisturbed flux level. When the intensity and duration of single-simple bursts are plotted in a graph, a two-pronged scatter of points is found. This may be numerically described by three regions designated as regions 1, 2 and 3 and corresponding numbers assigned to the bursts. These regions are outlined in the diagram provided on page 52. Simple 1 bursts have intensities less than 10 flux units and durations between 1 minute and 10 minutes (previous to January 1968 the limit was set at 7½ flux units and 7½ minutes). Simple 2 bursts have intensities greater than 10 flux units and durations ranging from 1 minute to 60 minutes depending upon the intensity. Simple 3 bursts have durations in the range from 10 minutes to several hours but with intensities seldom exceeding 50 flux units. Visual inspection of the records immediately suggests "Impulsive Burst" for describing the Simple 2 burst and "Long Enduring Burst" for the Simple 3 event. Bursts with duration less than 1 minute and with intensity much greater than the threshold noise are termed Spikes.

Single bursts with two or more prominent peaks also fall into the numerical categories outlined for the simple bursts. Such bursts with duration and intensity similar to the Simple 2 bursts are termed "Complex Bursts", while bursts with parameters similar to the Simple 3 burst are still designated as Simple 3 events. In both cases, the time of commencement and peak intensity of the various components may be described under the entry of Components.

When a number of single bursts occur in succession and the flux level returns to the steady pre-burst level for each event and remains there for durations ranging from a few minutes to several burst durations, the composite event is termed a "Group". The number of individual bursts is given, the maximum intensity of one event and the overall duration. Individual events are described as usual.

Irregularities observed in the otherwise smooth or gradual changes in a simple or complex burst are ripples, small rapid fluctuations and spikes. These are described as "Fluctuations"; they are not given any numerical values, but their presence is indicated by the addition of the letter "F" to the main descriptive term. Components of complex bursts are regarded as "Fluctuations" when the intensity is less than 15% of the main peak. Any structure of bursts in region 1 is also designated by "F" when not severely masked by the variations of the threshold.

When the complexity of a small burst is such that it is difficult to tabulate individual parts, or many rapid fluctuations blur the otherwise smooth variation of a simple or complex burst, the event is termed a "Period of Irregular Activity".

A gradual increase in flux preceding a more intense burst is designated as a "Precursor", while an enhanced level following a burst is designated a "Post Burst Increase". These may occur separately with bursts or in association with one another with respect to a more intense burst. When the precursor and post-burst increase have the same intensity, or may be smoothly joined together, the two features are combined into a "Simple type 3" burst. This type of event is designated by the letter "A". The superposition of bursts with different durations, one on top of the other, can thus be tabulated. In each case, individual component intensities of single bursts are measured and listed separately.

A moderate rise of flux from 5 to 30 minutes duration with no accompanying decline during the following hours is designated as a "Rise Only". Gradual rises of greater duration are automatically considered in the calibration levels made every three hours. A similar description holds for the "Fall Only".

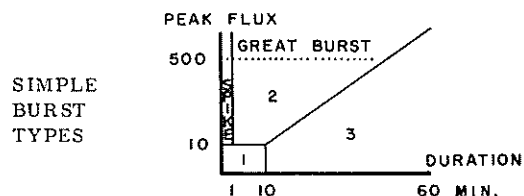
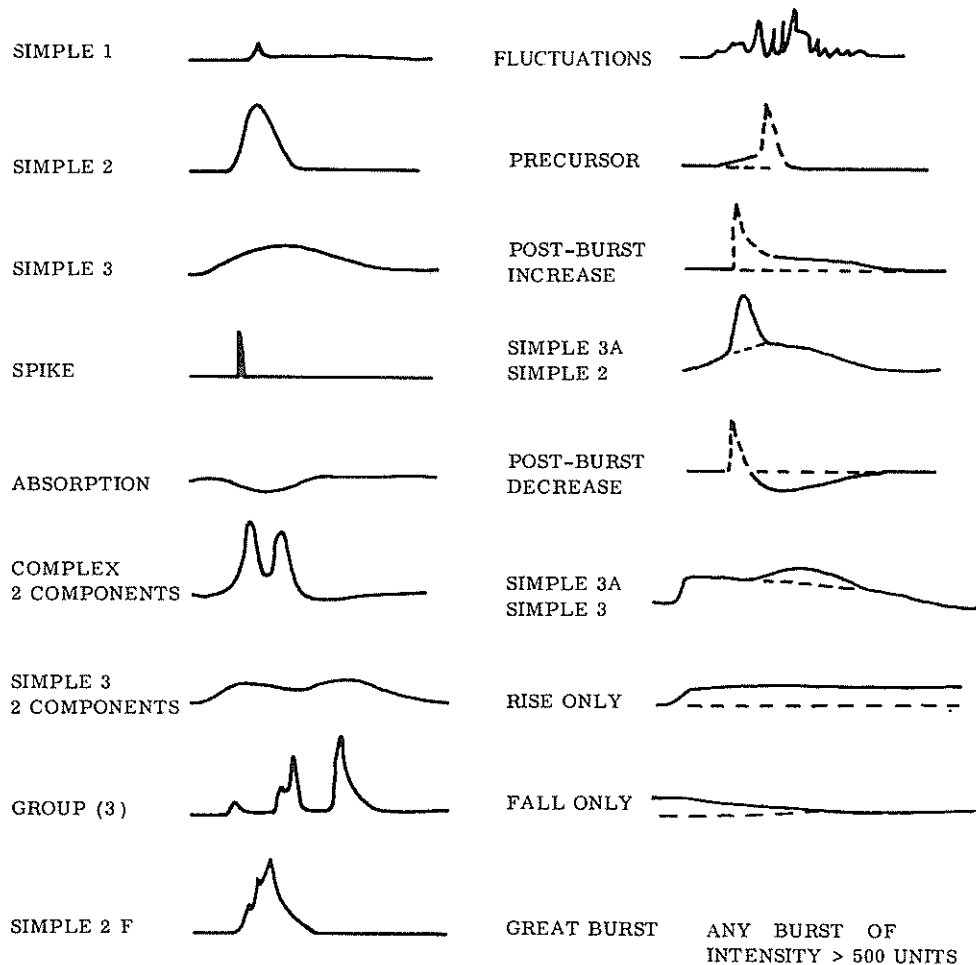
Microwave bursts with intensity greater than 500 flux units are of special geophysical interest but occur infrequently. They are described as "Great Bursts". The profiles generally exhibit great complexity; there may be an early, short duration impulsive burst followed by a second impulsive burst of comparable intensity but of greater duration. In the URANO code these great bursts are listed as Complex Bursts.

The types of bursts discussed all indicate an increase in radio emission from the sun and form the majority of events observed in the microwave region. The first clear indication of absorption occurred on May 19, 1951 as a "Post Burst Decrease" after the occurrence of an impulsive burst. The first clear indication of absorption alone occurred twice on June 20, 1967 and was recorded simultaneously at A.R.O. and D.R.A.O. These events are discussed in "Solar Radio Emission at 10.7 cm, 1947-1968" by A. E. Covington [*J. of Royal Astron. Soc. Can.*, 63, 125, 1969].

The burst peak intensity is measured in flux units without any adjustment for the varying sun-earth distance. For the smaller bursts, the errors in intensity will be only slightly greater than those entering into the calibration and estimated as $\pm 5\%$. For the more intense bursts, the errors are estimated as $\pm 15\%$. The continuous intensity scale may be replaced by using the following 9 flux intervals: below 1 unit, 1-9, 10-49, 50-99, 100-499, 500-999, 1000-2499, 2500-4999, and above 5000 [Harvey, *Astrophys. J.* 139, 16-44, 1964]. Mean flux is estimated or calculated using the listed intensity and duration and the actual burst profile for each event.

The commencement of a burst is taken when the enhancement of the flux shows a departure from the steady level of approximately 1 flux unit. For many of the bursts, this may be determined to within a few seconds with the exception of some of the long enduring bursts which have been described as "Gradual Rise and Fall" bursts. For these the uncertainty in determining the start may be as great as 5 minutes. The letter "E" appearing after the time of start indicates that the burst was already in progress at this time. Profiles of typical bursts are produced on page 52.

MICROWAVE BURST TYPES - 2695 MC/S - OTTAWA, CANADA



TYPE OF SIMPLE BURST DESIGNATED BY
NUMBER OR DESCRIPTION ASSIGNED TO
REGION CONTAINING THE MAGNITUDE
OF PEAK FLUX AND THE DURATION

SOLAR X-RAY RADIATION (A.11ab)

Naval Research Laboratory — SOLRAD 9 (1968-17A) -- The graphs presented are a pictorial display of the solar X-ray flux in the 0.5 to 3Å, 1 to 8Å, and 8 to 20Å bands as measured by ionization chambers aboard the Naval Research Laboratory's SOLRAD 9 satellite (Explorer 37). The data were stored in the satellite's memory with a time resolution of one minute. Hourly averages of these data have been published in the second month after observation in *Part I* of these *Solar-Geophysical Data* reports. A complete description of the SOLRAD 9 satellite can be found in NRL Report #6800, titled *The NRL SOLRAD 9 Satellite, Solar Explorer B, 1968-17A*.

Each plot gives the solar X-ray data for one complete day (UT). The date of each plot is given by the six-digit number, denoting year, month, and day, at the top of the plot. The integers scaling the abscissa of each plot represent the hours of Universal Time (UT). Except for the lowest cycle, the ordinate of the plot is logarithmically scaled in X-ray flux units of ergs/cm²-sec multiplied by the indicated power of ten. The units of the lowest cycle are digital counts which indicate charged particle interference with the X-ray experiments.

A point is normally generated at every minute on the plot for each detector and the background of the 0.5 to 3Å experiment. Lines are drawn connecting data points for each experiment. The lines are continuous until two data points in succession are missing and then a break in the line occurs. In each plot, the top curve represents the solar X-ray data from the 8 to 16Å ionization chamber, and the next lower curve represents data from the 1 to 8Å ionization chamber. A 2×10^6 K graybody solar emission spectrum [Kreplin, R. W., *Annales de Geophysique*, 17, 151, 1961] is used in converting from detector current to energy flux in the 8 to 20Å and 1 to 8Å bands. The third curve from the top represents solar X-ray data from the 0.5 to 3Å ionization chamber. A 10×10^6 K graybody solar emission spectrum is used in obtaining the 0.5 to 3Å energy flux values. Since the 0.5 to 3Å band solar emission is generally below the threshold level of the detector, the curve representing these data will be quite intermittent, and completely missing at times.

Gaps which occur simultaneously in all data lines are indicative of satellite night. At time, the x-ray flux data point immediately before (or after) a gap due to satellite night will be much lower than preceding (or subsequent) points. This is caused by attenuation of solar x-rays by passage through the Earth's atmosphere as the satellite passes from sunlight to darkness (or emerges from darkness into sunlight).

Charged-particle interference with the X-ray detectors, which can cause the plotted flux levels to be higher or lower than the actual flux, is indicated by the lowest data line. The ionization chamber current caused by the charged particle background is digitized and recorded as a "count". The number of counts is linearly related to the current generated in the 0.5 to 3Å ionization chamber by penetrating charged particles when the detector is facing away from the sun. Counts of 10 to 15 indicate no particle interference with the detectors. Counts of 20 to the maximum value of 127 indicate increasing amounts of particle interference. Data obviously contaminated by particle interference are not plotted, and this causes randomly spaced data gaps of 30 minutes or less, especially in the 0.5 to 3Å and 1 to 8Å data curves. However, when extremely large solar flares occur, the 0.5 to 3Å amplifier is driven into saturation and cannot recover before the background data sample is taken. This causes a high reading in the "Background Counts" curve which is not due to particle contamination.

At times, the energy flux curves look like step functions. This occurs when the energy flux represented by a single digital count in the analog-to-digital conversion is a significant fraction of the total solar flux at that time.

The flux values presented in the plots are all based on graybody solar emission spectra and assume a constant solar temperature for the solar source region whether the region is relatively quiet or a solar flare is in progress. These assumptions may be inadequate for quantitative correlations, especially in ionospheric research. A method for converting the SOLRAD 9 constant source temperature, graybody-spectrum based values for the 0.5 to 3Å and 1 to 8Å bands to values based on a variable source temperature and an emission spectrum which considers thermal bremsstrahlung and radiative recombination mechanisms and line emission can be obtained from: Dr. D. M. Horan, Code 7125.7, Naval Research Laboratory, Washington, D. C. 20390, U.S.A.

SOLAR COSMIC RAY PROTONS (A.12aa, A.12ab)

Solar Proton Monitoring Experiment (SPME) -- The Solar Proton Monitoring Experiment (SPME) is a joint effort by C. O. Bostrom and J. W. Kohl of the Johns Hopkins University Applied Physics Laboratory and D. J. Williams of the NOAA Space Environment Laboratory. The personnel listed above are those responsible for the construction, spacecraft integration, (JHU/APL) and calibration of the experiment and the data reduction, handling and presentation (JHU/APL and NOAA) of the monitor data. The initial conception, design, and proposal of the SPME were carried out by C. O. Bostrom, D. J. Williams, D. E. Hagge and F. B. McDonald.

The SPME was successfully launched aboard the NASA satellites Explorers 34 (IMP-F, 1967-51A) and 41 (IMP-G, 1969-53A) on May 24, 1967 and June 21, 1969, respectively. Explorer 34 reentered the earth's atmosphere on May 3, 1969 and Explorer 41 reentered on December 23, 1972. Continuous data from the SPME have been presented for the lifetimes of Explorers 34 and 41. Similar equipment was launched aboard Explorer 43 (IMP-I, 1971-19A) on March 13, 1971. These data were used to supplement the Explorer 41 data through 1972 and continue as the sole source at present.

The primary purpose of the SPME is to provide systematic monitoring of solar cosmic rays over at least half a solar cycle. The basic requirements set forth for such a monitoring program were:

- 1) to furnish simple reliable flux and spectral measurements.
- 2) to operate over a wide flux range and in particular provide coverage for very large events,
- 3) to provide a simple and easily reproducible detector system to form the basis of an operational monitoring program.

The SPME satisfies the above requirements. Data from the experiment are continuously being made available to the scientific community through *Solar-Geophysical Data*.

The SPME consists of an array of solid state detectors designed to measure proton intensities in the following energy ranges: $E_p \geq 10$ Mev, $E_p \geq 30$ Mev, and $E_p \geq 60$ Mev.

Since the overall design goal was to obtain a standard, reliable and easily reproducible detection scheme specifically aimed at monitoring solar cosmic rays, the method chosen was to use separate detectors for each energy range and to employ combinations of discriminator levels and shielding thicknesses to define the energy response of each channel. Such a method allows for accurate absolute flux determinations and for unit to unit comparisons when using a series of payloads to monitor the solar flux over an extended time period (≥ 0.5 solar cycles).

The following table indicates the SPME response to alpha particles which will introduce an ambiguity in the solar proton flux observations. To estimate the size of this uncertainty reproduced as Figure 1 is Figure 29-5 from Fichtel [Part 29, *Proceedings of AAS-NASA Symposium on the Physics of Solar Flares*, Oct. 1963, edited by W. N. Hess, NASA SP-50] which shows the proton to helium nuclei ratio observed during 1960 as a function of energy per nucleon. From this figure it is seen that a maximum uncertainty of $\sim 10\%$ may be expected due to the alpha particle flux at the energies shown in Figure 1.

Proton and Alpha Particle Energy Sensitivities of SPME

Channel	E_p	E_α
1	≥ 60 Mev	≥ 240 Mev
2	≥ 30 Mev	≥ 120 Mev
3	≥ 10 Mev	≥ 40 Mev

A more detailed description of the detectors follows.

Channel 1 ($E_p \geq 60$ Mev) and Channel 2 ($E_p \geq 30$ Mev):

Each of these two higher energy channels consists of three solid state detectors mounted on orthogonal axes and surrounded by a hemispherical shield. Figure 2 shows the assembly of these units. This arrangement is a straightforward method of obtaining a large area and a relatively smooth geometric factor when using disk shaped detectors.

The shielding thickness is by far the most important factor in determining the energy threshold in this particular arrangement. The thicknesses used are 5.6 mm Cu and 1.6 mm Cu and are indicated in Figure 2.

The detectors used in this assembly are surface barrier solid state detectors, fully depleted, 700 microns thick, having a usable surface area of 0.83 cm^2 and a noise level nominally < 20 kev at the operating bias voltage. These units fully deplete at < 150 volts and are operated at 200 volts.

The three detector outputs are fed in parallel to a preamp-amplifier-discriminator package and thence to the data processing electronics. Three 20 kev detectors yield a total detector noise level of ~ 35 kev in channels 1 and 2. This coupled with a preamp noise level of 25 kev yields a measured total system noise level of ~ 40 kev.

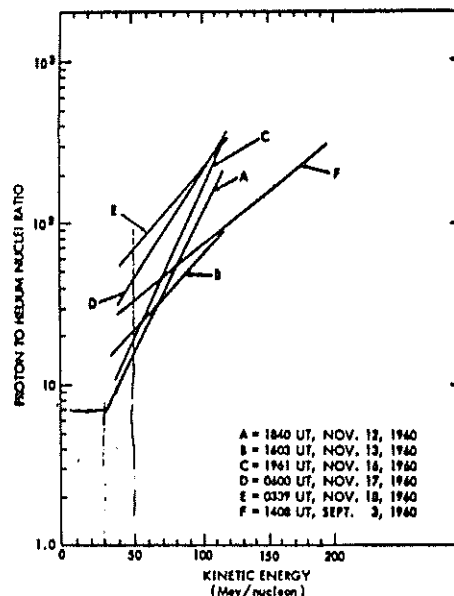


Figure 1

At minimum ionizing energies, the proton energy loss in 700 μ of silicon is ~ 280 kev. A discriminator bias level of 150 kev is both well below the minimum ΔE_p of 280 kev and well above the system noise level of 40 kev. The 150 kev discriminator level causes but a negligible shift of the energy threshold (<10 kev). Also, the response of the unit is relatively independent of discriminator level shifts.

Due to the high bias levels, the shielding thicknesses and mode of operation radiation damage effects will be negligible for several years for channels 1 and 2.

Channel 3 ($E_p \geq 10$ Mev):

This detector consists of a 3 mm cubic Li drifted solid state detector surrounded by a 170 mg/cm² (0.63 mm) Al shield. Figure 3 is a diagram of this unit.

The detector has a noise level of <50 kev at its operating bias of 200 volts. The discriminator level of 300 kev will raise the energy threshold ~ 25 kev. Radiation damage effects in channel 3 will be negligible for at least a year.

All data from the SPME published as monitoring data satisfy the following requirements:

- 1) final orbit determinations have been made,
- 2) final time corrections have been made,
- 3) all data quality flags indicate that the individual data point is "good".

Data that satisfy these requirements are then used to construct hourly averages of the respective energy channels. The ≥ 60 Mev and ≥ 30 Mev channels are sampled for 19.2 seconds once every 2 minutes 43.8 seconds. The ≥ 10 Mev channel is sampled twice every 2 minutes 43.8 seconds at 19.2 seconds per sample. Thus the maximum number of points in an hourly average is 22 for the ≥ 60 Mev and ≥ 30 Mev channels and 44 for the ≥ 10 Mev channel. If the number of "good" data points is less than 5 the hourly average is not constructed.

These hourly averages are then tabulated in a grid where the hours of the day run to the right and the days of the month run from top to bottom. The day is identified as both day of the month and day of the year. The tabular entries are nominally four characters each. The decimal point will be automatically shifted to the right as the intensity increases until it finally disappears when the intensity is ≥ 1000 protons cm⁻² sec⁻¹. If the intensity becomes $\geq 10,000$ protons cm⁻² sec⁻¹, the blank space between columns is utilized so that intensities up to 99,999 protons cm⁻² sec⁻¹ may be accommodated. The entries all begin with a low intensity format of 0.XX. The following is an example of how the entries appear for an intensity increasing from 0.55 protons cm⁻² sec⁻¹ to 55000 protons cm⁻² sec⁻¹:

0.55
5.50
55.0
550
5500
55000

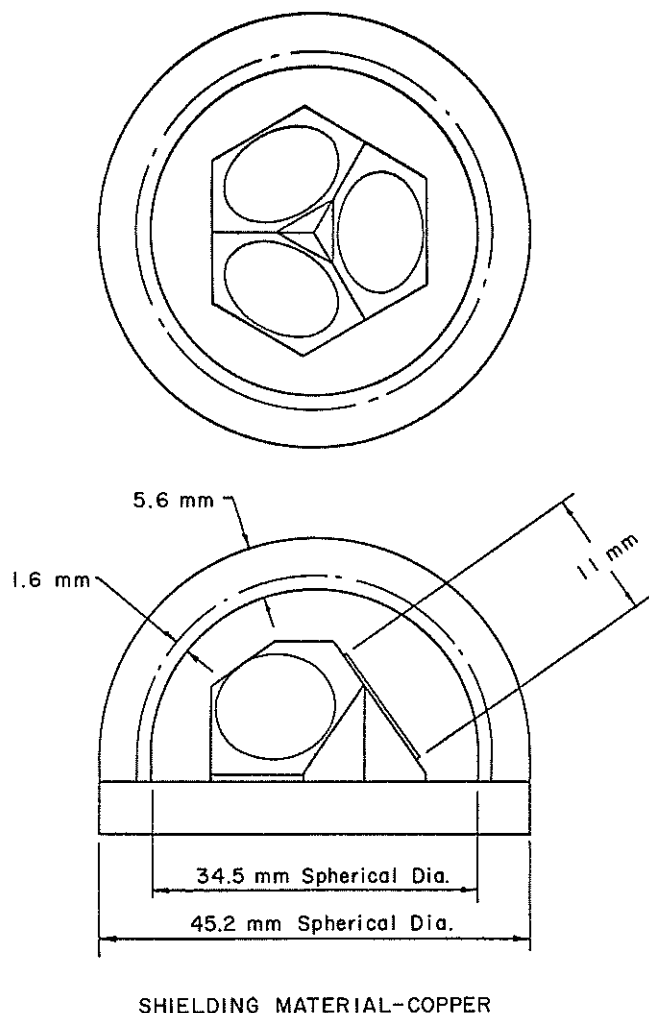


Figure 2

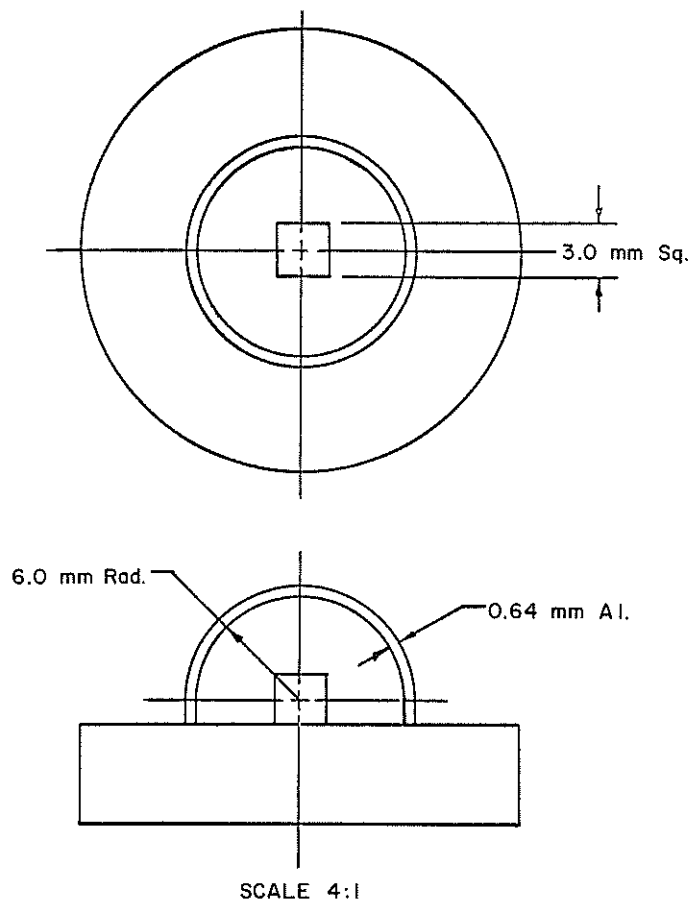


Figure 3

The hourly averages are also plotted vs. time in monthly blocks. The plots of hourly averaged fluxes for the various channels should also be self-explanatory. The two plots below the plot of flux values are included to show the satellite position in orbit at the time of the flux measurement. The lower plot is simply a projection of the orbit on the ecliptic plane with the lower circle representing the earth and the upper circle the sun. For example, during September 11, 1967, the semi-major axis of the Explorer 34 (IMP-F) orbit projected to the earth-sun line (see plot for September 1967 in the March 1968 *Solar-Geophysical Data*).

The middle plot (which resembles a fully rectified sine wave) shows the radial distance to satellite as a function of time. At the cusps, the satellite is at perigee, and at the crests the satellite is at apogee. Respective apogees for Explorers 34 and 41 are $\sim 34R_E$ and $\sim 28R_E$. The vertical scale is linear. Note the response of the detectors to the radiation belts at perigee; this shows up very clearly in the ≥ 10 Mev channel and is usually but a very few high points for the ≥ 60 Mev and ≥ 30 Mev channels.

The response of the ≥ 10 Mev channels in the radiation belts is very noticeable since this channel also responds to electrons of energy ≥ 515 kev. This low an electron energy threshold makes this channel respond to the radiation belt for a much larger radial extent (at times out to 10 earth radii) than channels 1 and 2 whose electron thresholds are several Mev in energy. The actual time profiles, due to the radiation belts, displayed by the ≥ 10 Mev channel on the hourly plots are highly variable due to the great variations in these trajectories through the trapping regions.

The flux values listed and plotted are accurate to $\pm 25\%$ for the ≥ 60 Mev and ≥ 30 Mev channels and to $\pm 50\%$ for the ≥ 10 Mev channel only during the times of solar cosmic ray events.

The directional factor becomes more nearly 4π for galactic cosmic rays due to their much higher characteristic energy. Therefore, the background fluxes which are due to galactic cosmic rays are incorrect as shown on the plots. These have not been corrected because more accurate start times and initial fluxes for solar events may be obtained if the detector response is seen to rise from its own background.

The ≥ 60 Mev and ≥ 30 Mev channels indicate a similar background flux whereas the ≥ 10 Mev channel shows a slightly different background flux value. This is due to differences in i) edge effects in a cube versus disk detector, and ii) differences in satellite shielding. These effects are more important at galactic cosmic ray energies than at the solar cosmic ray energies of this experiment.

MAGNETOGRAMS OF GEOMAGNETIC STORMS (D.1e)

In the past the Kp and Ci indices have provided some information on geomagnetic disturbances. However, during the last few years there has been an increasing demand for more quantitative indices with finer time resolution and based upon records from a more suitable distribution of observatories. The indices Kn, Ks, and Km have been developed and continue to satisfy the requirement for 3-hourly indices of activity as observed at mid-latitude locations. Both the Dst and AE indices have been devised to fulfill the need for quantitative indices having finer time resolution. Dst provides an estimate of the field of the ring current although ignoring its asymmetry. AE provides an estimate of the field of the auroral electrojets.

Recent progress in magnetospheric physics has made it clear that a comprehensive study of the asymmetric growth of the ring current belt is essential in understanding the mechanism of its formation and the generating mechanism of magnetospheric storms as well. For this purpose, Dst is not necessarily the most suitable index. Auroral electrojets have a lifetime of order one to three hours and the increasing availability of 2.5-min AE(11) provides indices having excellent time resolution for the study of these high-latitude magnetic variations. However, the delay inherent in acquisition and processing of all magnetograms used in deriving AE(11) and the desirability of including a record of magnetic variations at mid-latitude and equatorial locations suggest that no combination of indices are completely self-sufficient.

For these reasons, actual records of magnetic variations at a number of observatories are still very useful. In this publication, one or two interesting geomagnetic events are chosen for each month and are illustrated by reconstructed H-component magnetograms. The magnetograms have been reduced from the original records to display the same amplitude scale and time base. It is planned to include reduced magnetograms from about 10 of the 16 observatories listed below although delays in receipt of some magnetograms may necessitate using records from substitute stations. If an adequate coverage of auroral zone observatories is available, preliminary AU and AL graphs will also be prepared for each event. No reduced magnetograms will be prepared for months having activity of only minimal interest.

Table of Observatories

	Geog. Coord.		Geomag. Coord.			Geog. Coord.		Geomag. Coord.	
	Lat.	Long.	Lat.	Long.		Lat.	Long.	Lat.	Long.
Narssarssuaq	61.20	314.60E	71.21	36.79E	Dixon Island	73.55	80.57E	63.02	161.57E
Leirvogur	64.18	338.30	70.22	71.04	Tixie Bay	71.58	129.00	60.44	191.41
Fort Churchill	58.80	265.90	68.70	322.77	Tashkent	41.33	69.62	32.33	144.02
Barrow	71.30	203.25	68.54	241.15	San Juan	18.12	293.85	29.60	03.12
Great Whale River	55.27	282.22	66.58	347.36	Kakioka	36.23	140.18	26.02	205.95
Cape Chelyuskin	77.72	104.28	66.26	176.46	Honolulu	21.32	202.00	21.07	266.53
Abisko	68.36	18.82	66.04	115.08	Davao	07.08	125.58	-04.05	294.50
College	64.87	212.17	64.63	256.52	Tangerang	-06.17	106.63	-17.64	175.44

These reduced magnetograms and index graphs are now produced by J. H. Allen and H. Kroehl of the National Geophysical and Solar-Terrestrial Data Center from magnetograms furnished by the World Data Center A for Solar-Terrestrial Physics. From January 1967 until the present Dr. S.-I. Akasofu was responsible for supplying these records.

DATA FOR SEVEN MONTHS BEFORE MONTH OF PUBLICATION

TABLE OF CONTENTS

	<u>Page</u>
H.62 <u>Abbreviated Calendar Record</u>	60
C.1f <u>Flare Index (by Region)</u>	61

ABBREVIATED CALENDAR RECORD (H.62)

The Abbreviated Calendar Record is a monthly summary chronological account of solar and geophysical activity and events published in the seventh month after observation. It is intended to give a background for the early interpretation of solar-geophysical results. It continues the series published in *IQSY NOTES* beginning with data for January 1964 in No. 7, through data for December 1966 in No. 21, and for January 1967 through November 1968 in *STP Notes* No. 1-3, 5, and 7. (A Condensed Calendar Record has continued in *STP NOTES*, data for December 1968 through April 1971 were published in Nos. 7-10.) It is similar to the Calendar Record compiled for the IGY and IGC-1959 [*Annals of the IGY*, Vol. 16] and compiled for 1960-1965 [*Annals of the IQSY*, Vol. 2]. It is prepared from data reports available at the World Data Center A for Solar-Terrestrial Physics. However, it is compiled rapidly, including some provisional data, and should not be relied on for details of solar and geophysical events in preference to standard publications.

The format is as follows:

The period covered on each date is 0000 to 2400 UT (Universal Time). At the beginning of each month will be a chart of the sun for the month locating the calcium plages, as reported by the McMath-Hulbert Observatory, at the latitude and longitude of their Central Meridian passage by the last two digits of the plage serial number. The general activity of the region is approximately evaluated, mainly from area and intensity of plage and associated sunspots, by use of the symbols: G = great activity, M = moderate activity and S = small activity. Beginning with September 1973 data this is superimposed on the revised (when time permits) H α synoptic charts as originally published at the beginning of the second section of Part I (Prompt Reports).

For each date a series of time lines are presented. In the first block the duration of flares of importance $\geq 1f$ is shown by a horizontal line, followed by the importance with a slant line separating the last two digits of the serial number of the calcium plage region in which the flare occurred. These are selected from the grouped flare reports as published in these *Solar-Geophysical Data* reports. Only the flares in the confirmed list are used. Under the word "FLARES" is given the daily flare index (see page 44 of this text) and the hours of flare patrol on which the index is based. Fixed frequency solar noise bursts are indicated by vertical tick marks by wavelength (frequency) range at the time of beginning of the burst. The ranges are defined as dekameter = <40 MHz, meter = 40-400 MHz, decimeter = 400-1500 MHz, and centimeter = >1500 MHz. Spectral events of types II and IV are shown at the time of beginning by the appropriate Roman numeral. Noise storms at meter wavelength are indicated by horizontal lines. On the next two lines are vertical tick marks at the time of beginning to show sudden ionospheric disturbances and solar x-ray bursts from Explorer 37 (0.5-3Å, 1-8Å, 8-20Å).

The Ap for the day is given in the left-hand portion of the final two lines which give the eight Kp centered in the appropriate three-hour time blocks, and the time of storm sudden commencements, if any, by a triangle. The daily planetary Ap index is derived from the 3-hourly Kp indices, which are based on reports from a selected standard group of geomagnetic observatories. The Ap index increases with increasing magnetic activity to a maximum of 400. The data are provided by the Permanent Service of Geomagnetic Indices (Göttingen) of IAGA. [*Annals of the IGY*, Vol. 4, pp. 227-236]. Adjacent to the sc triangle the exact time of the sc is given with the number of observatories reporting it in the parentheses.

At the right-hand side of these last two lines are given the ionospheric indices, Ip and Ia. These indices are computed by the method of Y. Hakura, Y. Takenoshita and K. Matsuoka in "Influence of solar activity on the ionosphere blackout index" [*J. Radio Res. Labs. Japan*, 14, No. 73, 1967]. If "-" is entered, it signifies less than 12 hours of data, so no value has been computed. The index Ip is for polar cap blackout, and the index Ia is for auroral zone blackout. The indices are on a scale from "0" representing 0.4 hours or less of blackout per day increasing to "9" representing 20.1 to 24 hours of blackout per day. Ionospheric f-min data from selected stations are used. The indices differ from Hakura et al. in that College data have been substituted for Point Barrow for Ia, and Resolute Bay and Thule data are available for Ip.

Below the time lines at the left-hand side are given the 10 cm flux. This is solar radio noise at 2800 MHz as observed at the Algonquin Radio Observatory by National Research Council, Canada, at about 1700 UT daily. It is expressed in unit of $10^{-22} \text{ Wm}^{-2} \text{ Hz}^{-1}$. It is the observed flux, which should be used for most solar-terrestrial studies. The values adjusted for the varying Sun-Earth distance are published elsewhere. Next is the provisional daily Zürich relative sunspot number, R_z , as communicated by Prof. M. Waldmeier of the Swiss Federal Observatory. It is based on observations at Zürich, Arosa and Locarno only. Final values of R_z , issued after the end of each calendar year, usually differ slightly from the provisional ones. If available at time of publication these final values are used. Next are given the McMath calcium plage region numbers on their date of CMP together with their latitude and number of rotations, if more than one, in the parentheses, and the Mt. Wilson sunspot region numbers, together with their latitude, magnetic classification by α , β , γ or δ and largest spot (preceding "p" or following "f") and a digit encoding field strength where:

1 = 100 - 500 gauss
 2 = 600 - 1000
 3 = 1100 - 1500
 4 = 1600 - 2000
 5 = 2100 - 2500

6 = 2600 - 3000 gauss
 7 = 3100 - 3500
 8 = 3600 - 4000
 9 = 4100 - 4500
 10 =>4500

If the Mt. Wilson sunspot is at CMP on a different date than the calcium plage was, this date is given in parentheses following the sunspot information. If the calcium or sunspot region numbers are in parentheses, this signifies the regions were never actually at the Central Meridian; these had either died while on the Eastern Hemisphere or were born on the Western Hemisphere.

Word statements are given for each of the five disturbed or five or ten quiet magnetic days. Auroral displays are usually mentioned only if the southern limit reached ϕ (geomagnetic latitude) less than 60° . Remarks concerning auroral displays over Western Europe are provided by Mary Hallissey and D. H. McIntosh. N. V. Pushov provides descriptions of aurora summarizing reports from a network of about 130 stations between 30° and 140° E. longitude. The North American sector data are no longer available. Comments on Forbush cosmic ray decreases are from the Deep River or Sulphur Mountain charts, limited to those of 3% or greater. Polar cap absorption data are provided by NOAA when confirmed. Noctilucent cloud dates are furnished by Mary Hallissey and D. H. McIntosh. Outstanding green corona as published in *Solar-Geophysical Data* Part I are mentioned by limb quadrant on date the peak would be at CMP. Peaks in red or yellow coronal line intensities are also given. Solar proton increases observed on Explorer 43 as published in *Solar-Geophysical Data* Part II are given with nominal time of maximum.

FLARE INDEX BY REGION (C.1f)

An index that characterizes the flare productivity of McMath calcium plage regions integrated over a disk passage has been developed by Constance Sawyer and Catherine Candelaria. The scale is consistent with the HAO flare index, and with the NOAA whole-disk index which is briefly described on page 44. The same formula:

$$\frac{7600}{T^*} \sum A_d^2$$

is used where A_d is the measured (apparent) area in square degrees and the same flares (IAU "confirmed") are counted, but the sum is taken for each region separately over all the days of its disk passage.

The total number of flares is also given and the dates on which the first and last flares were observed in the region. The "flare-index mean" is the flare-index sum divided by the interval in days from the first flare to the last flare.

DATA FOR

MISCELLANEOUS TIME PERIODS

RETROSPECTIVE WORLD INTERVALS (H.63)

Retrospective World Intervals selected by the Monitoring of Sun Earth Environment (MONSEE) program of the ICSU Special Committee on Solar-Terrestrial Physics will be presented as appropriate.

OTHER DATA

Information available either annually or on a non-routine publication basis will be given. The descriptive material necessary to understand the data will be included in the issue presenting the data. Data received too late for publication in the normal section may also appear here.

A C K N O W L E D G E M E N T S

These monthly reports would not be possible without the continuing support and cooperation of scientists throughout the world. Much of the data included have been obtained through either the International Ursigram and World Days Service program or the international exchange of geophysical observations between World Data Centers in accordance with the principles set forth in recommendations of relevant organizations of the International Council of Scientific Unions.

Special thanks are due to many individuals including the following:

<u>Name</u>	<u>Organization</u>	<u>Data Type</u>
C. H. Hossfield	American Association of Variable Star Observers Solar Division 540 N. Central Avenue Ramsey, New Jersey 07446	Sunspots, SID
P. S. McIntosh	Space Environment Laboratory NOAA Boulder, Colorado 80302	Sunspots, H α photographs H α synoptic charts
M. Waldmeier	Eidgen. Sternwarte Schmelzbergstrasse 25 8006 Zürich, Switzerland	Sunspots
Helen W. Dodson	McMath-Hulbert Observatory University of Michigan 895 Lake Angeles Rd. North Pontiac, Michigan 48055	Calcium plages, flares, SID
G. Godoli	Osservatorio Astrofisico Citta Universitaria Viale A. Doria 95123 Catania, Italy	Calcium plages, flares
R. Howard J. M. Adkins	Mount Wilson Observatory 813 Santa Barbara Street Pasadena, California 91106	Magnetic classifications of sunspots, solar magnetograms
J. W. Evans	Sacramento Peak Observatory Sunspot, New Mexico 88349	Coronal data
A. A. Giesecke M. Ishitsuka	Observatorio de Huancayo Instituto Geofisico del Peru Apartado 46 Huancayo, Peru	SID, solar radio noise, flares
R. G. Giovanelli	CSIRO Division of Physics City Road, Chippendale N.S.W., Australia 2008	Flares
V. Badillo	Manila Observatory P. O. Box 1231 Manila, Philippines	Flares, SID, solar noise Calcium plages
U. Kusoffsky	Stazione Astrofisica Svedese Via Fraita 4 I-80071 Anacapri, Italy	Flares
G. Olivieri	Observatoire de Meudon 92 Meudon, France	Flares
J. P. Castelli Wm. R. Barron	USAF Cambridge Research Laboratories L. G. Hanscom Field Code LIR Bedford, Massachusetts 01730	Solar noise
W. N. Christiansen Arthur Watkinson	School of Electrical Engineering University of Sydney Sydney, N.S.W. 2006, Australia	Solar noise

<u>Name</u>	<u>Organization</u>	<u>Data Type</u>
A. E. Covington M. B. Bell	Astrophysics Branch National Research Council Ottawa 27 Ontario, Canada	Solar noise
J. P. Hagen W. J. Decker	Department of Astronomy 525 Davey Laboratory The Pennsylvania State University University Park, Pennsylvania 16802	Solar noise
Pierre Kaufmann	Universidade Mackenzie, CRAAM Rua Maria Antonia, 403 Caixa Postal 8792 Sao Paulo 3, Brazil	Solar noise
A. Maxwell	Harvard Radio Astronomy Station Fort Davis, Texas 79734	Solar noise
H. Urbarz	Aussenstelle Astronomy Institut der Universitat Tübingen 7981 Weissenau Federal Republic of Germany	Solar noise
A. O. Benz	Microwave Laboratory Gloriastrasse 35 8006 Zürich, Switzerland	Solar noise
C. Slotje	Solar Radio Observatory Netherlands Foundation for Astronomy Dwingeloo, Netherlands	Solar noise
M. Pick	Observatoire de Meudon 92 Meudon, France	Solar noise
J. W. Warwick	Dept. of Astro-geophysics University of Colorado Boulder, Colorado 80302	Solar noise
J. P. Wild S. F. Smerd	CSIRO Division of Radio Physics P. O. Box 76 Epping N.S.W. 2121 Australia	Solar noise
J. H. Wolfe	NASA Electrodynamics Branch Ames Research Center Moffett Field, California 94035	Solar wind
A. J. Lazarus	Center for Space Research Massachusetts Institute of Technology Cambridge, Massachusetts 02139	Solar wind
D. S. Colburn C. P. Sonett	NASA/ARC Moffett Field, California 94035	IP Electric Field
F. L. Scarf	Systems Group of TRW Inc. Bldg. R-5, Rm 1280 One Space Park Redondo Beach, California 90278	IP Electric Field
N. F. Ness	Laboratory for Extraterrestrial Physics NASA/GSFC Greenbelt, Maryland 20771	IP Magnetic Field
F. Mariani	Marconi Institute of Physics University of Rome Rome, Italy	IP Magnetic Field
R. B. Doeker G. Heckman	Space Environment Services Center NOAA Boulder, Colorado 80302	Solar proton events Inferred IP Magnetic Fields

<u>Name</u>	<u>Organization</u>	<u>Data Type</u>
R. J. Thomas W. M. Neupert	Laboratory for Solar Physics NASA/GSFC Greenbelt, Maryland 20771	EUV maps X-ray maps
R. Tousey M. Koomen	Naval Research Laboratory Washington, D. C. 20375	White light corona
	Cable & Wireless Engineer in Chief's Department Mercury House Theobalds Road London, W. C. 1, England	SID
T. Fortini	Osservatorio Astronomico Di Monte Mario Via Del Parco Mellini Roma 00136, Italia	Flares
C. Hornback	Table Mountain Geophysical Monitoring Station Space Environment Laboratory NOAA Boulder, Colorado 80302	SID, Solar radio noise
S. Katahara	Ionospheric Sounding Station P. O. Box 578 Puunene, Maui, Hawaii 96784	SPA
A. P. Mitra	Radio Research Committee National Physical Laboratory of India Hillside Road New Delhi 12, India	SID
P. C. Yuen	Department of Electrical Engineering University of Hawaii Honolulu, Hawaii 96822	SFD
R. W. Kreplin D. M. Horan	Solar Radiation Section Naval Research Laboratory 7125.7 U. S. Department of Navy Washington, D. C. 20390	Solar X-rays
M. Bercovitch Margaret D. Wilson	National Research Council of Canada Ottawa, Ontario, Canada K1A 0R6	Cosmic rays
D. Venkatesan M. Tjoei	Department of Physics University of Calgary Calgary 44, Alberta, Canada	Cosmic rays
J. A. Simpson	LASR Enrico Fermi Institute University of Chicago 933 E. 56th Street Chicago, Illinois 60637	Cosmic rays, Solar cosmic ray protons
E. P. Keath	University of Texas - Dallas P. O. Box 30365 Dallas, Texas 75080	Cosmic rays
M. A. Pomerantz	Bartol Research Foundation Swarthmore, Pennsylvania 19081	Cosmic rays
M. Wada	Institute of Physical and Chemical Research Kaga-1, Itabashi Tokyo, Japan 173	Cosmic rays
O. Binder	Institut für Reine und Angewandte Kernphysik der Christian-Albrechts- Universität Kiel 23 Kiel, German Federal Republic	Cosmic rays

<u>Name</u>	<u>Organization</u>	<u>Data Type</u>
M. Siebert	Geophysikalisches Institut Herzberger Landstrasse 180 34 Göttingen, G.F.R.	Magnetic indices
D. Van Sabben	Koninklijk Nederlands Meteorologisch Instituut DeBilt, The Netherlands	Magnetic indices
M. Suguira	Magnetic and Electric Fields Branch NASA/GSFC Greenbelt, Maryland 20771	Magnetic indices
D. J. Poros	Computer Sciences Corporation Silver Spring, Maryland 20910	Magnetic indices
P. N. Mayaud	Institut de Physique de Globe Tour 14, 3e etage 9, Quai Saint-Bernard 75-Paris, France	Magnetic indices
R. Eyfrig	Fermeldetechnisches Zentralamt 61 Darmstadt, Postfach 800 G.F.R.	Radio quality figures
K. D. Boggs	Institute for Telecommunication Sciences Office of Telecommunications Boulder, Colorado 80302	Radio quality figures
C. O. Bostrom	Applied Physics Laboratory The Johns Hopkins University 8621 Georgia Avenue Silver Spring, Maryland 20910	Solar protons
W. R. Webber J. A. Lezniak	Physics Department University of New Hampshire Demeritt Hall Durham, New Hampshire 03824	Solar cosmic ray protons
D. J. Williams	Space Environment Laboratory NOAA Boulder, Colorado 80302	Solar protons
A. Frosolone	Space Weather Consultants P. O. Box 213 Moffett Field, California 94035	Pioneer spacecraft
A. Romaña	Observatorio del Ebro Roquetas (Tarragona) Spain	ssc, si, sfe
J. H. Allen H. Kroel	NGSDC/EDS/NOAA Boulder, Colorado 80302	Magnetograms

I N D E X F O R
S O L A R - G E O P H Y S I C A L D A T A

On the following pages will be found the serial number of the report or reports in which data of a given type for any given month will be found, beginning with data for July 1957 through December 1973.

S T O N Y H U R S T D I S K S

Two transparencies provide Stonyhurst disks in degrees from CMP in the size of most of the maps or drawings presented in the second section of these monthly reports. A second set of transparencies with meridians calibrated in days from CMP are included to fit the Mount Wilson magnetograms. The two sizes as calibrated in degrees or days from CMP are reversed from those published in the last Descriptive Text which may also be used with these maps.

The dates shown were for 1969 but are within one day of appropriate date for 1974. See any Ephemeris.

		Mo/Yr	Mo/Yr
<u>A. Solar and Interplanetary Phenomena</u>			
A.1	Sunspot Drawings	1/67	- present
A.1a	Sunspot Data (see A05a)	7/57	- present
A.2a	Zürich Provisional Relative Sunspot numbers, R_z	7/57	- present
A.2b	Zürich Final Sunspot numbers, R_z	7/57	- present
A.2c	American Relative Sunspot numbers, R_A	7/57	- present
A.2d	27-day Plot of Relative Sunspot numbers (see D.1c)	7/57	- present
A.2e	Sunspot Cycle (Smoothed numbers) Graphs - in each issue	7/57	- present
A.2f	Table of Observed and Predicted Smoothed Sunspot numbers - in each issue since IER-FB-294, updated each month, for period	10/64	- present
A.3a	Mt. Wilson Magnetograms	9/66	- present
A.3b	Mt. Wilson Sunspot Magnetic Field Classifications	1/62	- present
A.4	H α Spectroheliograms	1/67	- present
A.5	Calcium Plage Drawings - McMath (or Catania)	1/67	- present
A.5a	Calcium Plage (McMath) and Sunspot Regions	7/57	- present
A.5b	Daily Calcium Plage Index	12/70	- present
A.6	H α Synoptic Charts	6/73	- present
A.7a	Coronal Line Emission Indices (Provisional)	7/57	- 5/66
A.7b	Coronal Line Emission Indices (Final)	1/60	- present
A.7c	White-Light Corona (NRL OSO-7, 1971-083A)	2/72	- present
A.7d	Solar EUV Spectroheliograms FeXV 284 Å (GSFC OSO-7, 1971-083A)	5/72	- present
A.7e	Solar XUV Coronagraphs (NRL OSO-7, 1971-083A)	10/72	- 12/73
A.8aa	2800 MHz (ARO-Ottawa) Daily Observed Values of Solar Flux	7/57	- present
A.8ab	2800 MHz (Ottawa) Final - Daily Observed Values of Solar Flux	1/62	- 12/66
A.8ac	2800 MHz (ARO-Ottawa) Daily Values Solar Flux Adjusted to 1 A.U.	1/64	- present
A.8ad	2800 MHz (Ottawa) Final - Daily Values of Solar Flux Adjusted to 1 A.U.	1/64	- 12/66
A.8b	470 MHz (Boulder) Daily 3-hourly Averages	7/57	- 3/58
A.8c	167 MHz (Boulder) Daily 3-hourly Averages	7/57	- 12/58
A.8d	200 MHz (Cornell) Daily 3-hourly Averages	7/57	- 12/58
A.8e	9530 MHz (USNRL) Daily Averages	2/58	- 4/59
A.8f	3200 MHz (USNRL) Daily Averages	2/58	- 4/59
A.8g	15400, 8800, 4995, 2695, 1415, 606, 410, 245 MHz (AFCRL) Solar Flux Adjusted to 1 A.U. (15400 MHz began 11/67 and 245 MHz began 1/70)	1/67	- present
A.9a	9.1 cm (Stanford) Radio Maps of the Sun	4/60	- 8/73
A.9aa	9.1 cm Spectroheliogram Data - included in A.5a since 1/69		
A.9b	21 cm (Fleurs) Radio Maps of the Sun	12/64	- 12/73
A.9c	8.6 mm (Prospect Hill) Radio Maps of the Sun	4/70	- present
A.10a	169 MHz (Nancay) Interferometric Observations	7/57	- present
A.10b	408 MHz (Nancay) Interferometric Observations	11/65	- 8/71
A.10c	21 cm (Fleurs) East-West Solar Scans	10/65	- present
A.10d	43 cm (Fleurs) East-West Solar Scans	4/66	- present
A.10e	10.7 cm (Ottawa-ARO) East-West Solar Scans	6/68	- present
A.11aa*	Solar X-ray Background Levels (NRL)	1/64	- present
A.11ab*	Solar X-ray Background Levels (NRL Graphs)	3/65	- present
A.11ac*	Solar X-ray Background Levels (Boulder)	12/65	- 11/68
A.11ad*	Solar X-ray Background Levels (France)	4/66	- 5/66
A.11ae*	Solar X-ray Background Levels (Aberdeen, S. D.)	1/66	- 11/68
	Popular Name	Satellite Designation	
	*SOLRAD 7A	1964-1D	1/64 - 10/64
	*SOLRAD 7B	1965-16D	3/65 - 12/65
	*SOLRAD 8	1965-93A	
	(Explorer 30)		1/66 - 12/67
	*OGO-4	1967-73A	1/68 - 3/68
	*OSO-4	1967-100A	
	*SOLRAD 9	1968-17A	3/68 - 7/72
	(Explorer 37)		6/73 - present
	(Beginning 12/68 daily/hourly averages presented)		
	*SOLRAD-10	1971-58A	8/72 - 6/73
	(Explorer 44)		
A.11b	Solar X-ray Background Levels, 0-20Å Injun 1/SOLRAD-3, 1961-02	6/61	- 12/61

A. Solar and Interplanetary Phenomena (continued)

A.11c	Solar X-ray Background Levels (Vela 1,2; 1963-39A,C)	(10/63)	
A.11d	Solar X-ray Background Levels (McMath) (OSO-3; 1967-20A), 8-12Å	3/67 - 8/67	
A.11e	Solar X-ray (OSO-5; 1969-6A) Spectroheliograms (University College London, Leicester Univ.)	7/69 - 11/72	
A.11f	Solar X-ray (GSFC OSO-7, 1971-083A) Spectroheliograms	12/72 - present	
A.12aa+	Solar Protons, Daily-hourly Values, JPL/GSFC	5/67 - present	
A.12ab+	Solar Protons, Graphs, JPL/GSFC	5/67 - present	
	Popular Name	Satellite Designation	
	+Explorer 34	1967-51A, Ep >10, >30, >60 Mev	5/67 - 5/69
	+Explorer 41	1969-53A, Ep >10, >30, >60 Mev	6/69 - 12/72
	+Explorer 43	1971-19A, Ep >10, >30, >60 Mev	11/71 - present
A.12ba	Cosmic Ray Protons, Ep 0.6-13, 13-175, >175 Mev, Univ. of Chicago (Pioneer 6; 1965-105A and Pioneer 7; 1966-75A)	3/69 - present	
A.12bb	Cosmic Ray Protons, Ep >13.9, >64 or >40 Mev, Univ. of New Hampshire (Pioneer 8; 1967-123A and Pioneer 9; 1968-100A)	12/69 - present	
A.12c	Cosmic Ray Protons, Ep 5-21, 21-70 Mev, Aerospace (ATS-1; 1966-110A)	1/70 - 8/72	
A.13a	Solar Wind (Pioneer 6, 1965-105A; and Pioneer 7, 1966-75A) NASA Ames	12/65 - present	
A.13b	Solar Wind, M.I.T. Pioneer 6, 1965-105A Pioneer 7, 1966-75A	3/69 - 2/70* 6/69 - 12/69	
A.13c	Solar Wind (Vela 3, 1964-40A; Vela 5, 1965-58A)	1/69 - 6/72	
A.17	Interplanetary Magnetic Field Pioneer 8, 1967-123A Pioneer 9, 1968-100A	10/72 - present 4/72 - present	
A.17c	Inferred Interplanetary Magnetic Field	12/71 - present	
A.18	Interplanetary Electric Field Pioneer 8, 1967-123A Pioneer 9, 1968-100A	5/72 - present 4/72 - present	
		*started again 12/73	

*started again 12/73

B. Ionospheric (and Radio Wave Propagation) Phenomena

B.10	Radar Meteor Indices, perpetual, based upon 1958-1962 data for N45 latitude -- see issues 246, 251	
B.51aa	NARWS Quality Figures and Forecasts (NBS/ESSA)	7/57 - 12/65
B.51ab	NARWS Comparison Graphs (NBS/ESSA)	7/57 - 12/65
B.51ba	NPRWS Quality Figures and Forecasts (NBS)	7/57 - 12/65
B.51bb	NPRWS Comparison Graphs (NBS)	7/57 - 10/64
B.51ca	High Latitude Quality Figures and Forecasts (ESSA/OT)	11/64 - present
B.51cb	High Latitude Comparison Graphs (ESSA/OT)	11/64 - 11/73
B.52	North Atlantic Graphs of Useful Frequency Ranges (German PTT)	7/57 - present
B.53	Quality Figures Based Upon Frequency Ranges (German PTT)	1/70 - present

C. Flare-Associated Events

C.1a	H-α Solar Flares (Preliminary)	7/57 - present
C.1ba	H-α Solar Flares (Including Standardized Data) (Divided into Confirmed and Unconfirmed Flares as of 1/68)	9/66 - present
C.1c	H-α Subflares	7/57 - present, included in C.1a after 1/62 and in C.1ba
C.1d	H-α Flare Patrol (The most recent issue listed for a month contains the comprehensive flare patrol.)	7/57 - present
C.1e	H-α Flare Index (Daily)	9/69 - present
C.1f	H-α Flare Index (by Region)	9/70 - present
C.1g	Frequency of Occurrence of Confirmed Solar Flares	1/68 - 6/68
C.3a	2800 MHz (Ottawa) Outstanding Occurrences	7/57 - *(see p. 69)
C.3aa	2800 MHz (Ottawa) Hours of Observation	7/57 - with C.3a after 12/65
C.3b	470 MHz (Boulder) Outstanding Occurrences	7/57 - 3/58
C.3c	167 MHz (Boulder) Outstanding Occurrences	7/57 - 10/60
C.3ca	167 MHz (Boulder) Hours of Observation	1/59 - 12/59
C.3d	200 MHz (Cornell) Outstanding Occurrences	7/57 - 12/58
C.3e	9530 MHz (USNRL) Outstanding Occurrences	2/58 - 4/59
C.3f	3200 MHz (USNRL) Outstanding Occurrences	2/58 - 4/59

C. Flare-Associated Events (continued)

C.3g	200 MHz (Hawaii) Outstanding Occurrences	6/59 - 8/59
C.3h	108 MHz (Boulder) Outstanding Occurrences	1/60 - 6/66
C.3ha	108 MHz (Boulder) Hours of Observation	1/60 - with C.3h after 12/65
C.3i	221 MHz (Boeing-Seattle) Outstanding Occurrences (Interferometric) - Changed to 223 MHz in May 1963	4/62 - 7/63 5/65 - 11/65 6/65 - 3/66
C.3j	107 MHz (Haleakala) Outstanding Occurrences	7/64 - *
C.3k	10700, 2700, 960 MHz (Pennsylvania State Univ.) Outstanding Occurrences	7/66 - 4/69
C.3	486 MHz (Washington State Univ.) Outstanding Occurrences	11/67 - *
C.3m	18 MHz Bursts (Boulder) (reported in C.6 1/63 - 11/66, C.6ab prior to 1/63)	1/66 - *
C.3n	35000, 15400, 8800, 4995, 2695, 1415, 606, 410, 245 MHz (AFCRL - Sagamore Hill) Outstanding Occurrences (15400 MHz began 11/67, 35000 and 245 MHz began early 1969, 410 MHz began 1971)	3/67 - *
C.3p	184 MHz (Boulder) Outstanding Occurrences	11/67 - *
C.3q	7000 MHz (Sao Paulo) Outstanding Occurrences	10/67 - *
C.3r	408 MHz (San Miguel) Outstanding Occurrences	1/68 - *
C.3s	18 MHz (McMath-Hulbert) Bursts	12/72 - present
C.3t	43.25, 80 and 180 MHz (Culgoora) Selected Bursts	

*C.3 Solar Radio Events (fixed frequencies).

Note: Beginning with the data for April 1966, in CRPL-FB-261, the C.3 entries on Solar Radio Outstanding Occurrences for the western hemisphere observatories and frequencies were combined in a single table "Solar Radio Emission Outstanding Occurrences, C.3." This table is described along with changes in reporting observatories and frequencies on pages i and ii of issue CRPL-FB-261, and in the Descriptive Texts for succeeding years. Beginning with the index for June 1969, the table was expanded to world-wide coverage, and the various observatories were no longer indexed separately.

C.4aa	Solar Radio Spectrograms of Events (Fort Davis)	
	100 - 580 MHz	7/57 - 12/58
	25 - 580 MHz	1/59 - 12/62
	50 - 320 MHz	1/63 - 3/65
	25 - 320 MHz	4/65 - 12/66
	10 - 580 MHz	1/67 - 2/70
	10 - 1000 MHz	3/70 - 4/70
	10 - 2000 MHz	5/70 - 5/73
	10 - 4000 MHz	5/73 - present
C.4ab	2100-3900 MHz Solar Radio Spectrograms of Events (Fort Davis)	1/60 - 12/61
C.4b	Solar Radio Spectrograms of Events (Boulder)	
	7.6 - 41 MHz	3/61 - 8/68
	7.6 - 80 MHz	9/68 - present
C.4c	450-1000 MHz Solar Radio Spectrograms of Events (Owens Valley)	11/60 - 10/61
C.4d	Solar Radio Spectrograms of Events (Culgoora)	
	10 - 210 MHz	1/67 - 7/69
	8 - 2000 MHz	8/69 - 2/70
	8 - 4000 MHz	3/70 - 10/70
	8 - 8000 MHz	11/70 - present
C.4e	30-1000 MHz Solar Radio Spectrograms of Events (Weissenau, GFR)	3/68 - present
C.4f	Solar Radio Spectrograms of Events (AFCRL - Sagamore Hill)	
	19 - 41 MHz	1/68 - 7/70
	24 - 48 MHz	7/70 - present
C.4g	20-60 MHz Solar Radio Spectrograms of Events (Clark Lake)	4/70 - 9/70
C.4h	160-320 MHz Solar Radio Spectrograms of Events (Dwingeloo)	1/74 - present
C.4i	100-1000 MHz Solar Radio Spectrograms of Events (Dürnten)	1/74 - present
C.5a	Solar X-ray Events (Vela 1,2; 1963-39A,C)	(10/63)
C.5b	Solar X-ray Events (Univ. of Iowa)	
	Explorer 33; 1966-58A (2-12Å)	7/66 - 10/71
	Explorer 35; 1967-70A (2-12Å)	12/67 - 7/72
C.5c	Solar X-ray Events (NRL Tabulation)	1/64 - 10/64
	(See A.11ab for NRL Graphs and list of Satellites)	and 3/65 - present

C. Flare Associated Events (continued)

C.5d	Solar X-ray Events (McMath-Hulbert) OSO-3; 1967-20A (8-12Å)	3/67 - 8/67
C.6	Sudden Ionospheric Disturbances (SID)	1/63 - present
C.6aa	Sudden Ionospheric Disturbances (SWF)	7/57 - included in C.6 after 12/62
C.6ab	Sudden Ionospheric Disturbances (SCNA, SEA, bursts)	1/58 - included in C.6 after 12/62
C.6ac	Sudden Ionospheric Disturbances (SPA)	6/61 - included in C.6 after 12/62
C.7	Solar Proton Events - Direct Measurement - same as A.12	5/67 - present
C.8	Solar Proton Events - Riometer Confirmed Polar Cap Absorption Events (ESSA)	1/67 - 6/67
C.8ba	Solar Protons, 26 MHz Riometer Events (South Pole) Provisional	9/63 - 11/67
C.8bc	Solar Protons, 30 MHz Riometer Events (Frobisher Bay)	1/65 - 5/65
C.8be	Solar Protons, 30 MHz Riometer Events (Great Whale River)	6/65 - 2/67

D. Geomagnetic and Magnetospheric Phenomena

D.1a	Geomagnetic Indices Ci, Cp, Kp, Ap, aa*, Selected Days	7/57 - present
D.1b	27-day Chart of Kp for Year	7/57 - present
D.1ba	27-day Chart of Kp Indices	7/57 - present
D.1c	27-day Chart of C9 for Year	7/57 - present
D.1d	Principal Magnetic Storms	7/66 - present
D.1e	Reduced Magnetograms	1/67 - present
D.1f	Sudden Commencements and Solar Flare Effects	1/66 - present
D.1g	Equatorial Indices Dst	5/73 - present
* aa first published 1/74		

F. Cosmic Rays

F.1a	Cosmic Ray Daily Averages Neutron Monitors (Deep River - graph of hourly values, daily averages begin 11/65)	1/59 - 3/72
F.1b	Cosmic Ray Daily Averages Neutron Monitors (Climax)	9/60 - present
F.1c	Cosmic Ray Daily Averages Neutron Monitors (Dallas)	1/64 - present
F.1d	Cosmic Ray Daily Averages Neutron Monitors (Churchill)	5/64 - 6/72
F.1e	Cosmic Ray Daily Averages Neutron Monitors (Alert - graph of hourly values)	7/66 - present
F.1f	Cosmic Ray Daily Averages Neutron Monitors (Calgary - also graph of hourly values)	1/71 - present
F.1g	Cosmic Ray Daily Averages Neutron Monitors (Sulphur Mountain - also graph of hourly values)	1/71 - present
F.1h	Cosmic Ray Daily Averages Neutron Monitors (Thule - also graph of hourly values)	4/73 - present
F.1i	Cosmic Ray Daily Averages Neutron Monitors (Tokyo - also graph of hourly values)	12/73 - present
F.1j	Cosmic Ray Daily Averages Neutron Monitors (Kiel - also graph of hourly values)	12/73 - present

H. Miscellaneous

H.60	Alert and Special World Interval Decisions (IUWDS Geophysical Alerts)	7/57 - present
H.61	International Geophysical Calendar	1/62 - 12/62
H.62	Abbreviated Calendar Record	12/68 - present
H.63	Retrospective World Intervals	1/66 - 12/67

INDEX TO "SOLAR-GEOPHYSICAL DATA"

Key *	1957						1958											
	Jul	Aug	Sep	Oct	Nov	Dec	Jan	Feb	Mar	Apr	May	Jun	Jul	Aug	Sep	Oct	Nov	Dec
A.2a	156	157	158	159	160	161	162	163	164	165	166	167	168	169	170	171	172	173
A.2b	166	166	166	166	166	166	175	175	175	175	175	175	175	175	175	175	175	175
A.2c	157	158	159	160	161	162	163	164	165	166	167	168	169	170	171	172	173	174
A.5a	156	157	158	159	160	161	162	163	164	165	166	167	168	169	170	171	172	173
A.7	156	157	158	159	160	161	162	163	164	166	166	167	168	169	170	171	172	173
			165	165	165	165	165	171	171	171	171	171	171					
A.8aa	156	157	158	159	160	161	162	163	164	165	166	167	168	169	170	171	172	173
A.8b	156	157	158	159	161	162	163	164	165									
A.8c	156	157	158	159	162	162	163	164	165	167	168	169	170	172	173	174	175	176
A.8d	156	157	158	159	160	161	163	163	164	165	167	167	168	169	170	171	172	173
A.8e								176	175	174	172	170	170	170	170	171	172	173
A.8f								176	175	174	172	170	170	170	170	171	172	173
A.10a	171	171	171	171	171	171	171	171	171	171	171	171	171	171	171	171	172	173
B.51aa	157	158	159	160	161	162	163	164	165	166	167	168	169	170	171	172	173	174
B.51ab	157	158	159	160	161	162	163	164	165	166	167	168	169	170	171	172	173	174
B.51ba	157	158	159	160	161	162	163	164	165	166	167	168	169	170	171	172	173	174
B.51bb	157	158	159	160	161	162	163	164	165	166	167	168	169	170	171	172	173	174
B.52	157	159	159	160	161	162	163	164	165	166	167	168	169	170	171	172	173	174
C.1a	156	157	158	159	160	161	162	163	164	165	166	167	168	169	170	171	172	173
	166	167	168	168	169	169	170	170	171	171	172	172	173	173	174	174	175	175
	169	174	174	174	161	174	174		174	174	174					176		
	174		175		174													
C.1c	156	157	158	160	161	162	163	164	165	166	167	168	169	170	171	172	173	174
C.1d	158	158	158	159	160	161	162	163	164	165	166	167	168	169	170	171	172	173
	166	167	168	168	169	169	170	170	171	171	172	172	173	173	174	174	175	175
	176	176	176	176	176	176	176	176	176	176								
C.3a	156	157	158	159	160	161	162	163	164	165	166	167	168	169	170	171	172	173
C.3aa	158	158	158	161	161	161	164	164	164	167	167	167	170	170	170	173	173	173
C.3b	156	157	159	159	161	162	163	164	165									
C.3c	156	157	159	159	162	162	163	164	165	168	169	169	170	172	173	174	175	176
C.3d	156	157	158	159	160	161	163	163	164	165	167	167	168	169	170	171	172	173
C.3e								176	175	174	172	170	170	170	170	171	172	173
C.3f								176	175	174	172	170	170	170	170	171	172	173
C.4aa												174	168	169	170	171	172	174
C.6aa	157	158	159	160	161	162	163	164	165	166	167	168	169	170	171	172	173	174
C.6ab								171	172	173	174	175	176	177	178	178	179	
D.1a	157	158	159	160	161	162	163	164	165	166	167	168	169	170	171	172	173	174
D.1b	174	174	174	174	174	174	174	174	174	174	174	174	174	174	174	174	174	174
D.1c	190	190	190	190	190	190	190	190	190	190	190	190	190	190	190	190	190	190
H.60	158	158	158	159	160	161	162	163	164	165	165	166	168	168	170	171	172	173
										166	166		169					

* See "Key" on pages 67 and following.

INDEX TO "SOLAR-GEOPHYSICAL DATA"

Key *	1959												1960											
	Jan	Feb	Mar	Apr	May	Jun	Jul	Aug	Sep	Oct	Nov	Dec	Jan	Feb	Mar	Apr	May	Jun	Jul	Aug	Sep	Oct	Nov	Dec
A.2a	174	175	176	177	178	179	180	181	182	183	184	185	186	187	188	189	190	191	192	193	194	195	196	197
A.2b	187	187	187	187	187	187	187	187	187	187	187	187	186	187	188	189	190	191	192	193	194	195	196	197
A.2c	175	176	177	178	179	180	181	182	183	184	185	186	187	188	189	190	191	192	193	194	195	196	197	198
A.5a	174	175	176	177	178	179	180	181	182	183	184	185	186	187	188	189	190	191	192	193	194	195	196	197
A.7a	174	175	176	177	178	179	180	181	183	183	184	185	186	187	188	189	190	191	192	193	195	196	196	197
A.7b										185	185		189	189	189	193	193	193	196	196	196	199	199	199
A.8aa	174	175	176	177	178	179	180	181	182	183	184	185	186	187	188	189	190	191	192	193	194	195	196	197
A.8e	174	175	176	177																				
A.8f	174	175	176	177																				
A.9a																196	197	199	210	211	212	212	212	
A.10a	174	175	176	177	178	179	180	181	182	183	184	185	186	187	188	189	190	191	192	193	194	195	196	197
B.51aa	175	176	177	178	179	180	181	182	183	184	185	186	187	188	189	190	191	192	193	194	195	196	197	198
B.51ab	175	176	177	178	179	180	181	182	183	184	185	186	187	188	189	190	191	192	193	194	195	196	197	198
B.51ba	175	176	177	178	179	180	181	182	183	184	185	186	187	188	189	190	191	192	193	194	195	196	197	198
B.51bb	175	176	177	178	179	180	181	182	183	184	185	186	187	188	189	190	191	192	193	194	195	196	197	198
B.52	175	176	177	178	179	180	181	182	183	184	185	186	187	188	190	190	191	192	193	194	195	196	197	198
C.1a	174	175	176	177	178	179	180	181	182	183	184	185	186	187	188	189	190	191	192	193	194	195	196	197
	176	178	179	180	181	182	183	184	185	186	187	188	189	190	191	192	193	194	195	196	197	198	199	200
	178	185	185	185	185	185	185	185			191	189	191	191	194	194	201	195	201	201	201	199	201	201
	185											191	194	194			201				201			
													196											
C.1c	175	176	177	178	179	180	181	182	183	184	185	186	187	188	189	190	191	192	193	194	195	196	197	198
C.1d	174	175	176	177	178	179	180	181	182	183	184	185	186	187	188	189	190	191	192	193	194	195	196	197
	176	178	179	180	181	182	183	184	185	186	187	188	189	190	191	192	193	194	195	196	197	198	199	200
	178	185	185	185	185	185	185	185			191	191	191	191			202	202	202	202	202	202	202	202
	185					200																		
C.3a	174	175	176	177	178	179	180	181	182	183	184	185	186	187	188	189	190	191	192	193	194	195	196	197
C.3aa	176	176	176	179	179	179	182	182	182	185	185	185	188	188	188	191	191	191	194	194	194	197	197	197
C.3c	176	177	178	178	179	180	180	181	182	183	184	185	195	195	195	195	195	195	195	195	195	195		
C.3ca	182	182	182	182	182	182	182	182	182	183	184	185												
C.3e	174	175	176	177																				
C.3f	174	175	176	177																				
C.3g						180	182	185																
C.3h													186	187	188	189	190	191	192	193	194	195	196	197
C.4aa	182	182	182	184	184	184	188	188	188	192	192	192	197	197	197	198	198	198	199	199	199	200	200	200
C.4ab													197	197	197	198	198	198	199	199	199	200	200	200
C.4c													197	198										
C.6aa	175	176	177	178	179	180	181	182	183	184	185	186	187	188	189	190	191	192	193	194	195	196	197	198
C.6ab	180	181	182	183	184	184	184	185	186	187	187	188	188	189	189	190	191	192	193	194	195	196	197	198
D.1a	175	176	177	178	179	180	181	182	183	184	185	186	187	188	189	190	191	192	193	194	195	196	197	198
D.1b	186	186	186	186	186	186	186	186	186	186	186	186	198	198	198	198	198	198	198	198	198	198	198	198
D.1c	190	190	190	190	190	190	190	190	190	190	190	190	190	190	190	190	226	226	226	226	226	226	226	226
F.1a	195	195	195	195	195	195	195	195	195	195	195	195	195	195	195	195	195	195	195	195	195	196	197	198
																	205							
F.1b																				195	196	197	198	
H.60	174	175	176	177	178	179	180	181	182	183	184	185	186	187	188	189	190	191	192	193	194	195	196	197

* See "Key" on pages 67 and following.

INDEX TO "SOLAR-GEOPHYSICAL DATA"

Key *	1961												1962											
	Jan	Feb	Mar	Apr	May	Jun	Jul	Aug	Sep	Oct	Nov	Dec	Jan	Feb	Mar	Apr	May	Jun	Jul	Aug	Sep	Oct	Nov	Dec
A.2a	198	199	200	201	202	203	204	205	206	207	208	209	210	211	212	213	214	215	216	217	218	219	220	221
A.2b	211	211	211	211	211	211	211	211	211	211	211	211	211	223	223	223	223	223	223	223	223	223	223	223
A.2c	199	200	201	202	203	204	205	206	207	208	209	210	211	212	213	214	215	216	217	218	219	220	221	222
A.3b														210	211	212	213	214	215	216	217	218	219	220
A.5a	198	199	200	201	202	203	204	205	206	207	208	209	210	211	212	213	214	215	216	217	218	219	220	221
A.7a	198	199	200	201	202	203	205	205	207	207	208	209	210	210	211	212	213	214	215	216	217	218	219	220
A.7b	204	204	204	205	205	205	208	208	208	212	212	212	212	213	213	213	216	216	216	220	220	220	226	226
A.8aa	198	199	200	201	202	203	204	205	206	207	208	209	210	210	211	212	213	214	215	216	217	218	219	220
A.8ab														223	223	223	223	223	223	223	223	223	223	223
A.9a		213	213														213	214	215	216	217	218	219	220
A.10a	198	200	201	201	202	203	204	205	206	207	208	209	210	211	212	213	214	215	216	217	219	219	220	221
A.11b						249	249	249	249	249	249	249	249	222	212	213	214	215	216	217	218	219	220	221
B.51aa	199	200	201	202	203	204	205	206	207	208	209	210	210	211	212	213	214	215	216	217	218	219	220	221
B.51ab	199	200	201	202	203	204	205	206	207	208	209	210	210	211	212	213	214	215	216	217	218	219	220	221
B.51ba	199	200	201	202	203	204	205	206	207	208	209	210	210	211	212	213	214	215	216	217	218	219	220	221
B.51bb	199	200	201	202	203	204	205	206	207	208	209	210	210	211	212	213	214	215	216	217	218	219	220	221
B.52	199	200	201	202	203	204	205	206	207	208	209	210	210	211	212	213	214	215	216	217	218	219	220	221
C.1a	198	199	200	201	202	203	204	205	206	207	208	209	210	210	211	212	213	214	215	216	217	218	219	220
	201	202	203	204	205	206	207	208	210	210	211	212	212	213	214	215	216	217	218	219	220	221	222	224
	208	208	208	208	208	208	208	208																
C.1c	199	200	201	202	203	204	205	206	207	208	209	210	210	included in C.1a after Jan. 1962										
C.1d	198	199	200	201	202	203	204	205	206	207	208	209	210	210	211	212	213	214	215	216	217	218	219	220
	201	202	203	204	205	206	207	208	210	210	211	212	212	213	214	215	216	217	218	219	220	221	222	223
	208	208	208	208	208	208	208	208																
C.3a	198	199	200	201	202	203	204	205	206	207	208	209	210	210	211	212	213	214	215	216	217	218	219	220
							206		209		209													
C.3aa	200	200	200	203	203	203	206	206	206	209	209	209	210	212	212	212	215	215	215	218	218	218	221	221
C.3h	198	199	200	201	202	203	204	205	206	207	208	209	210	210	211	212	213	214	215	216	217	218	219	220
C.3ha														210	211	212	213	214	215	216	217	218	219	220
C.3i														-	-	-	221	221	221	221	221	221	221	221
C.4aa	203	203	203	204	204	204	208	208	208	209	209	209	210	213	213	213	216	216	216	219	219	219	222	222
C.4ab	203	203	203	204	204	204	208	208	208	209	209	209	210	210	211	212	213	214	215	216	217	218	219	220
C.4b			207	207	207	207	207	207	207	207	208	209	210	210	211	212	213	214	215	216	219	219	219	220
C.6aa	199	200	201	202	203	204	207	206	207	208	209	210	210	211	212	213	214	215	216	219	219	219	220	221
C.6ab	199	200	201	202	203	204	205	206	207	208	209	210	210	211	212	213	214	215	216	219	219	219	220	221
C.6ac						204	205	206	207	208	209	210	210	211	212	213	214	215	216	219	219	219	220	221
D.1a	199	200	201	202	203	204	205	206	207	208	209	210	210	211	212	213	214	215	216	217	218	219	220	221
D.1b	208	208	208	208	208	208	208	208	208	208	208	208	208	221	221	221	221	221	221	221	221	221	221	221
D.1c	226	226	226	226	226	226	226	226	226	226	226	226	226	226	233	233	233	233	233	233	233	233	233	233
F.1a	199	200	201	202	203	204	204	206	207	208	209	210	210	211	212	213	214	223	223	223	223	223	223	222
							205																	
F.1b	199	200	201	202	203	204	205	206	207	208	210	210	210	211	212	213	214	215	216	217	218	219	220	221
H.60	198	199	200	201	202	203	204	205	206	207	208	209	210	210	211	212	213	214	215	216	217	218	219	220
H.61														207	207	207	207	207	207	207	207	207	207	207

* See "Key" on pages 67 and following.

INDEX TO "SOLAR-GEOPHYSICAL DATA"

Key *	1963												1964															
	Jan	Feb	Mar	Apr	May	Jun	Jul	Aug	Sep	Oct	Nov	Dec	Jan	Feb	Mar	Apr	May	Jun	Jul	Aug	Sep	Oct	Nov	Dec				
A.2a	222	223	224	225	226	227	228	229	230	231	232	233	234	235	236	237	238	239	240	241	242	243	244	245				
A.2b	235	235	235	235	235	235	235	235	235	235	235	235	247	247	247	247	247	247	247	247	247	247	247	247				
A.2c	223	224	225	226	227	228	229	230	231	232	233	234	235	236	237	238	239	240	241	242	243	244	245	246				
A.3b	222	223	224	225	none	227	228	229	230	231	232	233	234	235	236	237	238	239	240	241	242	243	244	245				
A.5a	222	223	224	225	226	227	228	229	230	231	232	233	234	235	236	237	238	239	240	241	242	243	244	245				
A.7a	222	223	224	225	226	227	228	229	230	231	232	233	234	235	236	237	238	239	240	241	242	243	244	245				
A.7b	226	226	226	228	228	228	231	231	231	234	234	234	237	237	237	240	240	240	243	243	243	248	248	248				
A.8aa	222	223	224	225	226	227	228	229	230	231	232	233	234	235	236	237	238	239	240	241	242	243	244	245				
A.8ab	233	233	233	233	233	233	233	233	233	233	233	233	245	245	245	245	245	245	245	245	245	245	245	245				
A.8ac													240	240	240	240	240	240	240	241	242	243	244	245				
A.8ad													245	245	245	245	245	245	245	245	245	245	245	245				
A.9a	222	-	-	225	226	227	228	229	230	231	232	233	234	235	236	237	238	239	240	241	242	243	244	245				
A.9b																								250				
A.10a	222	223	224	225	226	227	228	229	230	231	232	233	234	235	236	237	238	239	240	241	242	243	244	245				
A.11aa													243	247	247	241	241	241	244	244	245	245						
A.11c																249	255	264	266	266								
B.51aa	223	224	225	226	227	228	229	230	231	232	233	234	235	236	237	238	239	240	241	242	243	244	245	246				
B.51ab	223	224	225	226	227	228	229	230	231	232	233	234	235	236	237	238	239	240	241	242	243	244	245	246				
B.51ba	223	224	225	226	227	228	229	230	231	232	233	234	235	236	237	238	239	240	241	242	243	244						
B.51bb	223	224	225	226	227	228	229	230	231	232	233	234	235	236	237	238	239	240	241	242	243	244						
B.51ca																							245	246				
B.51cb																							245	246				
B.52	223	224	225	226	227	228	229	230	231	232	233	234	235	236	237	238	239	240	241	242	243	244	245	246				
C.1a	222	223	224	225	226	227	228	229	230	231	232	233	234	235	236	237	238	239	240	241	242	243	244	245				
	225	226	227	228	229	230	231	232	233	234	235	236	237	238	239	240	241	242	243	244	245	246	248	248				
C.1d	222	223	224	225	226	227	228	229	230	231	232	233	234	235	236	237	238	239	240	241	242	243	244	245				
	225	226	227	228	229	230	231	232	233	234	235	236	237	238	239	240	241	242	243	244	245	246	248	248				
C.3a	222	223	224	225	226	227	228	229	230	231	232	233	234	235	236	237	238	239	240	241	242	243	244	245				
C.3aa	224	224	224	227	227	227	230	230	230	233	233	233	236	236	236	239	239	239	242	242	242	245	245	245				
C.3b	222	223	224	225	226	227	228	229	230	231	232	233	234	235	236	237	238	239	240	241	242	243	244	245				
C.3ba	222	223	224	225	226	227	228	229	230	231	232	233	234	235	236	237	238	239	240	241	242	243	244	245				
C.3i	222	223	224	225	229	229	229																					
C.3k																				252	252	252	252	252				
C.4aa	225	225	225	228	228	228	230	230	230	234	234	234	237	237	237	240	240	240	243	243	243	246	246	246				
C.4b	222	223	224	225	226	227	228	229	230	231	232	233	234	235	236	237	238	239	240	241	242	243	244	245				
C.5a													249															
C.6	223	224	225	226	227	228	229	230	231	232	233	234	235	236	237	238	239	240	241	242	243	244	245	246				
	231	231	231	231	231	231	231	231																				
C.8ba													231	232	233	234	235	236	237	238	239	240	241	242	243	244	245	246
D.1a	223	224	225	226	227	228	229	230	231	232	233	234	235	236	237	238	239	240	241	242	243	244	245	246				
D.1b	233	233	233	233	233	233	233	233	233	233	233	233	245	245	245	245	245	245	245	245	245	245	245	245				
D.1c	233	233	233	233	233	233	233	233	233	233	233	233	245	245	245	245	245	245	245	245	245	245	245	245				
F.1a	223	224	225	226	227	228	229	230	231	232	233	234	235	236	237	238	239	240	241	242	243	244	245	246				
F.1b	223	224	225	226	227	228	229	230	231	232	233	234	235	236	237	238	239	240	241	242	243	244	245	246				
F.1c													243	243	243	243	243	243	243	243	243	244	245	246				
F.1d																												
H.60	222	223	224	225	226	227	228	229	230	231	232	233	234	235	236	237	238	239	240	241	242	243	244	245				

* See "Key" on pages 67 and following.

INDEX TO "SOLAR-GEOPHYSICAL DATA"

Key *	1965												1966											
	Jan	Feb	Mar	Apr	May	Jun	Jul	Aug	Sep	Oct	Nov	Dec	Jan	Feb	Mar	Apr	May	Jun	Jul	Aug	Sep	Oct	Nov	Dec
A.2a	246	247	248	249	250	251	252	253	254	255	256	257	258	259	260	261	262	263	264	265	266	267	268	269
A.2b	258	258	258	258	258	258	258	258	258	258	258	258	271	271	271	271	271	271	271	271	271	271	271	271
A.2c	247	248	249	250	251	252	253	254	255	256	257	257	258	259	260	261	262	263	264	265	266	267	268	269
A.3a																								
A.3b	246	247	248	249	---	251	252	253	254	255	256	257	258	259	260	261	262	263	264	265	266	267	268	269
A.5a	246	247	248	249	250	251	252	253	254	255	256	257	258	259	260	261	262	263	264	265	266	267	268	269
A.7a	247	248	248	249	250	251	252	253	---	256	257	257	258	259	260	261	262							
A.7b	249	249	249	252	252	252	256	256	256	258	258	258	261	261	261	264	264	264	267	267	267	270	270	270
A.8aa	246	247	248	249	250	251	252	253	254	255	256	257	258	259	260	261	262	263	264	265	266	267	268	269
A.8ab	257	257	257	257	257	257	257	257	257	257	257	257	269	269	269	269	269	269	269	269	269	269	269	269
A.8ac	246	247	248	249	250	251	252	253	254	255	256	257	258	259	260	261	262	263	264	265	266	267	268	269
A.8ad	257	257	257	257	257	257	257	257	257	257	257	257	269	269	269	269	269	269	269	269	269	269	269	269
A.9a	246	247	248	249	250	251	252	253	254	255	256	257	258	259	260	261	262	263	264	265	266	267	268	269
A.9b	250	250	254	254	257	257	257	259	260	263	263	263	263	263	263	263	266	266	266	267	267	267	---	269
A.10a	246	---	---	---	---	---	---	253	254	255	257	257	258	259	260	261	262	264	264	265	266	267	268	269
A.10b											257	257	258	259	260	261	262	264	264	265	266	267	268	269
A.10c										255	256	257	258	259	260	261	262	263	264	265	266	267	268	269
A.10d																261	262	263	264	265	266	267	268	269
A.11aa			279	279	279	279	279	279	279	279	276	276	276	276	264	276	276	276	265	267	267	269	269	269
A.11ab			286	286	286	286	286	286	286	286										279		272	273	274
A.11ac												270	270	270	270	271	271	271	271	271	271	271	271	271
A.11ad																267	267							
A.11ae													261	261	261	261	262	263	264	265	266	---	272	---
A.13a												306	306	306	306	306	306	306	306	306	306	306	306	306
B.51aa	247	248	249	250	251	252	253	254	255	256	257	258												
B.51ab	247	248	249	250	251	252	253	254	255	256	257	258												
B.51ba	247	248	249	250	251	252	253	254	255	256	257	258	259	260	261	262	263	264	265	266	267	268	269	270
B.51ca	247	248	249	250	251	252	253	254	255	256	257	258	259	260	261	262	263	264	265	266	267	268	269	270
B.51cb	247	248	249	250	251	252	253	254	255	256	257	258	259	260	261	262	263	264	265	266	267	268	269	270
B.52	247	248	249	250	251	252	253	254	255	256	257	258	259	260	261	262	263	264	265	266	267	268	269	270
C.1a	246	247	248	249	250	251	252	253	254	255	256	257	258	259	260	261	262	263	264	265	266	267	268	269
	249	250	251	252	253	255	255	256	257	258	259	260	261	262	263	264	265	266	267	268				
C.1ba																268					269	272	273	274
																					271			
C.1d	246	247	248	249	250	251	252	253	254	255	256	257	258	259	260	261	262	263	264	265	266	267	268	269
	249	250	251	252	253	255	255	256	257	258	259	260	261	262	263	264	265	266	267	268	269	272	273	274
C.3a	246	247	248	249	250	251	252	253	254	255	256	257	258	259	260	261	262	263	264	265	266	267	268	269
C.3aa	248	248	248	251	251	251	254	254	254	257	257	257												
C.3ha	246	247	248	249	250	251	252	253	254	255	256	257	258	259	260	261	262	263	---	---	---	---	---	---
C.3ha	246	247	248	249	250	251	252	253	254	255	256	257												
C.3i					251	252	253	253	254	255	256													
C.3j						252	253	253	254	255	256	257	258	259	260	261	262	263	---	---	---	---	---	---
C.3k	252	252	252	256	256	256	263	263	263	263	263	263	258	259	260	261	262	263	264	265	266	267	268	269
C.3l																								
C.3n													260	260	260	261	262	263	264	265	266	267	268	269
C.4aa													261	261	261	264	264	264	267	267	267	270	270	270
C.4b	246	247	248	249	250	251	252	253	254	255	256	257	258	259	260	261	262	263	264	265	266	267	268	269
C.5b																				275	275	275	275	277
C.5c			279	279	279	279	279	279	279	279	276	276	276	276	264	276	276	264	265	267	267	269	269	269
C.6	247	248	249	250	251	252	253	254	255	256	257	258	259	260	261	262	263	264	265	266	267	268	269	270
C.8bc	247	248	249	250	251																			
C.8be						252	253	254	255	256	257	258	259	260	261	262	263	264	265	266	267	268	269	270
D.1a	247	248	249	250	251	252	253	254	255	256	257	258	259	260	261	262	263	264	265	266	267	268	269	270
D.1b	258	258	258	258	258	258	258	258	258	258	258	258	270	270	270	270	270	270	270	270	270	270	270	270
D.1c	258	258	258	258	258	258	258	258	258	258	258	258	270	270	270	270	270	270	270	270	270	270	270	270
D.1d																								
D.1f													270	270	270	270	270	270	270	270	270	273	273	273
F.1a	247	248	249	250	251	252	253	254	255	256	257	258	259	260	261	262	263	264	265	266	267	268	269	270
F.1b	247	248	249	250	251	252	253	254	255	256	257	258	259	260	261	262	263	264	265	266	267	268	269	270
F.1c	247	248	249	250	251	252	253	254	255	256	257	258	259	260	261	275	275	275	275	275	275			
F.1d	247	248	249	250	251	252	253	254	255	256	257	258	259	260	261	274	274	274	274	274	274	274	274	274
F.1e																			265	266	267	268	269	270
H.60	246	247	248	249	250	251	252	253	254	255	256	257	258	259	260	261	262	263	264	265	266	267	268	269
H.63													282	282	282	282	282	282	282	282	282	282	282	282

* See "Key" on pages 67 and following.

INDEX TO "SOLAR-GEOPHYSICAL DATA"

Key *	1967												1968												
	Jan	Feb	Mar	Apr	May	Jun	Jul	Aug	Sep	Oct	Nov	Dec	Jan	Feb	Mar	Apr	May	Jun	Jul	Aug	Sep	Oct	Nov	Dec	
A.1	271	272	273	274	275	276	277	278	279	280	281	282	283	284	285	286	287	288	289	290	291	292	293	294	
A.2a	270	271	272	273	274	275	276	277	278	279	280	281	282	283	284	285	286	287	288	289	290	291	292	293	
A.2b	282	282	282	282	282	282	282	282	282	282	282	282	295	295	295	295	295	295	295	295	295	295	295	295	
A.2c	270	271	272	273	274	275	276	277	278	279	280	281	282	283	284	285	286	287	288	289	290	291	292	293	
A.3a	271	272	273	274	275	276	277	278	279	280	281	282	283	284	285	286	287	288	289	290	291	292	293	294	
A.3b	270	271	272	273	274	275	276	277	278	279	280	281	282	283	284	285	286	287	288	289	290	291	292	293	
A.4	271	272	273	274	275	276	277	278	279	280	281	282	283	284	285	286	287	288	289	290	291	292	293	294	
A.5	271	272	273	274	275	276	277	278	279	280	281	282	283	284	285	286	287	288	289	290	291	292	293	294	
A.5a	270	271	272	273	274	275	276	277	278	279	280	281	282	283	284	285	286	287	288	289	290	291	292	293	
A.7b	271	272	273	275	275	276	277	278	279	280	282	282	283	284	285	286	287	288	289	290	291	292	293	294	
A.8aa	270	271	272	273	274	275	276	277	278	279	280	281	282	283	284	285	286	287	288	289	290	291	292	293	
A.8ac	270	271	272	273	274	275	276	277	278	279	280	281	282	283	284	285	286	287	288	289	290	291	292	293	
A.8g	270	271	272	273	274	275	276	277	278	279	280	281	282	283	284	285	286	287	288	289	290	291	292	293	
A.9a	271	272	273	274	275	276	277	278	279	280	281	282	283	284	285	286	287	288	289	290	291	292	293	294	
A.9b	271	272	273	274	275	276	277	278	---	280	281	282	283	284	285	286	---	288	289	290	291	292	293	294	
A.10a	270	271	272	273	---	---	277	277	279	279	280	---	---	---	284	285	287	287	288	289	290	291	292	293	
A.10b	270	271	272	273	275	275	276	277	279	279	280	281	282	283	284	285	287	287	288	289	290	291	292	293	
A.10c	270	271	272	273	274	275	276	277	278	280	280	281	282	283	284	285	286	287	288	289	290	291	292	293	
A.10d	270	271	272	273	274	275	276	277	278	280	280	281	282	283	284	285	286	287	288	289	290	291	292	293	
A.10e	---	---	---	---	---	---	---	---	---	---	---	---	---	---	---	---	---	287	288	289	290	291	292	293	
A.11aa	271	272	273	274	275	276	277	278	279	280	281	282	283	284	285	286	287	288	289	290	291	292	293	294	
A.11ab	275	276	277	278	279	280	281	---	---	---	---	---	---	---	---	---	---	288	289	290	291	292	293	---	
A.11ac	271	272	273	274	275	---	---	278	279	280	281	---	---	---	---	---	---	288	289	290	291	292	293	---	
A.11ae	---	272	273	274	---	276	277	---	279	280	---	---	---	---	---	---	---	288	289	290	291	292	293	---	
A.11d	---	---	278	279	279	280	281	282	---	---	---	---	---	---	---	---	---	288	289	290	291	292	293	---	
A.12aa	---	---	---	---	282	282	282	282	283	284	285	286	287	288	289	290	291	292	293	298	298	298	300	301	
A.12ab	---	---	---	---	282	282	282	282	283	284	285	286	287	288	289	290	291	292	293	298	298	298	300	301	
A.13a	305	305	305	305	305	305	305	305	305	305	305	281	281	282	283	284	285	286	287	288	289	290	291	292	
B.51ca	271	272	273	274	275	276	277	278	279	280	281	282	283	284	285	286	287	288	289	290	291	292	293	294	
B.51cb	271	272	273	274	275	276	277	278	279	280	281	282	283	284	285	286	287	288	289	290	291	292	293	294	
B.52	271	272	273	274	275	276	277	278	279	280	281	282	283	284	285	286	287	288	289	290	291	292	293	294	
C.1a	270	271	272	273	274	275	276	277	278	279	280	281	282	283	284	285	286	287	288	289	290	291	292	293	
C.1ba	275	276	277	278	279	280	281	282	283	284	285	286	287	288	289	290	291	292	293	294	295	296	297	298	
C.1d	270	271	272	273	274	275	276	277	278	279	280	281	282	283	284	285	286	287	288	289	290	291	292	293	
C.1g	275	276	277	278	279	280	281	282	283	284	285	286	287	288	289	290	291	292	293	294	295	296	297	298	
C.3a	270	271	272	273	274	275	276	277	278	279	280	281	282	283	284	285	286	287	288	289	290	291	292	293	
C.3k	270	271	272	273	274	275	276	277	278	279	280	281	282	283	284	285	286	287	288	289	290	291	292	293	
C.31	270	271	272	273	274	275	276	277	278	279	280	281	---	283	284	---	---	---	---	---	---	290	291	---	293
C.3m	---	---	---	---	---	---	---	---	---	---	280	281	282	283	284	285	286	287	288	289	290	291	292	293	
C.3n	270	271	272	273	274	275	276	277	278	279	280	281	282	283	284	285	286	287	288	289	290	291	292	293	
C.3p	---	---	272	273	274	275	276	277	278	279	280	281	282	---	---	---	---	---	288	289	290	291	292	293	
C.3q	---	---	---	---	---	---	---	---	---	280	281	---	282	283	284	285	286	287	288	289	290	291	292	293	
C.3r	---	---	---	---	---	---	---	---	279	280	281	---	282	283	284	285	286	287	288	289	290	291	292	293	
C.3s	---	---	---	---	---	---	---	---	---	---	---	---	282	---	284	285	286	287	288	289	290	291	292	293	
C.4aa	277	277	277	277	277	277	277	278	279	280	281	282	283	284	285	286	287	288	289	290	291	292	293	294	
C.4b	270	271	272	273	274	275	276	278	279	280	281	282	283	284	285	286	287	288	289	290	291	292	293	294	
C.4d	277	277	277	277	277	277	277	278	279	280	281	282	283	284	285	286	287	288	289	290	291	292	293	294	
C.4e	---	---	---	---	---	---	---	---	---	---	---	---	---	---	285	286	287	288	289	290	292	292	293	294	
C.4f	---	---	---	---	---	---	---	---	---	---	---	---	283	284	285	286	287	288	289	290	291	292	293	294	
C.5b	278	278	278	280	280	281	281	283	283	284	285	287	287	288	289	290	291	292	293	294	295	296	297	299	
C.5c	271	272	273	274	275	276	277	278	279	280	281	282	283	284	285	286	287	288	289	290	291	292	293	294	
C.5d	---	---	278	279	279	280	281	282	---	---	---	---	---	---	---	---	---	---	---	---	---	---	---	---	
C.6	271	272	273	274	275	276	277	278	279	280	281	282	283	284	285	286	287	287	288	289	290	291	292	293	
C.8	284	284	284	284	284	284	---	---	---	---	---	---	287	288	289	290	291	292	293	294	295	296	297	298	
C.8ba	---	---	---	---	274	275	276	277	278	279	280	281	---	---	---	---	---	---	---	---	---	---	---	---	
C.8be	271	272	---	---	---	---	---	---	---	---	---	---	---	---	---	---	---	---	---	---	---	---	---	---	
D.1a	271	272	273	274	275	276	277	278	279	280	281	282	283	284	285	286	287	288	289	290	291	292	293	294	
D.1b	282	282	282	282	282	282	282	282	282	282	282	282	294	294	294	294	294	294	294	294	294	294	294	294	
D.1c	282	282	282	282	282	282	282	282	282	282	282	282	294	294	294	294	294	294	294	294	294	294	294	294	
D.1d	271	272	273	274	275	276	277	278	279	280	281	282	283	284	285	286	287	288	289	290	291	292	293	294	
D.1e	297	---	---	---	---	---	---	---	---	---	---	---	---	---	---	---	---	---	---	---	298	298	---	---	
D.1f	277	277	277	280	280	280	283	283	283	285	285	2													

♣

* See "Key" on pages 67 and following.

INDEX TO "SOLAR-GEOPHYSICAL DATA"

Key *	1971											
	Jan	Feb	Mar	Apr	May	June	July	Aug	Sep	Oct	Nov	Dec
A.1	319	320	321	322	323	324	325	326	327	328	329	330
A.2a	318	319	320	321	322	323	324	325	326	327	328	329
A.2b	331	331	331	331	331	331	331	331	331	331	331	331
A.2c	318	319	320	321	322	323	324	325	326	327	328	329
A.3a	319	320	321	322	323	324	325	326	327	328	329	330
A.3b	319	320	321	322	323	324	325	326	327	328	329	330
A.4	319	320	321	322	323	324	325	326	327	328	329	330
A.5	319	320	321	322	323	324	325	326	327	328	329	330
A.5a	319	320	321	322	323	324	325	326	327	328	329	330
A.5b	320	320	321	322	323	324	325	326	327	328	329	330
A.7b	319	320	321	322	323	324	325	326	327	328	329	330
A.8aa	318	319	320	321	322	323	324	325	326	327	328	329
A.8ac	318	319	320	321	322	323	324	325	326	327	328	329
A.8g	318	319	320	321	322	323	324	325	326	327	328	329
A.9a	319	320	321	322	323	324	325	326	327	328	329	330
A.9b	319	320	321	322	323	324	325	326	327	328	329	330
A.9c	319	320	321	322	323	324	325	326	327	328	329	330
A.10a	318	319	320	321	322	323	324	325	---	---	333	333
A.10b	318	319	320	321	322	323	324	325	---	---	---	---
A.10c	318	319	320	321	322	323	324	325	326	327	328	329
A.10d	318	319	320	321	322	323	324	325	326	327	328	329
A.10e	318	319	320	321	322	323	324	325	326	327	328	329
A.11aa	319	320	321	322	323	324	325	326	327	328	329	330
A.11ab	323	324	325	326	327	328	329	330	331	332	333	334
A.11e	319	322	321	322	323	324	325	326	327	328	329	330
A.12aa	328	328	328	328	328	330	330	336	336	336	338	338
A.12ab	328	328	328	328	328	330	330	336	336	336	338	338
A.12ba	318	319	320	321	322	323	324	325	326	327	328	329
A.12bb	318	319	320	321	322	323	324	325	326	329	329	---
A.12c	318	319	320	321	322	323	324	325	326	327	328	329
A.13a	318	319	320	321	322	323	324	325	326	327	328	329
A.13c	318	319	320	321	322	323	324	325	326	327	328	329
B.51ca	319	320	321	322	323	324	325	326	327	328	329	330
B.51cb	319	320	321	322	323	324	325	326	327	328	329	330
B.52	319	320	321	322	323	324	325	326	327	328	329	330
B.53	319	320	321	324	324	324	325	326	327	328	330	330
C.1a	318	319	320	321	322	323	324	325	326	327	328	329
C.1ba	323	324	325	326	327	328	329	330	331	332	333	334
C.1d	318	319	320	321	322	323	324	325	326	327	328	329
C.1e	323	324	325	326	327	328	329	330	331	332	333	334
C.1f	324	325	326	327	328	329	330	331	332	333	334	335
C.3	323	324	325	326	327	328	329	330	331	332	333	334
	---	319	320	321	322	323	324	325	326	327	328	329
C.4aa	319	320	321	322	323	324	325	326	327	328	329	330
C.4b	319	320	321	322	323	324	325	326	327	328	329	330
C.4d	319	320	321	322	323	324	325	326	327	328	329	330
C.4e	319	320	321	322	323	324	325	326	327	328	329	330
C.4f	319	320	321	322	323	324	325	326	327	328	329	330
C.4g	---	---	321	322	323	324	328	328	---	---	333	333
C.5b	323	324	325	326	327	328	329	330	331	332	333	334
C.5c	319	320	321	322	323	324	325	326	327	328	329	330
C.6	319	320	321	322	323	324	325	326	327	328	329	330
D.1a	319	320	321	322	323	324	325	326	327	328	329	330
D.1b	330	330	330	330	330	330	330	330	330	330	330	330
D.1c	330	330	330	330	330	330	330	330	330	330	330	330
D.1d	319	320	321	322	323	324	325	326	327	328	329	330
D.1e	323	324	325	326	327	328	329	---	---	---	---	334
D.1f	319	320	321	322	323	324	325	326	327	328	329	330
F.1a	319	320	321	322	323	324	325	326	327	328	329	330
F.1b	319	320	321	322	323	324	328	328	328	328	329	330
F.1c	319	320	321	322	323	324	325	326	327	328	333	333
F.1d	319	320	321	322	323	324	325	326	327	328	333	333
F.1e	319	320	321	322	323	324	325	326	327	328	329	330
F.1f	319	320	321	322	323	324	325	326	327	328	329	330
F.1g	319	320	321	322	323	324	325	326	327	328	329	330
H.60	318	319	320	321	322	323	324	325	326	327	328	329
H.62	324	325	326	327	328	329	330	331	332	333	334	335

* See "Key" on pages 67 and following.

INDEX TO "SOLAR-GEOPHYSICAL DATA"

Key *	1972											
	Jan	Feb	Mar	Apr	May	June	July	Aug	Sep	Oct	Nov	Dec
A.												
A.1	331	332	333	334	335	336	337	338	339	340	341	342
A.2a	330	331	332	333	334	335	336	337	338	339	340	341
A.2b	343	343	343	343	343	343	343	343	343	343	343	343
A.2c	330	331	332	333	334	335	336	337	338	339	340	341
A.3a	331	332	333	334	335	336	337	338	339	340	341	342
A.3b	331	332	333	334	335	336	337	338	339	340	341	342
A.4	331	332	333	334	335	336	337	338	339	340	341	342
A.5	331	332	333	334	335	336	337	338	339	340	341	342
A.5a	331	332	333	334	335	336	337	338	339	340	341	342
A.5b	331	332	333	334	335	336	337	338	339	340	341	342
A.7b	331	332	333	334	335	336	337	338	339	340	341	342
A.7c	---	332	333	334	335	336	337	338	339	340	341	342
A.7d	---	---	---	---	335	336	337	338	339	340	341	342
A.8aa	330	331	332	333	334	335	336	337	338	339	340	341
A.8ac	330	331	332	333	334	335	336	337	338	339	340	341
A.8g	330	331	332	333	334	335	336	337	338	339	340	341
A.9a	331	332	333	334	335	336	337	338	339	340	341	342
A.9b	331	332	333	334	335	336	337	338	339	340	341	342
A.9c	331	332	333	334	335	336	338	338	339	340	341	342
A.10a	333	333	334	334	334	335	336	337	338	340	340	341
A.10c	330	331	332	333	334	335	336	337	338	339	340	341
A.10d	330	331	332	333	334	335	336	337	338	339	340	341
A.10e	330	331	332	333	334	335	336	337	338	339	340	341
A.11aa	331	332	333	334	335	336	337	338	339	340	341	342
A.11ab	335	336	337	338	339	340	341	342	343	344	345	346
A.11e	331	332	333	334	335	336	337	338	339	340	342	---
A.12aa	338	337	337	338	339	340	341	342	343	345	345	346 & 353
A.12ab	338	337	337	338	339	340	341	342	343	345	345	346 & 353
A.12ba	330	331	332	333	334	335	336	337	---	339	340	---
A.12bb	---	---	---	333	334	335	336	337	338	339	340	341
A.12c	330	331	332	333	334	335	336	337	---	---	---	---
A.13a	330	331	332	333	334	335	336	337	---	339	340	341
A.13c	330	331	332	333	334	335	---	---	---	---	---	---
A.17	---	---	---	333	334	335	336	337	338	339	340	341
A.18	---	---	---	333	334	335	336	337	338	339	340	341
B.												
B.51ca	331	332	333	334	335	336	337	338	339	340	341	342
B.51cb	331	332	333	334	335	336	337	338	339	340	341	342
B.52	331	332	333	334	335	336	337	338	339	340	341	342
B.53	331	332	333	334	335	336	337	338	339	340	341	342
C.												
C.1a	330	331	332	333	334	335	336	337	338	339	340	341
C.1ba	335	336	337	338	339	340	341	342	343	344	345	346
C.1d	330	331	332	333	334	335	336	337	338	339	340	341
C.1e	335	336	337	338	339	340	341	342	343	344	345	346
C.1f	336	337	338	339	340	341	342	343	344	345	346	347
C.3	335	336	337	338	339	340	341	342	343	344	345	346
C.4aa	330	331	332	333	334	335	336	337	338	339	340	341
C.4b	331	332	333	334	335	336	337	338	339	340	341	342
C.4d	331	332	333	334	335	336	337	338	339	340	341	342
C.4e	331	332	336	334	335	336	337	338	339	340	341	342
C.4f	331	332	333	334	335	336	337	338	339	340	341	342
C.4g	---	333	---	334	335	---	---	---	---	---	---	---
C.5b	335	337	338	338	341	341	341	---	---	---	---	---
C.5c	331	332	333	334	335	336	337	338	339	340	341	342
C.6	331	332	333	334	335	336	337	338	339	340	341	342
D.												
D.1a	331	332	333	334	335	336	337	338	339	340	341	342
D.1b	342	342	342	342	342	342	342	342	342	342	342	342
D.1c	342	342	342	342	342	342	342	342	342	342	342	342
D.1d	331	332	333	334	335	336	337	338	339	340	341	342
D.1e	---	---	---	---	337	340	---	342	343	---	345	346
D.1f	331	332	333	334	335	336	337	338	339	340	341	342
F.												
F.1a	331	332	334	334	335	336	337	350	350	350	350	350
F.1b	331	332	333									
F.1c	331	342	333	334	335	336	337	338	339	340	341	342
F.1d	331	342	342	342	342	336	348	348	348	348	348	348
F.1e	331	332	334	334	335	336	337	350	350	350	350	350
F.1f	331	332	333	334	335	336	337	338	339	340	341	342
F.1g	331	332	333	334	335	336	337	338	339	340	341	342
H.												
H.60	330	331	332	333	334	335	336	337	338	339	340	341
H.62	336	337	338	339	340	341	342	343	344	345	346	347

* See "Key" on pages 67 and following.

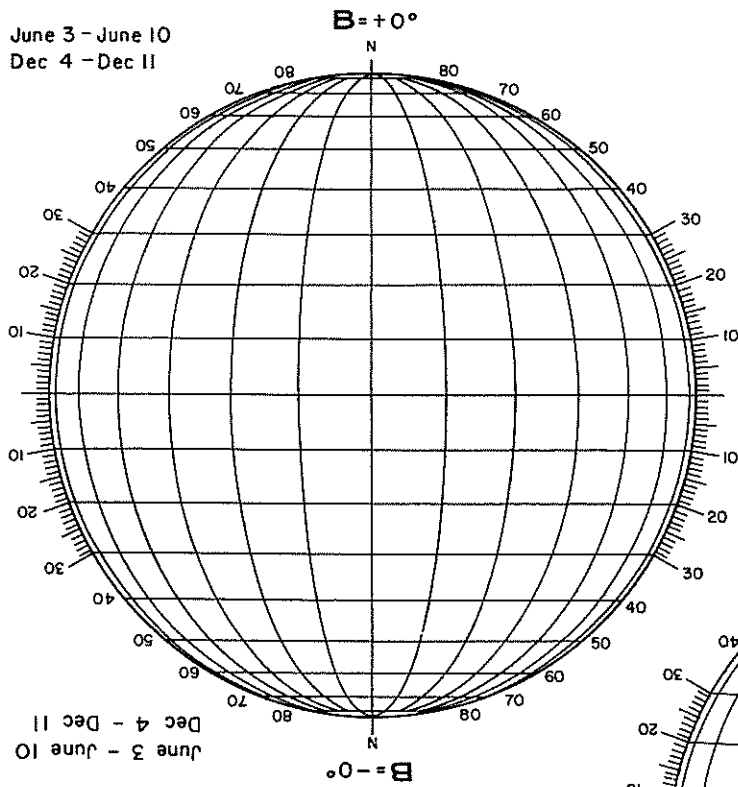
INDEX TO "SOLAR-GEOPHYSICAL DATA"

Key *	1973											
	Jan	Feb	Mar	Apr	May	June	July	Aug	Sep	Oct	Nov	Dec
A.												
A.1	343	344	345	346	347	348	349	350	351	352	353	354
A.2a	342	343	344	345	346	347	348	349	350	351	352	353
A.2b												
A.2c	342	343	344	345	346	347	348	349	350	351	352	353
A.3a	343	344	345	346	347	348	349	350	351	352	353	354
A.3b	343	344	345	346	347	348	349	350	351	352	353	354
A.4	343	344	345	346	347	348	349	350	351	352	353	354
A.5	343	344	345	346	347	348	349	350	351	352	353	354
A.5a	343	344	345	346	347	348	349	350	351	352	353	354
A.5b	343	344	345	346	347	348	349	350	351	352	353	354
A.6	---	---	---	---	---	348	349	350	351	352	353	354
A.7b	343	344	345	346	347	348	349	350	351	352	353	354
A.7c	343	344	345	346	347	348	349	350	351	352	353	354
A.7d	343	344	345	346	347	348	349	350	351	352	353	354
A.7e	343	344	345	346	347	348	349	350	351	352	353	354
A.8aa	342	343	344	345	346	347	348	349	350	351	352	353
A.8ac	342	343	344	345	346	347	348	349	350	351	352	353
A.8g	342	343	344	345	346	347	348	349	350	351	352	353
A.9a	343	344	345	346	347	348	349	350	---	---	---	---
A.9b	343	344	345	346	347	348	349	350	351	352	353	354
A.9c	---	---	---	---	---	---	---	350	351	352	353	354
A.10a	343	344	345	346	347	348	349	350	351	352	353	354
A.10c	342	343	344	345	346	347	348	349	350	351	352	353
A.10d	342	343	344	345	346	347	348	349	350	351	352	353
A.10e	342	343	344	345	346	347	348	349	350	351	352	353
A.11aa	343	344	345	346	347	348	349	350	351	352	353	354
A.11ab	347	348	349	350	351	352	353	354	---	---	---	---
A.11e	---	---	---	---	---	---	---	---	---	---	---	---
A.11f	343	344	345	346	347	348	349	350	351	352	353	354
A.12aa	350	353	353	353	353	---	---	---	---	---	---	---
A.12ab	350	353	353	353	353	---	---	---	---	---	---	---
A.12ba	342	---	---	---	---	347	---	349	350	---	352	353
A.12bb	342	343	344	345	346	347	348	349	350	351	352	353
A.12c												
A.13a	342	---	---	---	346	347	---	349	350	---	352	353
A.13c												
A.17	342	---	---	---	346	347	---	349	350	---	---	353
A.17	342	343	344	345	346	347	348	349	350	351	352	353
A.17c	348	348	348	348	348	348	348	349	350	351	352	353
A.18	342	---	---	---	346	347	---	349	350	---	---	353
A.18	342	343	344	345	346	347	348	349	350	351	352	353
B.												
B.51ca	343	344	345	346	347	348	349	350	351	352	353	354
B.51cb	343	344	345	346	347	348	349	350	351	352	353	354
B.52	343	344	345	346	347	348	349	350	351	352	353	354
B.53	343	344	345	346	347	348	349	350	351	352	353	354
C.												
C.1a	342	343	344	345	346	347	348	349	350	351	352	353
C.1ba	347	348	349	350	351	352	353	354	---	---	---	---
C.1d	342	343	344	345	346	347	348	349	350	351	352	353
C.1e	347	348	349	350	351	352	353	354	---	---	---	---
C.1f	348	349	350	351	352	353	354	---	---	---	---	---
C.3	347	348	349	350	351	352	353	354	---	---	---	---
C.3t	342	343	344	345	346	347	348	349	350	351	352	353
C.4aa	344	344	345	346	347	348	349	350	351	352	353	354
C.4b	343	344	345	346	347	348	349	350	351	352	353	354
C.4d	343	344	345	346	347	348	349	350	351	352	353	354
C.4e	343	344	345	346	347	348	349	350	351	352	353	354
C.4f	343	344	345	346	347	348	349	350	351	352	353	354
C.5b												
C.5c	343	344	345	346	347	348	349	350	351	352	353	354
C.6	343	344	345	346	347	348	349	350	351	352	353	354
D.												
D.1a	343	344	345	346	347	348	349	350	351	352	353	354
D.1b	354	354	354	354	354	354	354	354	354	354	354	354
D.1c	354	354	354	354	354	354	354	354	354	354	354	354
D.1d	343	344	345	346	347	348	349	350	351	352	353	354
D.1e	---	348	349	350	351	352	---	---	---	---	---	---
D.1f	343	344	345	346	347	348	349	350	351	352	353	354
D.1g	---	---	---	---	347	348	349	350	351	352	353	354
F.												
F.1a	346	346	346	347	348	349	349	350	351	352	353	354
F.1b												
F.1c	343	344	345	346	347	348	349	350	352	352	353	354
F.1d												
F.1e	346	346	346	347	348	349	349	350	351	352	353	354
F.1f	343	344	345	346	347	348	349	350	351	352	353	354
F.1g	343	344	345	346	347	348	349	350	351	352	353	354
F.1h				346	347	348	349	350	351	352	353	354
H.												
H.60	342	343	344	345	346	347	348	349	350	351	352	353
H.62	348	349	350	351	352	353	354	---	---	---	---	---

* See "Key" on page 67 and following.

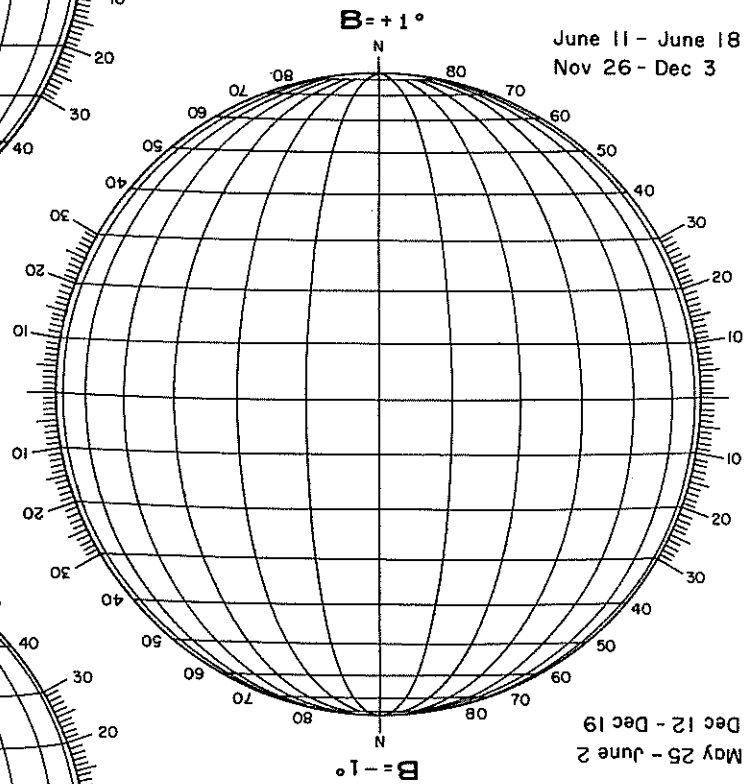
DAYS FROM CENTRAL MERIDIAN

June 3 - June 10
Dec 4 - Dec 11



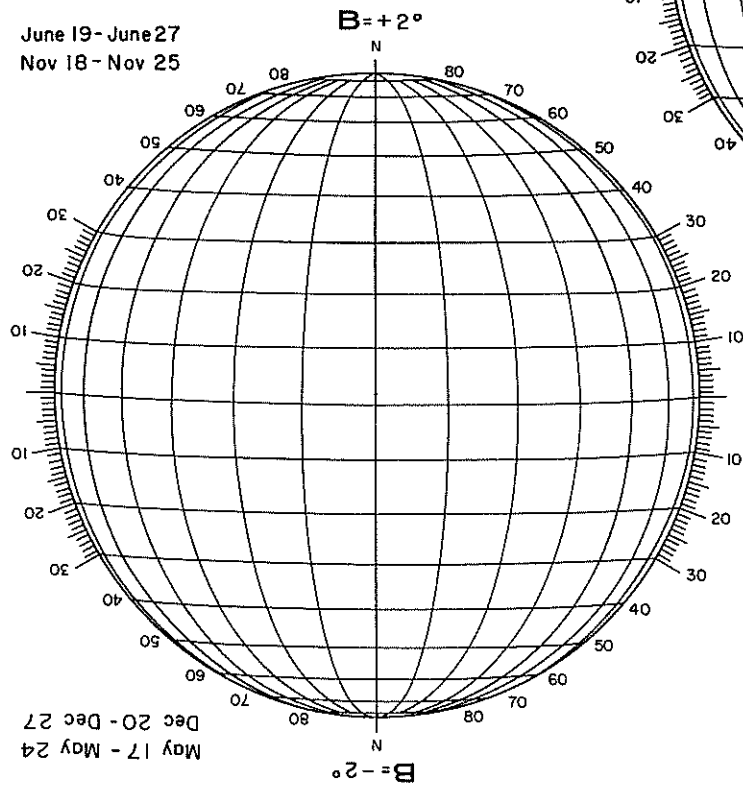
June 3 - June 10
Dec 4 - Dec 11

June 11 - June 18
Nov 26 - Dec 3



May 25 - June 2
Dec 12 - Dec 19

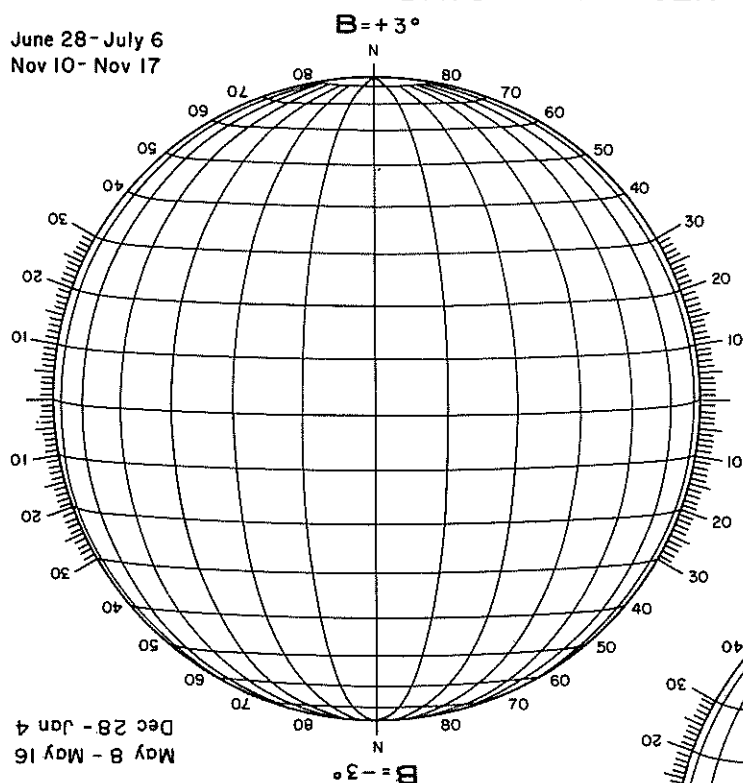
June 19 - June 27
Nov 18 - Nov 25



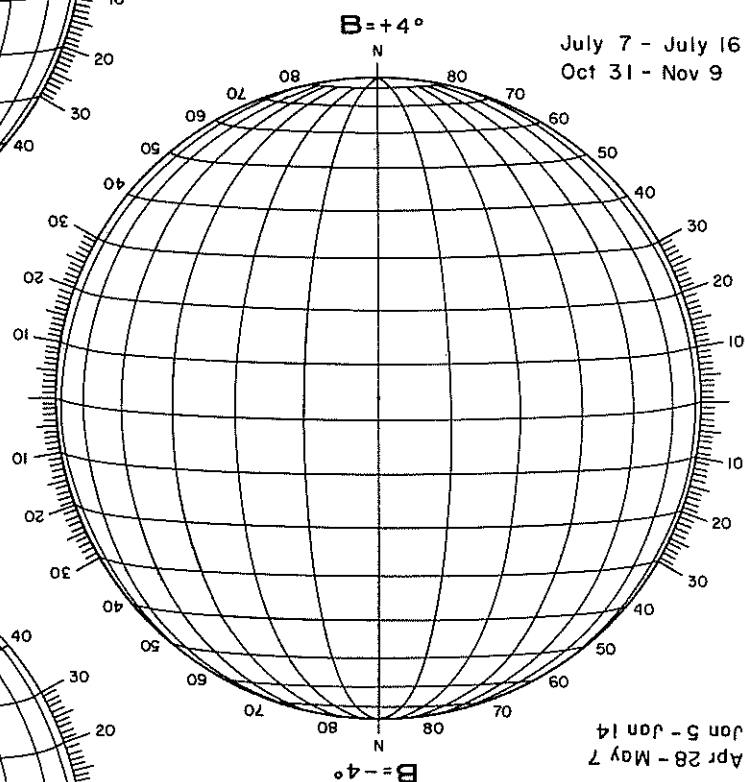
May 17 - May 24
Dec 20 - Dec 27

DAYS FROM CENTRAL MERIDIAN

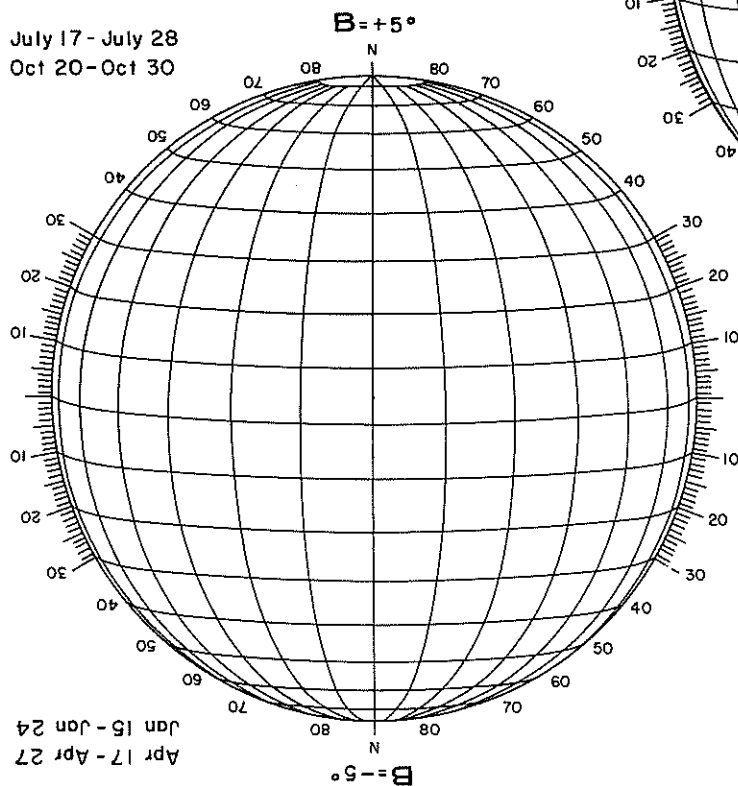
June 28 - July 6
Nov 10 - Nov 17



July 7 - July 16
Oct 31 - Nov 9

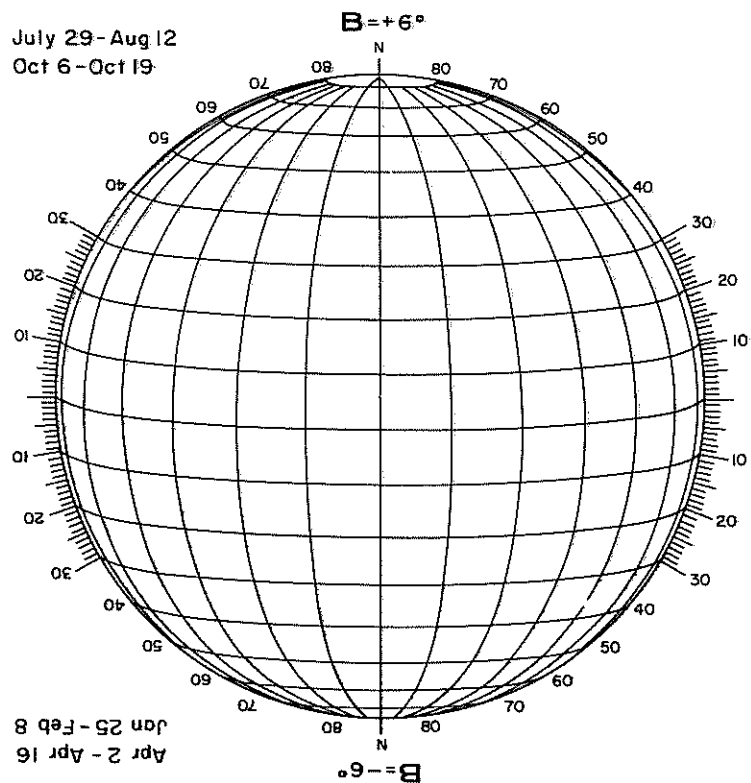


July 17 - July 28
Oct 20 - Oct 30

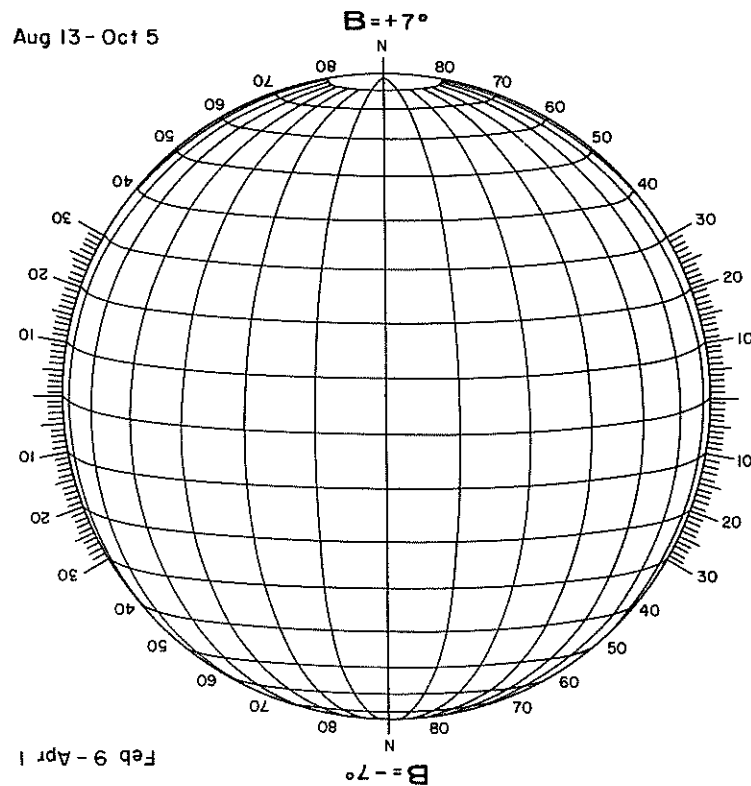


DAYS FROM CENTRAL MERIDIAN

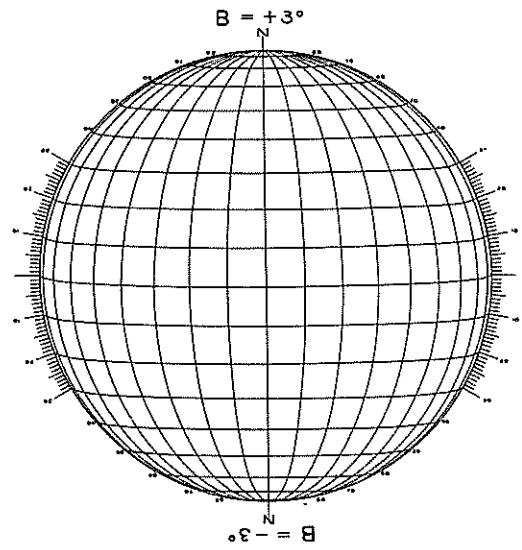
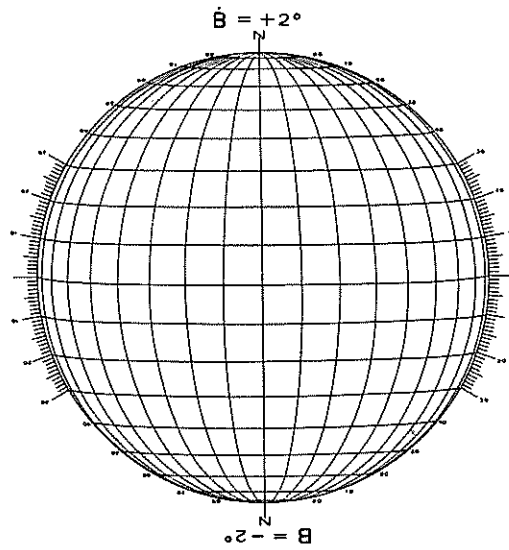
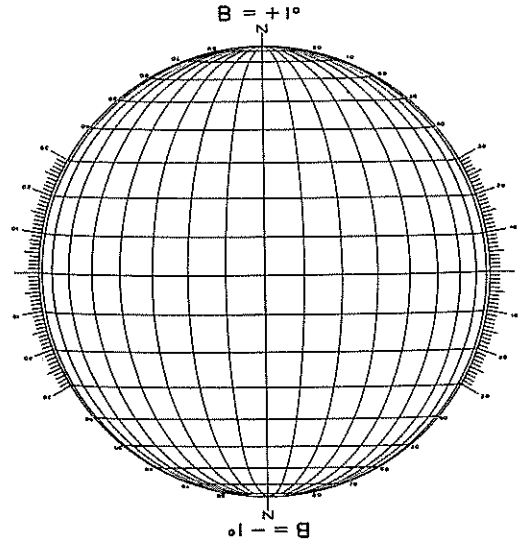
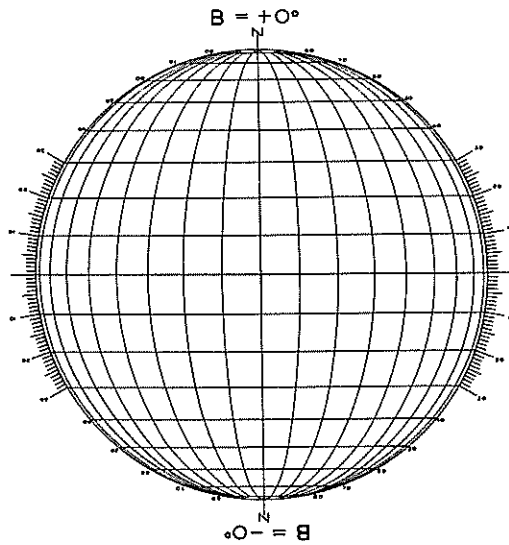
July 29-Aug 12
Oct 6-Oct 19

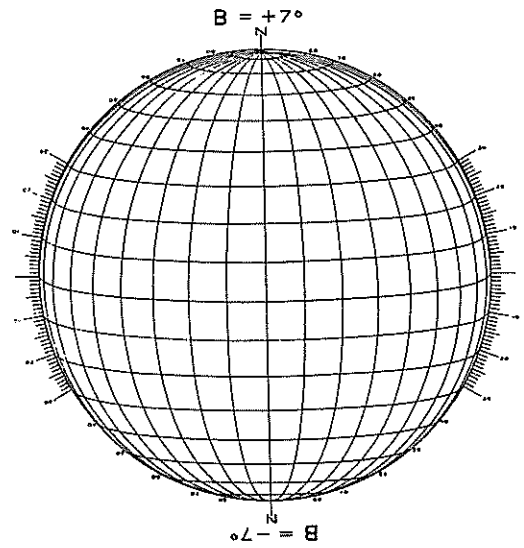
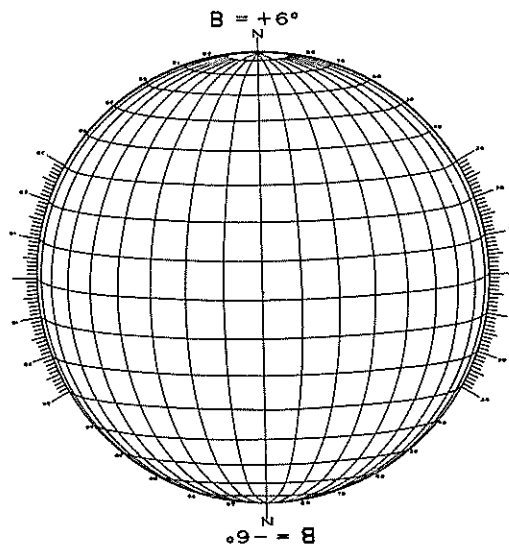
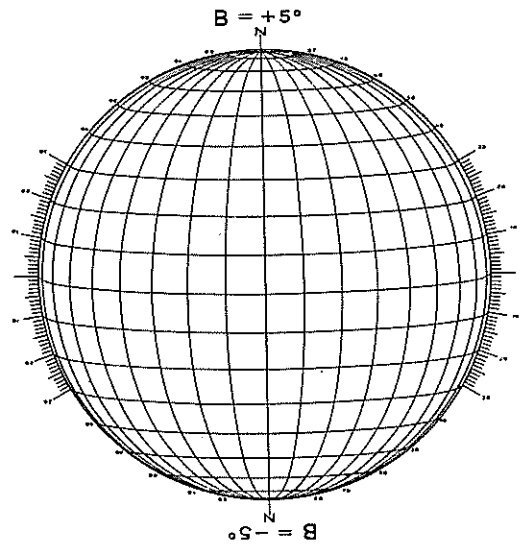
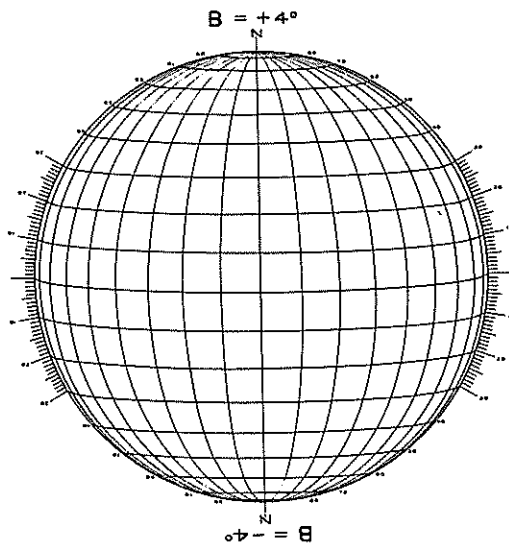


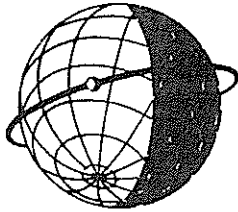
Aug 13 - Oct 5



DEGREES FROM CENTRAL MERIDIAN



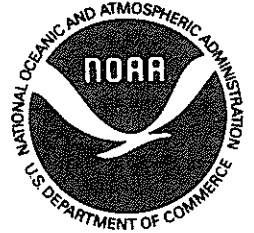




WORLD DATA CENTER A

FOR

SOLAR-TERRESTRIAL PHYSICS



The ICSU Panel on WDCs has recommended that it would be appropriate courtesy to acknowledge in publications that data were obtained from the originating station or investigator through the intermediary of the WDCs. The following statement is suggested:

"Data used in this study were provided by WDC-A for Solar-Terrestrial Physics, NOAA E/GC2, 325 Broadway, Boulder Colorado 80303, USA."